

HOST PATHOGEN INTERACTION, AND COPPER RESISTANCE IN
XANTHOMONADS ASSOCIATED WITH CITRUS CANCKER

By

ALBERTO MARTIN GOCHEZ

A DISSERTATION PRESENTED TO THE GRADUATE SCHOOL
OF THE UNIVERSITY OF FLORIDA IN PARTIAL FULFILLMENT
OF THE REQUIREMENTS FOR THE DEGREE OF
DOCTOR OF PHILOSOPHY

UNIVERSITY OF FLORIDA

2014

© 2014 Alberto Martin Gochez

To my wife Dolores, the love of my life
To my sons Nicolas, Francisco and Santiago, my pride and joy

ACKNOWLEDGMENTS

I want to thank my committee chair Dr. Jeffrey B. Jones, for all his support and advice since the first day. I would like to especially acknowledge to all my committee members, Drs. James Graham, James Preston, Jeffrey Rollins, and Nian Wang for all their support, useful criticism and fruitful discussions. Very special thanks go to Dr. Robert Stall and Jerry Minsavage, for all their advice, recommendations and expertise guidance that made my years here in Fifield Hall more productive; to Dr. Blanca Canteros from INTA Bella Vista, for share all her wisdom with me and support from the first moment my decision to start this PhD. Also I want to thank Dr. Jason Hurlbert, from Winthrop University, SC, for his expertise collaboration in this dissertation.

During the last 4 years I have collaborated with many colleagues from the 2560 lab for whom I have great regard and I wish to extend my warmest thanks and wishes of best luck. First, I want to thank Neha Potnis, and Deepak Shantaraj, for their patience when teaching me molecular techniques, for always finding some time to discuss new ideas, and for their friendship. Also I want to thank Franklin Behlau, Francisco Figueiredo, Jason Hong, Mine Hantal, Yang Hu, Will Rockey and Sujana Timilsina, and all the numerous lab mates, and graduate student who shared unforgettable moments with me. I want to express my sincere gratitude to Jessica Ulloa who helped me in every step of this PhD, and also to Dr. Botond Balogh who stayed always on call. I also want to extend thanks to my parents, who have always taught me with their example; to my brothers that never lost contact through the years; and a special lovely thanks to my wife Dolores, for staying by my side all the time, no matter if the moments were difficult or happy. Thanks go to my kids, Nicolas, Francisco and Santiago, for giving me complete happiness.

TABLE OF CONTENTS

	<u>page</u>
ACKNOWLEDGMENTS.....	4
LIST OF TABLES.....	8
LIST OF FIGURES.....	9
ABSTRACT	12
CHAPTER 1	14
HOST PATHOGEN INTERACTION, AND COPPER RESISTANCE IN XANTHOMONADS ASSOCIATED WITH CITRUS CANKER.....	14
Introduction	14
Citrus Production Overview	14
Citrus Canker	14
Characteristics of the citrus canker pathogens.....	15
<i>Xanthomonas citri</i> Strains.....	16
Pathogenic variation of Xc-A strains	18
<i>X. fuscans</i> pv. <i>aurantifolii</i> type B and C strains	21
Characterization of the Interaction between <i>Xanthomonas</i> and Citrus Hosts	24
Characterization of <i>Xanthomonas</i> Pathogenomes Associated with citrus canker.....	26
Control Methods of Plant Pathogenic CuR Strains	29
Activation and Function of the CuR Operon	34
Project Goal and Objectives	36
CHAPTER 2	37
IDENTIFICATION AND CHARACTERIZATION OF THE GENE <i>avrGf2</i> PRESENT IN <i>Xanthomonas fuscans</i> pv. <i>aurantifolii</i> TYPE C.....	37
Introduction	37
Material and Methods	39
Bacterial Strains and Media.....	39
Growth of Plants and Inoculum Preparation	39
Bacterial Growth Curves and Electrolyte leakage Experiments.....	40
Molecular Techniques	41
Sequence Comparison of Gene <i>avrGf2</i> and Phylogenetic Approach.....	42
Results.....	43
Identification of <i>AvrGf2</i> in Xfa-C as an Elicitor of HR in Grapefruit	43
The effector <i>XopAG-avrGf2</i> is Present Only in Xfa-C Strains.....	45
Xc-A* Elicits HR in Grapefruit.....	46
<i>AvrGf2</i> and <i>AvrGf1</i> Differ in HR in Grapefruit	46
Phylogenetic Analysis between <i>avrGf2</i> Gene and Members of the <i>XopAG</i> Effector Family	47

Discussion	47
CHAPTER 3	<u>7169</u>
MOLECULAR CHARACTERIZATION OF AvrGf2, A XopAG EFFECTOR THAT IS REQUIRED FOR ELICITATION OF HR IN GRAPEFRUIT	<u>7169</u>
Introduction	<u>7169</u>
Material and Methods	<u>7472</u>
Bacterial Strains and Media.....	<u>7472</u>
Growth of Plants and Inoculum Preparation	<u>7472</u>
Bacterial Growth Curves and Electrolyte Leakage Experiments	<u>7573</u>
Aminoacid Sequence Comparison of XopAG Effectors.....	<u>7573</u>
Swapping of the C Terminal Domains from <i>avrGf1</i> to <i>avrGf2</i> Gene.....	<u>7674</u>
Mutational Analysis of <i>avrGf2</i> 'CLNA' Motif.....	<u>7775</u>
Mutation of a Cyclophilin Binding Site in <i>avrGf2</i> , and Phenotype Characterization of Mutants	<u>7775</u>
Determination of the Interaction between a Citrus Cyclophilin and XopAG Effectors Using a Yeast Two Hybrid Approach	<u>7876</u>
Determination of the Interaction between a Citrus Cyclophilin and AvrGf2 Using a Transient Silencing Approach <i>in planta</i>	<u>7977</u>
Results.....	<u>8179</u>
The XopAG-effectors AvrGf1 and AvrGf2 Share Related Functional Features.....	<u>8179</u>
The C-terminal Part of XopAG-AvrGf2 Effector is Essential for Elicitation of HR in Citrus.....	<u>8280</u>
The XopAG AvrGf2 Effector Contains a Cyclophilin Binding Site that Determines the Elicitation of HR in Citrus	<u>8384</u>
A Constitutively Expressed Cyclophilin in Grapefruit Interacts with AvrGf1 and AvrGf2.....	<u>8583</u>
Discussion	<u>8684</u>
CHAPTER 4	<u>105400</u>
SEQUENCING OF THE COPPER RESISTANT <i>Xanthomonas citri</i> STRAIN A44. EFFECTOR PROFILE AND PLASMID ARRANGEMENT.....	<u>105400</u>
Introduction	<u>105400</u>
Material and Methods	<u>108403</u>
Bacterial Strains Media and Inoculum Preparation.....	<u>108403</u>
Growth of Plants.....	<u>109404</u>
Bacterial Population Dynamics <i>in planta</i>	<u>109404</u>
Infectivity Titration	<u>109404</u>
Isolation of Plasmid DNA.....	<u>110405</u>
Cosmid Cloning and Genome Finishing	<u>111406</u>
PCR Analysis	<u>111406</u>
Genome Sequencing and Alignment.....	<u>112407</u>
Gap Closure and Assembly Validation	<u>113408</u>
Effector Analysis.....	<u>114409</u>

Results.....	<u>114109</u>
Pathogenicity Assessment for CuR Strain Xc-A44	<u>114109</u>
Genome Alignment and Assessment of Genes Related to Virulence between Xc-A44 and Xc-A306	<u>115110</u>
The <i>pthA</i> TALE Genes are Carried in the Pathogenicity Plasmid pXc123	<u>115110</u>
Comparison of Strain A44 Copper Resistance Plasmid with Other Xanthomonads	<u>117112</u>
Discussion	<u>119114</u>
CHAPTER 5	<u>143138</u>
SUMMARY AND DISCUSSION	<u>143138</u>
LIST OF REFERENCES	<u>147142</u>
BIOGRAPHICAL SKETCH.....	<u>164155</u>

LIST OF TABLES

<u>Table</u>		<u>page</u>
2-1	Bacterial strains, plasmid vectors, and plasmid constructs used in this study	<u>5152</u>
2-2	Primers utilized in the present work.....	<u>5758</u>
3-1	Comparison of <i>GF-Cyp</i> gene expression in grapefruit leaves in a transient gene silencing experiment using <i>Agrobacterium tumefaciens</i> and QRT-PCR.	<u>Error! Bookmark</u>
3-2.	Comparison of the areas under the curve (AUC) of the electrolyte leakage analysis data performed in transient silenced young GF leaves separately infiltrated with suspensions of 5×10^6 CFU/ml of <i>Agrobacterium tumefaciens</i> .	<u>Error! Bookmark</u>
4-1	Putative Type III effectors (T3E) present in the Xc-306 and Xc-A44 plasmids.	128
4-2	General features of Xc-A44 and Xv1111 CuR plasmids analyzed using Gene Calling method in IMG/ER.	<u>Error! Bookmark not defined.</u> 137
4-3	Gene summary of Xc-A44pCuR region '00056'.....	<u>140139</u>
4-4	Gene summary of Xc-A44pCuR region '00052'.....	<u>141140</u>

LIST OF FIGURES

<u>Figure</u>	<u>page</u>
2-1 AvrGf2 expression in citrus canker producing strains results in elicitation of a hypersensitive reaction in Duncan grapefruit leaves..	<u>Error! Bookmark not defined.</u> 59
2-2 Disease reactions observed in leaves of Duncan grapefruit; Hamlin orange; Eureka lemon; and Satsuma mandarin.	<u>Error! Bookmark not defined.</u> 60
2-3 Population dynamics in Key lime (KL), and Duncan grapefruit (DG) leaves inoculated with bacterial suspensions adjusted 5×10^5 CFU/ml. Electrolyte leakage analysis of the same bacterial species in DG leaves infiltrated with bacterial suspensions adjusted to 5×10^8 CFU/ml.	<u>Error! Bookmark not defined.</u> 64
2-4 Strains of <i>Xanthomonas fuscans</i> pv. <i>aurantifolii</i> type –B (Xfa-B) contain a transposon insertion in <i>avrGf2</i>	<u>Error! Bookmark not defined.</u> 62
2-5 Hybridization of <i>avrGf2</i> with total genomic DNA of <i>Xanthomonas</i> strains.	<u>Error! Bookmark not defined.</u>
2-6 Population dynamics in Duncan grapefruit (DG) leaves following infiltration of bacterial suspensions adjusted to 5×10^5 CFU/ml..	<u>Error! Bookmark not defined.</u> 64
2-7 Hypersensitive and susceptible reaction observed after 15 days in Duncan GF leaves infiltrated with bacterial suspensions adjusted to 5×10^8 CFU/ml.	<u>Error! Bookmark not defined.</u>
2-8 Hypersensitive reaction observed after 5 days in Duncan Grapefruit leaves infiltrated with bacterial suspensions adjusted to 5×10^8 CFU/ml..	<u>Error! Bookmark not defined.</u>
2-9 Expression of <i>avrGf1</i> and <i>avrGf2</i> in Xc-A results in elicitation of HR and reduces XccA growth in Duncan grapefruit leaves.	<u>Error! Bookmark not defined.</u> 67
2-10 Population dynamics in Key lime (KL), and Duncan grapefruit (DG) leaves following infiltration with bacterial suspensions adjusted to 5×10^5 CFU/ml.	<u>Error! Bookmark not defined.</u>
2-11 Neighbor-joining tree with a Bootstrap test of inferred phylogeny calculated using MEGA 5 for XopAG effector family genes and close related nucleotides sequenced recovered from Genbank..	<u>Error! Bookmark not defined.</u> 69
2-12 Neighbor-joining tree with a Bootstrap test of inferred phylogeny calculated using MEGA 5 for XopAG effector family genes and close related aminoacid sequenced recovered from Genbank..	<u>Error! Bookmark not defined.</u> 70
3-1 Clustal W multiple sequence alignment of translated proteins AvrGf1 (from XC-Aw) and AvrGf2 (from Xfa-C)..	<u>Error! Bookmark not defined.</u> 92
3-2 Three C-terminal domains were predicted in AvrGf1 and AvrGf2 using MEME Suite.....	<u>Error! Bookmark not defined.</u> 93

3-3	Three C-terminal domains were predicted in nine XopAG effectors (from five different bacterial genera) using MEME Suite. .. Error! Bookmark not defined.	94
3-4	The effect of site directed mutagenesis of CLNA motif in <i>avrGf2</i> gene on HR elicitation. Error! Bookmark not defined.	95
3-5	The effect of site directed mutagenesis of GPxL motif in <i>avrGf2</i> gene on HR elicitation. Error! Bookmark not defined.	96
3-6	The effect of GPxL motif and mutation derivatives in <i>avrGf2</i> . Error! Bookmark not defined.	97
3-7	Yeast two-hybrid assay showing the interaction between the <i>Citrus paradisi</i> cyclophilin (GF-Cyp) and XopAG <i>avrGf1</i> and <i>avrGf2</i> . Error! Bookmark not defined.	98
3-8	Quantification of the expression of <i>GF-Cyp</i> in a transient gene silencing experiment using <i>Agrobacterium tumefaciens</i> in GF leaves. Error! Bookmark not defined.	100
3-9	Transient silencing experiment in young grapefruit (GF) leaves infiltrated separately with a suspension of <i>Agrobacterium tumefaciens</i> strains adjunted to a concentration of 5×10^8 CFU/ml..... Error! Bookmark not defined.	101
3-10	Transient silencing experiment in young grapefruit (GF) leaves infiltrated separately with suspensions of <i>Agrobacterium tumefaciens</i> strains adjusted to a concentration of 5×10^5 CFU/ml. Error! Bookmark not defined.	102
3-11	Electrolyte leakage analysis in transient silenced young GF leaves separately infiltrated with suspensions of 5×10^6 CFU/ml of <i>Agrobacterium tumefaciens</i> strains..... Error! Bookmark not defined.	103
4-1	Population dynamics in Duncan grapefruit (DG) leaves following infiltration with 5×10^5 CFU/ml of <i>Xanthomonas citri</i> type A CuS and CuR.. Error! Bookmark not defined.	
4-2	Citrus canker lesion development on Duncan grapefruit leaves following infiltration with a suspension of <i>Xanthomonas citri</i> Xc-A306 CuS or Xc-A44 CuR. Error! Bookmark not defined.	126
4-3	BLAST Dot Matrix representation of alignment based on chromosomal sequence comparison between Xc-A306 (X axis) and Xc-A44 (Y axis).. Error! Bookmark not d	
4-4	Total genomic and plasmid extractions of strains were subjected to electrophoresis and probed with <i>pthA</i> probe. .. Error! Bookmark not defined.	132
4-5	Two functional copies of the gene, <i>pthA4</i> were identified in cosmid library clones 'NLS8' and '5-4-2'..... Error! Bookmark not defined.	133
4-6	Circular representation of Xc-A44p129 using CGView server based on sequences obtained from Xc-A44 high-throughput sequencing contigs and library clones.. Error! Bookmark not defined.	134

- 4-7 Plasmid profiles of *Xanthomonas* CuR strains following agarose gel electrophoresis.[Error! Bookmark not defined.](#)135
- 4-8 A. BLAST Dot Matrix representation for the alignment obtained for sequence comparison between Xv1111 pCuR and Xc-A44 pCuR..[Error! Bookmark not defined.](#)136
- 4-9 Circular representation of Xc-A44pCuR using BRIG..[Error! Bookmark not defined.](#)138
- 4-10 Gene Orthologous Neighborhoods comparison among Xc-A44pCuR region designated '00056', and '00052' and Xc-A306 chromosome.[Error! Bookmark not defined.](#)141

ABSTRACT

HOST PATHOGEN INTERACTION, AND COPPER RESISTANCE IN XANTHOMONADS ASSOCIATED WITH CITRUS CANCKER

By

Alberto Martin Gochez

May 2014

Chair: Jeffrey Jones
Co-chair: James H. Graham.
Major: Plant Pathology

Citrus canker is a bacterial disease caused by *Xanthomonas citri* type A (Xc-A) and *X. fuscans* pv. *aurantifolii* (Xfa). The disease reduces yield and affects marketing of the fruits. Most of the strategies for citrus canker control are based on application of copper sprays. Two strains, Xc-Aw and Xfa type C (Xfa-C), isolated in Florida and Brazil, elicit a hypersensitive reaction (HR) in grapefruit (*Citrus paradisi*) leaves. The major objectives of this dissertation are: 1) to identify and characterize the gene from Xfa type C that elicits HR in citrus species, and 2) to characterize chromosomal and plasmid rearrangements in copper resistant (CuR) strain Xc-A44. The gene responsible for the Xfa type C strain eliciting an HR in citrus species except Key lime (*C. aurantifolia*) was identified and designated *avrGf2*. A non-functional copy of this effector is present in Xfa-B strains. Compared with the previously characterized gene *avrGf1*, *avrGf2* elicited a faster form of HR in citrus. The two avirulence genes, *avrGf1* and *avrGf2*, both members of the XopAG family, have 45% identity at the amino acid level and contain chloroplast localization signals. Based on amino acid sequence comparisons, two C-terminal motifs were identified in AvrGf1 and AvrGf2 effectors and

also in several XopAG already described. The effector AvrGf2 shows a putative C-terminal domain (CLNAXYD), and a cyclophilin-binding site (GPxL), which was determined to be essential for HR elicitation. The genome sequence of strain Xc-A44, shows a similar T3E profile as well high sequence identity with the chromosome of the reference strain Xc-A306, although there are considerable differences in their plasmids. The first plasmid difference is associated with the pathogenicity plasmid, which has an approx. size of 123 Kbp. Plasmid Xc-A44p123 has differences in the sequence and number of its TALEs; this plasmid contained two functional copies of *pthA4* gene, and nucleotide sequences that resemble a recombination of plasmids pXAC33 and pXAC64 from strain Xc-A306. The second plasmid (pCuR) has two sequence insertions with homology to the Xc-A44 and Xc-A306 chromosome. The insertions found in Xc-A44pCuR have sequence identities with transposon genes previously identified in several *Xanthomonas* species.

CHAPTER 1

HOST PATHOGEN INTERACTION, AND COPPER RESISTANCE IN XANTHOMONADS ASSOCIATED WITH CITRUS CANCKER

Introduction

Citrus Production Overview

Citrus is the highest valued crop in world agriculture. In the last 10 years, mainly as a consequence of emerging diseases like Huanglongbing (HLB) and citrus canker, the ranking of the world planted area, and production per region/country varied. According the Food and Agriculture Organization of the United Nations (FAO(2013), the five most important citrus producers are Brazil with 21 million tons (Mtons), China (14 Mtons), United States (12 Mtons), and Mexico (6 Mtons). Citrus fruits are commercialized as processed product (juice) or sold as fresh fruit. In the US, citrus is almost totally used in the internal market; 60% of the production is destined for juice and the remainder for fresh market (source: NASS-USDA). Moreover, Brazil uses 70% of fruit harvest for juice industry, which is almost totally exported (98%), principally to the United States. For some countries such as Spain and Italy, their production (5.7 and 3.8 Mtons respectively) is primarily for fresh market, while production in other countries such as Argentina (2.6 Mtons), South Africa (2.3 Mtons), and Peru (0.94 Mtons) focuses specifically on producing high quality fruits for exportation.

Citrus Canker

In many citrus growing regions citrus canker is a major disease. The causal agent of citrus canker *Xanthomonas citri* type A (Xac) incites symptoms (also called pustules or cankers) on leaves, fruit and young twigs. Growing tissues are most susceptible to citrus canker (Lee, 1921, Goto, 1972, Stall et al., 1982, Gottwald &

Graham, 1992). Canker lesions serve as an inoculum source for new infections in the same or different plants (Stall et al., 1979, Timmer et al., 2000). The combination of wind and rain carry the bacterial cells from existing lesions to susceptible tissues (Serizawa & Inoue, 1975, Timmer et al., 1991, Canteros, 2005). The infection cycle of this pathogen is favored during storms, when the wind velocity of raindrops is greater than 8 m / sec (Serizawa & Inoue, 1975, Kuhara, 1978) which allows the bacterium to overcome the stomatal pressure resistance, enter through the stomatal opening and reach the mesophyll space. The bacterium also enters plants through wounds (Serizawa & Inoue, 1975). The resistance to the passage of water into stoma varies among citrus species, and also depends on the innate resistance of the mesophyll (McLean & Lee, 1922, Stall & Seymour, 1983, Schubert et al., 2001).

Although citrus canker was recognized as a new disease in 1913 (Berger, 1914), Fawcett and Jenkins (1933) found citrus canker symptoms in herbarium specimens collected in 1827-1831 (*Citrus medica*, from India), and in 1842-1844 (*C. aurantifolia*, originally from Indonesia), and in 1865 (from Japanese samples erroneously identified as citrus scab at this time) (Loucks, 1934). In 1915 Clara Hasse (1915) isolated the causal agent and demonstrated the infective agent was a bacterium completing Koch's postulates.

Characteristics of the citrus canker pathogens

Initially classified as *Pseudomonas citri* (Hasse, 1915), subsequent revisions in nomenclature include *Bacterium citri* (ex Hasse) Doidge, 1916; *Bacillus citri* (ex Hasse) Holland, 1920; *Phytomonas citri* (ex Hasse) Bergey et al. 1923; *Xanthomonas citri* (ex Hasse) Dowson, 1939; and *Xanthomonas campestris* pv. *citri* (ex Hasse) Dye, 1978.

More recently Vauterin et al. (1995) proposed *Xanthomonas axonopodis* pv. *citri* (Hasse) Vauterin et al., 1995 for the citrus canker type A pathogen (Vauterin & Swings, 1997). Schaad et al. (2005) proposed placing *X. axonopodis* pv. *citri* in *X. smithii* subsp. *citri*. However this name was determined to be illegitimate (Schaad et al., 2006).

Currently the nomenclature of these bacterial groups varies depending on the working group (Brunings & Gabriel, 2003, Graham et al., 2004, Bull et al., 2012).

- *Xanthomonas citri* subsp. *citri* (ex Hasse 1915) Gabriel et al. 1989; *Xanthomonas axonopodis* pv. *citri* (Hasse 1915) Vauterin et al. 1995, *Xanthomonas campestris* pv. *citri* (Hasse) Dye 1978, *Xanthomonas citri* (ex Hasse) nom. rev. Gabriel et al., *Xanthomonas axonopodis* pv. *citri* (Hasse) Vauterin et al., (1995) (sin = *Pseudomonas citri* Hasse, *Xanthomonas citri* (Hasse) Dowson (Xc)
- *Xanthomonas citri* f. sp. *aurantifoliae* (Namekata & Oliveira, 1972), *Xanthomonas campestris* pv. *aurantifolii* (Gabriel et al. 1989), *Xanthomonas axonopodis* pv. *aurantifolii* (Vauterin et al. 1995), *X. fuscans* pv. *aurantifolii* (Schaad et al., 2005) (Xfa).

***Xanthomonas citri* Strains**

In a review by Civerolo & Stall (1991), the authors suggested that based on physiological and pathogenic characteristics, three groups of xanthomonads that cause citrus canker disease should be separated as: A, B, and C strains. These three groups (Xc-A, Xfa-B and Xfa-C) were partially characterized using various techniques including RFLP (Hartung and Civerolo, 1987), fatty acid methyl ester analysis (Vauterin et al. 1991; Vauterin et al. 1996a), DNA-DNA hybridization (genomic annealing experiments) (Egel, 1991; Egel et al. 1991; Vauterin et al. 1990; Vauterin et al., 1991), and analysis of polymerase chain reaction (PCR) products following amplification of *hrp* regions (Leite et al., 1994).

De Souza Carvalho et al. (2005) characterized the genetic diversity of 22 Xc-A strains from South America extracting plasmids for each strain to compare size and number, and digesting total genomic DNA with restriction enzymes (*XbaI* and *VspI*) to compare RFLPs by pulse-field-gel electrophoresis. After combining results, the authors observed high coefficients of similarity for strains isolated in similar geographical locations (from 0.83 to 1 for strains isolated in seven Brazilian states and between 0.62 and 0.83 for strains from Argentina, Bolivia, Paraguay and Uruguay). There was also variability in plasmid sizes (only 5 types of plasmid ranging in size from 57.7 to 83 Kbp).

A detailed study was performed in which 157 strains from Brazil were compared for type III effector (T3E) profiles using a qualitative PCR-Southern blot technique (Jaciani et al., 2012). Low genetic variability was observed for strains isolated in the northern part of the country, but more diversity was present in the strains isolated in the southern part, where the disease was more prevalent. In China Xc-A strains from 9 citrus growing regions were characterized for variability of TAL effectors. As a result of the analysis of 105 strains, some showed differential pathogenicity on a set of citrus hosts; these strains varied in the number of TAL effectors ranging from 3 to 5 *pthA* genes. The comparison of the strains through the hybridization with a probe based on the Xc-A3213 *pthA* gene, allowed separation of strains into 14 genotypes, with more than 80% of the strains being placed in two major groups. The lack of hybridization observed in some strains was correlated with lower virulence of these specific strains (Ye et al., 2013), and could be correlated with variation in the sequences of the *pthA* genes (Lin et al., 2005, Lin et al., 2011). Interestingly, a slight modification in the

number of repeats of the gene *pthA4*, produced changes in the pathogenicity of the bacterium, specifically in the induction of the citrus canker symptoms (Lin et al., 2013).

A specific TALE (PthA4) is responsible for the elicitation of citrus canker symptom through the activation of specific genes in the host (Shantharaj et al., 2013). Recently, it was confirmed that the TALE, PthA4, up-regulated the host gene *CsLOB-1*, a member of the lateral organ boundaries (LOB) transcription factor family, and *CsSWEET1*, a homolog of the SWEET sugar transporter and rice disease susceptibility gene family (Hu et al., 2013). Also, it was demonstrated that the effector, PthA4, interacts *in planta* with the C-Terminal Domain (CTD) of RNA Polymerase II, inhibiting the activity of a CTD-associated cyclophilin that works as a negative regulator of cell growth (Domingues et al., 2012), and also with the protein CsMAF1, which represses the tRNA synthesis and cell growth, through its interaction with the RNA polymerase III (Soprano et al., 2013).

Pathogenic variation of Xc-A strains

Symptoms of citrus canker were first identified in commercial crops in northern Yemen in 1988 (Cook, 1988), Saudi Arabia, Oman, Iraq (Ibrahim & Bayaa, 1989), United Arab Emirates (El-Goorani, 1989), Iran (Alizadeh & Rahimian, 1990), and Ethiopia (Derso et al., 2009). Following inoculation of diverse citrus (Key lime and Marsh grapefruit) and *Poncirus* species, it was determined that the pathogenicity of these strains was different compared to typical Xc-A strains, and also Xfa-B and Xfa-C strains, and for this reason, this group of strains isolated in the Southwest of Asia were designated Xc-A* (Verniere et al., 1998). Indirect ELISA tests with polyclonal antibodies specific for Xc-A, Xfa-B and Xfa-C did not show high affinity for the Xc-A* strains. PCR

with primers specific for Xc-A, showed that the Xc-A* strains grouped with Xc-A strains (Verniere et al., 1998).

Characterization of several Xc-A* strains isolated from Key lime (KL) in Iran based on pathogenicity, biochemical and physiological characteristics, plasmid profiles, DNA fingerprints, SDS-PAGE analysis of total soluble proteins, and phage susceptibility, revealed that some of the Xc-A* strains were only pathogenic on KL; however, these strains still showed enough similarity with typical Xc-A strains, that they should be considered as a subgroup of Xc-A (Graham et al., 2004, Mohammadi et al., 2001).

In May of 2000, in Southeastern Florida, USA (Palm Beach County, located in the vicinity of Lake Worth and Wellington), symptoms of citrus canker were observed on Key lime (Rybak, 2005) and Alemow leaves (*C. macrophylla*, a hybrid between citron and pummelo) (Sun et al., 2004, Saunt, 2000). The association with symptoms on only certain hosts, and a differential physiological and genetic profile in the isolates compared to the common Xc-A, allowed the researchers to postulate that the group of strains isolated in Wellington were different from all the other previously isolated strains, and for those reasons were designated Xc-Aw (Sun et al., 2004).

In 2002, Cubero and Graham analyzed different citrus pathogenic xanthomonads using molecular techniques such as rep-PCR with ERIC and BOX primers developed by Louws et al.,(1995), and sequence comparison of ribosomal (16S, 23S) fragments, internal transcriber sequence (ITS) regions, and *pthA* gene sequences. Based on the amplified fragments, diverse dendrograms were made to show the relationships among

the strains. The rep-PCR comparisons revealed similarities between the Xc-A, Xc-A*, and Xc-Aw strains and differences with Xfa-B and Xfa-C strains which were located in different clusters. The analysis showed a higher degree of similarity between the strains of Xc-A* and Xc-Aw than with typical Xc-A strains isolated from around the world (Cubero & Graham, 2002).

In a review by Brunings & Gabriel (2003), they discuss the two phylogenetic groups, the Asian group consisting of strains belonging to Xc (strains A, A* and Aw) and the South American group composed of strains B and C (which were classified as *X. a. pv. aurantifolii*). Due to the similarity of elicited symptoms, they assume that strains from both groups possess similar pathogenetic mechanisms, and in an attempt to determine the specific host range of each strain, they indicated that the Xc-Aw strains had a *pthAw* gene (Brunings & Gabriel, 2003).

Sun et al. (2004) made a comparison of several Xc-A strains, its variants (Xc-Aw and Xc-A*), Xfa-B strains, and a *X. axonopodis* pv *citrumelo* strain. They performed serological and molecular characterizations using ELISA, PCR, fatty acids analysis, pulsed-field gel electrophoresis (PFGE) of genomic DNA, and Biolog® differentiation, which confirmed the similarities between the Xc-A strains, and more closely between Xc-A* and Xc-Aw strains. Also, based on the PFGE patterns obtained by digestion of total genomic DNA with restriction enzymes *Xba I* and *Spe I*, a dendrogram was created which separated the Xfa-B strain from the others strains. In a DNA-DNA hybridization test the A strains including Xc-A, Xc-A*, and Xc-Aw strongly hybridized, but weakly hybridized with Xfa-B and *X. axonopodis* pv *citrumelo* (Sun et al., 2004).

***X. fuscans* pv. *aurantifolia* type B and C strains**

The strains identified as citrus canker type B, were isolated in South America between the years 1929-1990, and were less aggressive than the A type strains, which were not introduced into the region until the 1970s (Canteros, 1984). As a first attempt of classification, Fawcett & Bitancourt (1937) postulated that two types of cankers existed and designated type A to be the most aggressive and common type and type B for those identified in Argentina and Paraguay that were less pathogenic. This designation for these strains has been broadly accepted, but was based only on field observations, and it was never based on the characterization of isolates of any of these two types of cankers.

Goto et al. (1980) characterized different strains of group A and B, isolated in Japan and Entre Rios (Argentina), respectively. The comparison of strains was based on symptom development, physiological tests, serological properties, and differential phage susceptibility. The characterization supported the separation of the strains into groups that correlated with field observations, specifically differences in aggressiveness. Goto et al. (1980) suggested that the strains that produced the less aggressive citrus canker B should be referred to as a different pathovar than *citri*. Also, these authors reported that *X. citri* f. sp. *aurantifolia* (type C, recently discovered in those years) had pathological, physiological and serological characteristics that differed from the A and B types. This variant was presented as highly virulent (aggressive) in Key lime, slightly pathogenic in Tahiti lime, and avirulent (non-pathogenic) in other citrus (Goto et al., 1980).

In 1979, Stall et al. (1979) experimentally described difficulties in growing citrus canker type B strains on nutrient agar media. In 1985, Canteros & Zagory (1985)

developed a specific culture medium that facilitated the isolation and culture of type B strains. That medium allowed the growth of all A and B type strains and facilitated subsequent characterization. These authors found that group A strains, that grew on King B medium, nutrient agar, SMB, Wakimoto and Emerson's media, differed from group B strains which could only be grown on SMB media (sucrose, peptone, dipotassium phosphate, magnesium sulfate, and Difco purified agar) (Canteros de Echenique et al., 1985).

According to Canteros (2005), when the A strain epidemic spread from Brazil to Argentina, the endemic B strains were displaced. The isolation of B strains was complicated because this bacterium did not grow on simple media such as nutrient agar (like the A strains); for this reason few strains were preserved (Stall et al., 1979, Canteros de Echenique et al., 1985). However, Xfa-B is still considered a quarantine hazard. A possible explanation for why the type B strains disappeared from the field after the introgression of the Xc-A strain was shown in an *in vitro* experiment in 2011 (Canteros et al., 2011) in which Xfa-B strains were inhibited on media by Xc-A strains. The compound produced by Xc-A that was inhibitory to B strains has not been determined.

The group C strains were isolated and described first in Brazil based on serological characterization (Namekata and Oliveira, 1971). It was proposed initially to designate these strains as *Xanthomonas citri* forma especialis *aurantifoliae* (Oliveira & Namekata 1971) due to their ability to infect only Key lime (Namekata and Oliveira, 1971). In recent years, there have been several other pathogenic studies of

xanthomonads strains isolated from South America which exhibit a differential pathogenicity response compared to typical Xc-A strains (Jaciani et al., 2009, Chiesa et al., 2013).

In 1989 Gabriel et al. (1989) suggested the reinstatement of the species *X. citri* for the strains of type A group, and suggested the name of *X. campestris* pv *aurantifolii* for the strains that produce citrus canker type B and C. This was the first mention of the name *X. campestris* pv. *aurantifolii* that includes both types B and C strains. The proposal was based primarily on the results obtained by comparing restriction fragment length polymorphism (RFLP), which is based on determining fragments of genomic DNA of the bacteria cut by restriction enzymes, and hybridized with specific DNA probes from *X. c.* pv. *malvacearum* and *X. c.* pv. *citrumelo*. After the analysis of the bands, they determined that the citrus pathogenic strains could be differentiated into two groups, the first one corresponding to the type A strains (*X. citri*), and the second cluster to the type B and C strains (*X. c.* pv. *aurantifolii*). Subsequent reviews found no sufficient basis for this proposed name change, because the methodology used by the authors (RFLP) was considered inappropriate (Young et al., 1991; Vauterin et al., 1991).

In 2004, Graham et al. (2004) published a review concerning the factors that affected eradication of the citrus canker disease causal organism. In that work, type B and C strains were both designated for the first time as *X. axonopodis* pv. *aurantifolii* based on the taxonomic designation for the Xfa-B and Xfa-C strains proposed by Schaad et al. (2005).

Characterization of the Interaction between *Xanthomonas* and Citrus Hosts

Resistance to citrus canker is a quantitative character. It has been determined in commercial varieties under a natural infection range of susceptibility/resistance from: very susceptible (grapefruits, Key lime), to very resistant like the mandarin species Ponkan and Okitsu (*C. reticulata*, and *C. unshiu*) (Civerolo, 1984, Leite Jr, 2000, Das et al., 2009, Stall et al., 1981). Some biotechnological efforts have been attempted to increase the natural resistance to canker in citrus through induced mutations, hybridization (Deng et al., 1992), and transgenes using constitutive expression of antibodies which recognize the bacterium *in planta* (Chandrika & Gabriel, 2003). Regardless of these strategies, little progress has been made using any of the methodologies.

The characterization of the hypersensitive response (HR) is essential for its subsequent use as a tool in breeding programs (Hibberd et al., 1987a). The underlying specificity of this defense reaction is primarily due to the recognition of the pathogen by the host (Klement & Goodman, 1967). This recognition produced by the interaction of an inducer (or elicitor) of the pathogen and a host recognition factor (Bonas et al., 1991, Wei et al., 1992) triggers a series of processes that determine the life or death fate of the invaded cell, with the consequent death of the pathogen. Both components involved in this recognition, are produced by genes termed avirulence genes (avr genes) in the pathogen and resistance genes (R genes) in the host (Staskawicz et al., 1984, Willis et al., 1991). In 2009, the gene *avrGf1* was identified in Xc-Aw (DPI strain12879), as the avirulence gene, which elicits an HR in grapefruit leaves (Rybak et al., 2009). The authors provided the first conclusive evidence that this gene specifically induces an HR in citrus.

The divergence observed in the type III effectors (T3Es) of strains Xc-A, Xc-Aw, Xfa-B and Xfa-C is an example of host-bacterial adaptation based on the existence of different effector repertoires. In the case of Xc-Aw, the presence of a single gene (*avrGf1*) excludes the bacterium from a range of other citrus species, except KL, (Rybak et al., 2009), This was demonstrated experimentally by elimination of the *avr* gene, which produces a mutant strain Xc-Aw Δ *avrGf1* less pathogenic than Xc-A strains (Rybak et al., 2009, Jalan et al., 2012). This observed reduction in virulence of strain Xc-Aw 12879 revealed the specialization of the bacterium compared with Xc-A306. Similarly, inactivation of the host limiting factor (an *avr* gene which elicits HR) allows the pathogen to interact again with a wide spectrum of possible hosts (Bogdanove et al., 2010), and enhances the selection of new variability (Kirchner & Roy, 2002), and/or the exchange of new pathogenic elements with other bacteria (Barash & Manulis-Sasson, 2009).

In recent years, a close relationship between bacterial effectors and cyclophilins was uncovered (Coaker et al., 2005, Aumüller et al., 2010). In 2006, Coaker, *et al.* (2006) demonstrated that a single mutation of a cyclophilin binding site (GPxL motif), present in *Pseudomonas* effector *avrRpt2*, blocked protease activity *in vitro*. In 2009, Block, *et al.* (2009) revealed that another T3E, *HopG1* from *P. syringae*, a member of the XopAG effector class, also has this putative cyclophilin binding site (GPxL motif), and suppresses pathogen-associated molecular pattern (PAMP)-triggered immunity (PTI). Interestingly, previous work (Jamir et al., 2004) also demonstrated that this T3E (*HopPtoG*, from *P. syringae* DC3000) suppresses HR elicitation in tobacco; specifically

mediating suppression of *PR1a* gene. The analysis of this specific host-pathogen interaction mediated by single effectors present in the pathogen strains Xc-Aw and Xfa-C will help in understanding the phenomenon of resistance to xanthomonads associated with citrus canker, and provide effective and durable sources of resistance for new biotechnological approaches.

Characterization of Xanthomonads Pathogenomes Associated with citrus canker

The major landmark in characterization of Xc-A was the complete genome sequencing of the strain Xc-A306, in 2002 (da Silva et al., 2002). The genome of this strain consists of a 5.27 megabase pairs (Mbp) chromosome encoding approximately 4500 genes, and two plasmids, pXAC64 and pXAC33, which are 64.9 and 33.7Mbp, respectively (da Silva et al., 2002). Some of the most interesting features discovered in the Xc-A genome were the large number of cell wall degrading enzymes, proteases, iron receptors, genes related to energy metabolism pathways, type II and type III secretion systems, genes for the flagella structural units, and chemotactic protein genes (*tsr*), as well the xanthomonadin (*pig* genes) and xanthan gum synthesis gene cluster (*gumB* to *gumM*), which are important in the epiphytic phase of the life cycle (Dunger et al., 2007). There are genes for biofilm production that result in formation of bacterial aggregates in the apoplast and which define the proliferation of the bacterium and symptom development (Rigano et al., 2007).

Strain Xfa-B69 (NC_005240.1) has a 37 mpb self-transmissible plasmid designated pXcB by Brunings et al (2001). This plasmid pXcB shares similar characteristics with pXAC64 (present in Xc-A 306). Both plasmids, pXcB and pXAC64, contain a cluster of *vir* genes, and type IV secretion system (T4SS) necessary for

production of the conjugation machinery. According to Bruning & Gabriel (2003), the pXcB also has a homolog gene of pthA4, which was designated *pthB* (Brunings & Gabriel, 2003, El Yacoubi et al., 2007). These authors hypothesized that in the past, Xc-A could have transferred its pXAC64 by conjugation, through its T4SS, to a citrus non-pathogenic *Xanthomonas* strain (in this case *X. fuscans*). This idea could explain the appearance of a new pathovar of citrus pathogenic xanthomonad (the proposed *Xf* pv. *aurantifolii*); however, it is only an hypothesis, which needs to be tested experimentally.

After finalizing the sequencing of Xc-A306 genome, the São Paulo State Science Foundation (FAPESP) and FAPESP Genome Program also sequenced two other strains that cause citrus canker: *X. fuscans* pv. *aurantifolii* groups B (strain B69), and C (strain Xc70) (Moreira et al., 2010b). Comparison of the sequenced draft genomes with Xc-A306 focused on several aspects: effector composition (type III effectors, and type IV proteins), genes that allow biofilm formation, quorum sensing and sugar acquisition, flagellum gene organization, and lipopolysaccharides (LPS) synthesis. In general terms the Xfa-B strain genome had more similarities with the Xc-A306 genome (87%) than with Xfa- C genome (84%). The Xfa-B strain genome contains more known T3Es than Xfa-C strain, and some T3Es were common to Xc-A and Xfa-B, but not to Xfa-C. Also a few T3Es were present only in Xfa-C, an indication of divergence in the pathogenic mechanisms developed for each strain. Compared to the reference strain Xc-A306, the plasmid composition for Xfa-B and Xfa-C strains indicated that both strains share 46% of the sequence present in plasmid pXAC33, and also that Xfa-B strain shares 61% of pXAC64 sequence, while the Xfa-C strain shares 55%.

Through a comparative genomic analysis of strains Xc-A306 and Xc-Aw12879, Jalan et al. (2013b) indicated that besides *xopAG-avrGf1* that contributed to the host range specificity in Xc-Aw, other effectors present in Xac-Aw, like *xopAF* (which is also present in Xfa-B and Xfa-C) also contributes to the virulence of Xc-Aw. Although the complete genome of strain Xc-Aw12879 shows a close relationship with the Xc-A306 strain, numerous inversions and translocations between both chromosomes were found. Also Xc-Aw contains two unique plasmids: pXacw19, which does not share similarities with Xc-A306 plasmids, and pXacw58, which encodes two TAL effector genes designated *pthAw1* and *pthAw2*.

In 2010, several Xc-A, Xc-A*, and Xc-Aw strains, and also *X. citri* pv. *bilvae* strains, which cause citrus canker symptoms in KL (Patel et al., 1953), were characterized by amplified fragment length polymorphism (AFLP) and multilocus sequence analysis (MLSA) based on four partial housekeeping gene sequences (*atpD*, *dnaK*, *efp* and *gyrB*). Based on the high chromosomal sequence homology among the strains, the authors suggest the new designation, *X. c.* pv. *bilvae*, which is now considered a synonym of Xc-A* strains. The authors demonstrated a close genetic relationship between Xc-Aw and Xc-A* strains, which were identified as a highly variable subgroup of Xc-A strains (Ngoc et al., 2010).

Recently, a complete genome comparison (pan-genome analysis) of 25 sequenced strains of Xc-A, Xc-Aw and Xc-A* revealed a conserved core with 85% sequence similarity among the genomes of these three groups of strains. Most of the

variation between groups was observed between Xc-Aw and Xc-A* vs typical Xc-A strains. The variation was associated principally with chromosome deletions, transposition events, and plasmid insertions (Jalan et al., 2013a).

In an attempt to determine which factors determine the differential host pathogenicity in Xc-A* strains, Escalon et al. (2013), used a molecular database generated by an AFLP analysis from 55 Xc-A strains previously characterized by Bui et al. (2009). In this work, they identified 66 T3Es, where 28 were common in all Xc-A, Xc-A*, and Xc-Aw strains. Two of the effectors, XopAG and XopC1, appeared limited to Xc-A* and Xc-Aw strains. Interestingly, the T3E XopAG-*avrGf1*, was present in all the Xc-Aw strains tested, and also in all the Xc-A* strains that were pathogenic only in KL, while XopC1 was present only in 4 of the Xc-A* strains that exhibited a limited host range. The effector XopC1 did not elicit HR, and after the deletion of the effector XopC1, the pathogenicity of the strain Xc-A* Δ XopC1 was not affected. Except for the presence of the *avrGf1* gene, it was not possible to strictly correlate the presence of a specific combination of T3Es with the variable pathogenicity results registered for each Xc-A* strain. Compared with Xc-A and Xc-Aw strains, Xc-A* was the most diverse group. The presence of Xc-A* homologous T3Es in *X. c. pv. bilvae* suggest a fluid horizontal genetic exchange between different *Xanthomonas* species (Escalon et al., 2013).

Control Methods of Plant Pathogenic CuR Strains

Copper is a potent bactericide that works by damaging bacterial membranes and proteins (Cooksey, 1990a). In bacteria, the membrane proteins and membrane lipids constitute the major targets of free copper ions, which are able to oxidize sulfhydryl

groups (i. e. cysteine), causing inactivation of the proteins by damaging Fe-S clusters in cytoplasmic hydratases (Santo et al., 2011).

Following the emergence of bacterial spot of tomato in the US (1922), the first method of chemical control was copper sprays, and later, antibiotics. For a short period reliance on streptomycin as a control strategy reduced the need for copper bactericides. The advent and spread of streptomycin resistant *X. vesicatoria* strains in tomato and pepper Florida fields forced growers to rely heavily on Cu compounds and Cu mixtures of various formulations (Stall, 1964). The mixture of Cu and ethylene bis dithiocarbamates provides a better control of bacterial spot in the field than copper alone (Conover & Gerhold, 1981). The combination was more effective for control of *X. vesicatoria* CuR strains than copper alone. Dithiocarbamates (specifically mancozeb) must be added to any Cu bactericide at the time of spray application (Marco & Stall, 1983).

Ethylene bis dithiocarbamates have been commonly used as fungicides for almost 50 years (Gullino et al., 2010). Currently, it is not entirely clear how the combination of Cu and mancozeb kills CuR resistant strains of the bacterium. Initially, it was considered that the combination of copper and ethylene bis dithiocarbamates resulted in release of more Cu⁺⁺ ions into the suspension (Uden & Bigley, 1977), and this was responsible for killing CuR bacteria strains (Parsons & Edgington, 1981). In another study, there was no significant difference in the concentration of Cu⁺⁺ in mixtures of Cu and Mancozeb compared to copper alone on the surface of tomato leaflets (Jones et al., 1991), suggesting that the synergistic antibacterial effect observed

is not the result of increased ionic copper as a result of combining copper with ethylene bis dithiocarbamates (Jones et al., 1992).

Most of the control strategies for citrus canker were developed in Argentina in the late 1970s (Rodriguez, 2012). After the failure of an eradication program that destroyed almost 50% of the citrus in the northeast region of this country, a collaboration between the National Institute of Agricultural Technology (INTA-Argentina), the Institute of Food and Agricultural Sciences of the University of Florida (IFAS-UF), and the Department of Plant Industry of Florida (DPI) was initiated to study integrated control management of the disease, based on the use of windbreaks, sprays and timing of different copper compounds to protect young fruit and leaves, and the use of resistant citrus species like Satsuma mandarins (Rodriguez, 2012, Stall et al., 1979), selective pruning, and certification of free disease nurseries, (Canteros, 1984). Currently, the control of citrus canker worldwide is based on the application of copper sprays along with the use of windbreaks in the groves (Muraro et al., 2000, Behlau et al., 2010).

In 1983 Stall and Marcó (1983) determined that *X. vesicatoria* CuR strains were present in Florida. This was the first report of CuR in plant pathogenic bacteria. In that work, a collection of *X. vesicatoria* strains sampled since 1960 from different Florida locations were tested for viability in suspensions of copper compounds. It was also demonstrated that some strains isolated in 1968 were CuR (Marco & Stall, 1983). In 1986, it was confirmed that a conjugative plasmid of nearly 200 Kb (pXvCu) was responsible for the CuR phenotype in *X. euvesicatoria* (Stall et al., 1986). Following the report of widespread distribution of *X. vesicatoria* CuR strains in Florida fields

(Pohronezny et al., 1992), more recently CuR strains of *X. perforans* have also been identified as the predominant population in Florida (Horvath et al., 2012). In 1989, Canteros et al. (1989) identified *X. vesicatoria* (Race 1) CuR strains isolated in 1987 from bacterial spot symptoms in plants of tomato in Bella Vista, Argentina (Canteros, 1990). In 1994, Canteros isolated the first CuR strain of Xc-A in fruit and leaf lesions from lemons grown in Bella Vista (Canteros, 1996). Currently, only the Northeastern region of Argentina contains CuR strains of Xc-A (Canteros et al., 2013). In 2000, CuR strains of *X. alfalfae* subsp. *citrumelonis* (Xcm), which produce citrus bacterial spot, were isolated from citrus nurseries in Florida. The CuR in the Xcm strains was mediated by a conjugative plasmid of approx. 200 Kbp, and the comparison with the copper resistance determinants from *X. citri*, *S. maltophilia*, and *X. vesicatoria* revealed high sequence homology (92%) (Behlau et al., 2011).

In 1985 CuR strains of *Pseudomonas syringae* pv. *tomato* (*Ps tomato*) were reported in California (Bender & Cooksey, 1985). The different CuR strains isolated in the early 1980's were associated with variable plasmid profiles. Only the plasmid pPT23A (100 Kbp) and pPT23C (60 Kbp) were responsible for the CuR phenotype (Bender & Cooksey, 1986). Later Cooksey et al. (Cooksey et al., 1990) characterized CuR strains of *X. vesicatoria* strains which had plasmids of 100 kb (pXV10A), and *P. syringae* from Impatiens which have a 35 Kbp plasmid (pPSI1) (Cooksey, 1990b).

Two general types of CuR plasmids have been described in Gram-negative bacteria. One of them is represented by large CuR plasmids (approx 200 Kbp in size), which have been found in *X. citri*, *X. perforans* and *X. vesicatoria*. The other is comprised

of a group of smaller CuR plasmids, such as the ones identified in *Pseudomonas* and also in some *Xanthomonas* strains (from 35 to 100 Kbp) (Sundin et al., 1989, Cooksey, 1990a, Stall et al., 1986, Canteros, 1996). The CuR plasmids of *X. citri*, *X. perforans*, and *X. vesicatoria* are transmissible between bacterial strains within the same species and within the same genus. The size of the megaplasmids are variable, albeit at values close to 200 kb (Canteros, 1990). The megaplasmids that mediate CuR in *X. citri* and *X. vesicatoria* share sequence homology with the *cop* genes from *Pseudomonas* species. This homology was demonstrated by hybridization experiments with DNA probes based on sequence analysis of the *P. tomato* CuR plasmid and may indicate a common origin for all sizes of plasmids (Canteros et al., 2004).

An exception to CuR genes harbored on a plasmid was found first in *X. a. pv juglandis*, which has a chromosomal locus that mediates the CuR. The characterization of the 4.9 Kbp CuR loci shows a 20 Kbp chromosomal region with high sequence identity with the *Ps tomato* CuR plasmid (35 Kbp). This suggests a plasmid integration event may have occurred (Lee et al., 1994).

Another example of chromosomal CuR genes in plant pathogenic bacteria comes from Xv-P26, isolated from pepper in Taiwan (Basim et al., 1999). This strain contains a 7.6 Kbp chromosomal locus with genes that show homology with the regulatory *cop* genes from *Ps tomato*, but also two other genes that have homology with cation efflux system membrane proteins. The molecular characterization of several *X. vesicatoria* strains from the same region shows that no other strains possess these loci, so it was

postulated that Xv-P26 is a rare event of conjugation with a CuR bacterium from the environment, with subsequent chromosomal integration.

The acquisition and integration of CuR genes are reported from environments with high selective pressures. In heavy metal contaminated soils from the north of China, a CuR inhabitant was isolated and designated *Xanthomonas* strain IG-8, and possess a 9.2 Kbp locus, acquired by horizontal gene transfer and integrated into the chromosome. This locus contains the Cu-inducible *xmeRSA* cluster that encodes for an unspecific efflux pump that prevents sensitivity to several heavy metals such as Cu, Zinc, Cobalt, and Arsenic, and also antibiotics. Based on the comparison of the genes present at this locus, and the codon usage pattern observed in the genes surrounding the *xmeRSA* genes, indicate a possible origin from *X campestris*; although the resistance genes present high sequence identity with the *SmeABC* operon, characterized previously in *Stenotrophomonas maltophilia* (Ryan et al., 2007).

Activation and Function of the CuR Operon

Copper is an essential element used by bacteria in numerous metalloprotein structures, such as the Type 1, 2 and 3 “blue” copper-center proteins described respectively in plastocyanins, multi-copper oxidases, and tyrosinases (Fee, 1975). The first genetic element that mediated the CuR (a plasmid) was isolated from *E. coli* in 1985 (pRJ1004). The first CuR plasmid from *P. syringae* pv *tomato* was determined in 1986 (pPT23); its CuR genes were cloned in 1987 by Bender & Cooksey, and the genes *copABCD* were identified as an operon and sequenced in 1988 by Mellano & Cooksey (Cervantes & Gutierrez-Corona, 1994).

The CuR genes from *P. syringae* pv *tomato* were localized to a 4.5 kb region of the plasmid pPT23 which contains the *copABCD* operon. The *cop* operon is adjacent to and oriented in the same direction as CuR *pco* (plasmid copper) operon from *E. coli*; furthermore, it shows sequence homology via DNA hybridization experiments with the *cop* operon in several species of plant pathogenic bacteria (*Pseudomonas* and *Xanthomonas*), as well saprophytic bacteria (Cooksey et al., 1990).

The first CuR gene characterized in the *cop* operon was *copA* from *P. syringae* pv. *tomato*. The *copA* gene is inducible in the presence of Cu, and its presence was confirmed in several other CuR bacterial species (Voloudakis et al., 1993). The CopA protein has homology with the multicopper oxidase type I blue copper family, and is expressed in the bacterial periplasm; it has the capacity to bind up to 11 Cu molecules. Other proteins encoded at the *copABCD* operon are: CopB, an outer membrane protein, CopC, another periplasmic protein, and CopD, a protein associated with the inner membrane (Cervantes & Gutierrez-Corona, 1994).

In *Pseudomonas* the presence of *copA* alone was observed to provide some degree of CuR to the bacterium. The presence of *copAB* provides resistance to higher concentrations of Cu. The presence of *copCD* genes is required for complete resistance (Cervantes & Gutierrez-Corona, 1994). In *Pseudomonas*, strains which carried *copCD* accumulated 40% more Cu in the inner membrane than strains that did not have these genes, suggesting a participation of CopCD in Cu uptake (Cha & Cooksey, 1993).

There are variations between the mechanisms of activation of the *cop* operon. The *copABCD* operon in CuR *P. syringae* strains is induced specifically by a two component (*copRS*) system located at the end of the *copABCD* operon (*copABCERS*).

This induction system is similar in *E. coli* through *pcoRS* (Mills et al., 1993, Voloudakis et al., 1993), but is not similar in *X. vesicatoria*, where the gene *copL*, located upstream of *copA*, is constitutively expressed. The CopL protein, acts as a sensor of the Cu ion level in bacteria; in high concentrations of Cu, CopL induces the expression of *copA* and consequently the other *cop* genes (Rademacher & Masepohl, 2012).

A different arrangement and composition of the CuR genes was characterized in Xc-A44 (*copLABMGCDF*), and Xcm-1381 (*copLABMGF*). For both CuR operons, highly conserved nucleotide sequences ($\geq 92\%$) were identified in *Stenotrophomonas maltophilia* K279a and Xv-7882. New Cop proteins were annotated from Xc-A44 and Xcm-1381 CuR operons: CopM, a cytochrome c oxidase involved in electron transport, CopG a hypothetical export protein, CopC and CopD, transmembrane transporter proteins, and CopF, a putative copper-transporting p-type ATPase (Behlau et al., 2011).

Project Goal and Objectives

The goals of this project were i) to characterize the *avrGf2* from Xfa type C that induces HR in citrus, ii) to determine the importance of conserved domains shared in the XopAG effector family, and iii) to characterize sequence rearrangements in the chromosome and plasmids of copper resistant strain Xc-A44.

CHAPTER 2

IDENTIFICATION AND CHARACTERIZATION OF THE GENE *avrGf2* PRESENT IN *Xanthomonas fuscans* pv. *aurantifolii* TYPE C.

Introduction

Citrus canker is one of the most important bacterial diseases of citrus. The disease is caused by two species, *Xanthomonas citri* (Xc), which is associated with Asiatic Citrus canker and designated A-group strains (Xc-A) (Ah-You et al., 2009), and *X. fuscans* pv. *aurantifolii* (Xfa) (Schaad et al., 2006), which consists of B-group strains (Xfa-B) and C-group strains (Xfa-C) group strains. The Xfa-B group is less virulent than Xc-A group but produces symptoms in all citrus species. The B-type canker was reported for the first time in Argentina in 1929, was observed mainly on lemon (*C. limon*), but has not been found again in the field after 1991.

The C-type canker, initially designated as *X. citri* f. sp. *aurantifoliae* (Namekata & Oliveira, 1972), was isolated only from Key lime (KL, *C. aurantifolia*) in Sao Paulo State, Brazil. The Xfa-C strains elicit a hypersensitive reaction (HR) in grapefruit (GF, *C. paradisi*) leaves (Stall et al., 1981), and do not produce symptoms in other citrus hosts with the exception of KL. In 1999, a variant of Xfa-C, which produces a brown pigment in solid media, emerged in Sao Paulo State. According Nociti et al. (2006) the aggressiveness of the brown Xfa-C strains in KL is higher compared with the Xfa-C strains that do not produce the brown pigment.

Although an HR by Xfa-C strains was reported 30 years ago, the HR was only characterized recently by conducting population dynamics and electrolyte leakage assays in GF and KL that are used to confirm HR (Gochez et al., 2008). Moreira, et al. (2010) sequenced the genomes of Xfa-B and Xfa-C strains, and made a comparison of

type III effector (T3E) repertoires of these two strains and Xc-A. Their analysis showed that some putative effector classes are shared or absent. Of particular interest was one type III effector, XopAG, which appeared to be functional in Xfa-C, but contained a transposon insertion in Xfa-B that potentially rendered this effector non-functional.

Following the initial reference of an HR in grapefruit induced by C-type strains (Stall et al., 1981), a second type of HR in citrus was found to be associated with Xc-Aw strains isolated in Southeastern Florida (Rybak, 2005). In 2009, *avrGf1*, from Xc-Aw 12879 strain (Rybak et al., 2009), was characterized, and shown to be responsible for eliciting an HR in GF leaves. The authors provided the first conclusive evidence that this gene specifically induces an HR in GF. In 2013, the analysis of the genome of strain Xc-Aw 12879 showed that the gene *XopAG-avrGf1* is located on the chromosome (Jalan et al., 2013b).

Additional variation in Xc-A strains was identified in Southwest Asia based on differential pathogenicity responses in Citrus and Poncirus species. These strains were designated as Xc-A*, because some of the strains induced a resistance reaction in GF (Verniere et al. 1998). The resistance reaction caused in GF by an Xc-A* strain (Xc-A* 1974) was compared with the HR caused for strain Xc-Aw 12879 by Rybak et al. (2009). This comparison revealed that each strain (Xc-A* and Xc-Aw) induces a different type of HR in GF (Rybak et al., 2009). The genetic characterization of the Xc-A* strains revealed some similarity with typical Xc-A strains (Mohamadi et al. 2001; Graham et al. 2004), and its origin in Southwest Asia was presumed to result from illegal entries of infected plant material from India (Schubert et al. 2001, Li et al. 2005).

Furthermore some of these strains were also determined to contain the *avrGf1* gene, which shows high sequence homology with the *avr* gene described in Xc-Aw strains (Ngoc et al. 2009).

The objective of this work was to characterize the gene *avrGf2* from Xfa type C that induces an HR in GF, compare this gene with *avrGf1* that elicits HR in citrus except KL, and screen for the presence of this gene, or possibly related genes in other strains that induce an HR in Citrus.

Material and Methods

Bacterial Strains and Media

Strains utilized in this work are listed in Table 2-1. Strains of Xfa (B and C) and Xc-Aw were stored in sterile tap-water and were cultured on nutrient agar (NA) medium. Rifampicin resistant strains were obtained by plating 10^9 colony-forming-units (CFU)/ml, of a bacterial suspension from a 24 h culture, on NA containing 50 µg/ml of rifampicin and selecting rifampicin resistant colonies. *Escherichia coli* (Ec) strains were maintained on Luria-Bertani (LB) medium (Sambrook et al., 1989), suspended in nutrient broth (Difco™) containing 30% glycerol, and stored in a -80°C freezer. Conjugations were performed on nutrient yeast glycerol agar (NYGA) (Daniels et al., 1984). The media were amended, when necessary, with antibiotics at the following concentrations: rifampicin, 50 µg/ml; tetracycline, 10 µg/ml; and kanamycin, 40 µg/ml.

Growth of Plants and Inoculum Preparation

Citrus plants, Duncan GF, KL, Valencia orange, and Eureka lemon, were grown in steamed peat-vermiculite mix in 20 cm (diameter) pots in a greenhouse at 20-35°C. Plants were regularly fertilized with a slow-release fertilizer (Osmocote®).

Bacterial strains for plant inoculations were grown on nutrient agar for 18 h at 28°C. The bacterial suspension was adjusted to an optical density (O.D.) 600 nm = 0.3 (2–5×10⁸ colony-forming unit (CFU) per ml) with a spectrophotometer (Spectronic 20). For population dynamics studies bacterial suspensions were diluted to 5×10⁵ CFU/ml in sterile tap water.

Bacterial Growth Curves and Electrolyte leakage Experiments

Bacterial multiplication in leaves was determined following infiltration of a bacterial suspension adjusted to 5×10⁵ CFU/ml into the mesophyll with a syringe. Infiltrated areas were sampled at regular intervals, by determining colony counts on solid media after serial dilution (Stall & Cook, 1966, Hibberd et al., 1987b). Plant shoots with leaves of approximately the same age were marked and individual leaves were infiltrated with bacterial suspensions of a strain using a hypodermic syringe and needle as previously described (Hibberd et al., 1987a). The bacterial populations were determined over a 14-day period in both KL and GF. Every 48 h three disks of 0.5 cm² from infiltrated areas of leaves were sampled. Each disk was crushed separately in 0.5 ml of sterilized tap-water, serial dilutions were performed and dilutions were plated on NA to determine bacterial populations per cm² of infiltrated leaf tissue. Plants were maintained in a growth room at 28°C.

Electrolyte leakage was measured as conductivity in infiltrated plant tissue (Cook & Stall, 1968, Hibberd et al., 1987b). Only leaves that remained attached to the plant were collected for the analysis. Six leaf disks that measured 0.5 cm² each were placed in 3 ml of distilled water to measure conductivity. Three replicates per treatment were used, each replicate in different leaves of the same plant. Plants were maintained in a growth chamber at 28°C.

Molecular Techniques

Techniques used for cosmid cloning, enzyme digestion, ligation, map construction, subcloning, plasmid purification, and agarose gel electrophoresis were essentially as described by Sambrook et al. (1989). The genomic library of Xfa-C was constructed in the vector pLAFR3 (Ditta et al., 1980, Friedman et al., 1982, Staskawicz et al., 1984, Staskawicz et al., 1987), following digestion with the restriction enzyme *Sau3* (New England BioLabs Inc.), and individual clones were maintained in *E. coli* DH5 α (BRL).

Primers were synthesized by Sigma-Aldrich (Sigma-Aldrich Co., St. Louis, MO). Amplification of target genes from all bacteria was performed using a DNA thermal cycler (Bio-Rad-MyCyclerTM) and a Taq polymerase kit (Promega, Madison, WI). For extraction of template DNA, strains were individually grown overnight on NA, suspended in sterile deionized water (DI), boiled for 20 min, cooled on ice for 5 min, shaken thoroughly using a vortex mixer (Genie2), centrifuged at 15,000 rpm for 5 min and kept on ice prior to use of the supernatant in the PCR reaction mixture. Each PCR reaction mixture, prepared in 25 μ L total volume, consisted of 11.4 μ L of sterile water, 5 μ L of 5 \times PCR buffer, 1.5 μ L of 25 mM MgCl₂, 4 μ L deoxyribonucleoside triphosphates (0.8 mM each dATP, dTTP, dGTP, and dCTP), 0.5 μ L of each primer (stock concentration, 25 pmol μ L⁻¹), 2 μ L of template, and 0.2 μ L (5 U/ μ l) of Taq DNA polymerase. PCR reactions were initially incubated at 95°C for 5 min. This was followed by 30 PCR cycles which were run under the following conditions: denaturation at 95°C for 30 s, primer annealing for 30 s at 5°C below the minimum primer T_m calculated based on the following formula: $T_m = [81.5 + (41 * (\%GC/100)) - 21.6 - (500 / (\text{length}))]$, and DNA extension at 72°C for 45 s in each cycle. After the last cycle, PCR tubes were incubated for 10 min

at 72°C and then at 4°C. In every reaction, positive controls were included depending on the set of primers. PCR reaction mixtures were analyzed by 1% agarose gel electrophoresis (Bio-Rad Laboratories, Hercules, CA) with Tris-acetate-EDTA (TAE) buffer system. A λ -*EcoRI-HindIII* DNA marker (Promega, Madison, WI) was used as the standard molecular size marker for PCR product sizing. Reaction products were visualized by staining the gel with ethidium bromide (0.5 μ g mL⁻¹) for 20 min and then photographed using a UV transilluminator and Quantity One software (Bio-Rad Universal Hood II, Hercules, CA).

Southern hybridization experiments were performed on positively charged Nylon membranes and the DIG-High Prime DNA Labeling and detection kit, according to the manufacturer's instructions (Roche). Genomic DNA extractions were made using CTAB- DNA isolation method (Sambrook et al., 1989). The isolated DNA preparations were restriction digested with *EcoRI* endonuclease (Promega). The digested DNA was electrophoresed in 0.7% agarose gel, using as a size reference marker DIG labeled 0.12-21.2 Kbp DNA Molecular Weight Marker III (Roche).

Sequence Comparison of Gene *avrGf2* and Phylogenetic Approach

The nucleotide and amino acid sequences of avirulence genes *avrGf1* and *avrGf2*, and other members of the xopAG effector family were recovered from the online database <http://www.xanthomonas.org/t3e.html> and also from Genbank using BLASTX. The sequences were aligned by Clustal Ω , and compared in a phylogenetic analysis using Mega 5 software.

Results

Identification of AvrGf2 in Xfa-C as an Elicitor of HR in Grapefruit

To determine the gene or genes responsible for the Xfa-C HR elicitation in GF, a cosmid library from the Xfa-C strain was mobilized into the Xc-A306 strain by triparental mating and screened in GF for HR. One clone (pL351), converted the normally pathogenic strain Xc-A306 to avirulence on GF. The insert DNA of pL351 was digested with EcoRI and religated in pLAFR3, and the resulting clones were mobilized into Xc-A306. The recombinant plasmid p351-88-1 carrying an insert of 4402 bp exhibited HR activity. Further sequencing of the subclone pL351-88-1 and analysis using ORF Finder (<http://www.ncbi.nlm.nih.gov/gorf/gorf.html>) and tBLASTn, identified a 1527 bp open reading frame encoding a predicted product having 45% amino acid identity with XopAG-AvrGf1. The gene was designated *avrGf2* based on its Pfam domain homology with XopAG-AvrGf1.

An in-frame deletion construct of the *avrGf2* coding region in the vector pGEMT-Easy with a 2934 bp *EcoRI* fragment from library clone pL351-88-1 was created. PCR primers were designed in the outward directions to create the deletion and to add *BamHI* restriction enzyme sites. The PCR product was purified and digested with BamHI. After religation and transformation into *E. coli* DH5 α , a clone lacking the complete ORF of *avrGf2* and containing only flanking regions of *avrGf2* was chosen. The deletion was confirmed by sequencing the insert in the pGEMT-Easy vector. The ORF-deleted fragment of the gene with flanking regions was excised from pGEMTEasy and was cloned into the suicide vector pOK1. This deletion mutant gene was conjugated into Xfa-C (strain 10535) using homologous recombination, as previously described, and mutants were identified by PCR (Huguet et al. 1998). Following

identification of the Xfa-C $\Delta avrGf2$ strain, it was tested in GF and did not elicit an HR. A subsequent complementation of Xfa-C $\Delta avrGf2$ with pL351-88-1, restored the avirulent phenotype and confirmed that *avrGf2* was responsible for the HR (Figure 2-1).

A strain with a mutated *avrGf2* gene (Xfa-C $\Delta avrGf2$) was compared with the wild-type Xfa-C strain by inoculation of Duncan grapefruit, Hamlin orange; Eureka lemon; and Satsuma mandarin leaves by infiltration of a bacterial suspension adjusted to 5×10^8 CFU/ml. Visually, the symptoms caused by the Xfa-C $\Delta avrGf2$ strain were more similar to those produced by the wild-type Xc-A strain; a confluent and expanding lesion developed in a typical pathogenicity reaction in all the Citrus species tested (Figure 2-2). Internal bacterial populations and electrolyte leakage from KL and GF leaves infiltrated with strains Xc-A; Xfa-B; Xfa-C; Xfa-C $\Delta avrGf2$; and Xfa-C $\Delta avrGf2::avrGf2$, at a concentration of 5×10^5 CFU/mL, were compared (Fig. 2-3). In KL, Xc-A increased its population faster than all the other strains although all reached a population level of 10^6 at 8 days after inoculation and higher population at day 10. In GF populations of all strains were about equal for the first 2 days after inoculation. However, after day 4, the population of the Xfa-C strain was significantly smaller than that of the Xc-A strain. At day ten, the population of the Xc-A strain was highest (approx. 10^8), and the population of the Xfa-C strain was unchanged at about 10^4 CFU/cm². The population of the Xfa-C- $\Delta avrGf2$ strain was intermediate between those of the Xc-A and Xfa-C strains. The complementary strain containing the p351-88-1 clone (*avrGf2*) showed the smallest population levels. Electrolyte leakage analysis in GF leaves confirmed that Xfa-C and Xfa-C $\Delta avrGf2$:pL351-88-1 elicited rapid cell death in GF leaves, and differed from Xfa-C $\Delta avrGf2$ and Xc-A306, which were used as controls. Electrolyte leakage of Xfa-C and

Xfa-C $\Delta avrGf2$ was similar after the first 24 h, but leakage increased dramatically for Xfa-C in the next 48 h, showing a peak at 72 h after inoculation, while leakage caused by Xfa-C $\Delta avrGf2$ and Xc-A306 remained almost unchanged at 72 hpi. After 96 h, tissue damage caused by Xfa-C $\Delta avrGf2$ and Xc-A306 showed only a slight increase (Figure 2-3).

The effector XopAG-*avrGf2* is Present Only in Xfa-C Strains

Using PCR primers BandC F/R (Table 2-2), a functional copy of gene *avrGf2* was identified in both Xfa-C 10535 (type strain) and Xfa-C #94 (brown pigment producer) strains. A truncated version of gene *avrGf2* was present in all Xfa-B strains tested (Figure 2-4). Even though Xfa-B was reported first in South America, the presence of a functional copy of *avrGf2* shows that Xfa-C is the progenitor strain of Xfa-B. The *avrGf2* gene was not amplified from genomic DNA of strain Xc-Aw12879 or strain Xf-#93. No other XopAG effector other than *avrGf1* was found in the Xc-Aw12879 genome (Jalan et al., 2013b). Furthermore, using BLASTn, the whole sequence of the Xfa-C library clone containing p-GF13 (2934 bp) was compared against the Xc-Aw12879 genome. As a result, only partial sequence similarity with different parts of Xc-Aw12879 genome was observed.

The gene *avrGf2* was not found in strains Xfa-#93 or Xc-A* 290 using a PCR approach with the primers sets (Forward /Reverse): BandC, Gf2Up- Gf2Down, JGF2, NPIS, Up-BC, DownBC, and *avrGf1* (Table 2-2), nor through Southern blot hybridization using as a probe containing the entire *avrGf2* gene (amplified using primers *avrGf2EV* F/R), or the first 943 bases of gene *avrGf2*, (primers *avrGf2EV*-Forward and Up-BC2-Reverse).

Xc-A* Elicits HR in Grapefruit

The resistant reaction observed in GF appears different compared to the strong HR induced by Xfa-C. Internal bacterial populations were quantified in GF leaves using strains Xc-A*290 and Xc-A*406, with Xfa-C and Xc-A306 as controls. Following infiltration with strain Xc-A*290, populations were lower than Xc-A306, but not as low as with the Xfa-C strain. Xc-A*406, which produces a compatible disease reaction in GF leaves and had relatively higher populations levels compared to Xc-A*290 and Xfa-C but lower than Xc-A306 (Figure 2-6). Xc-A* strain 290 induces a slow necrosis in GF leaves following infiltration of 10^8 CFU/ml into leaves (Figure 2-7).

AvrGf2 and AvrGf1 Differ in HR in Grapefruit

Following infiltration of GF leaves with a high bacterial concentration (5×10^8 CFU/ml) of strains Xc-Aw and Xfa-C, the infiltrated areas showed two different types of resistance reactions, Xfa-C produced a stronger HR compared to strain Xc-Aw (Figure 2-8). When the *avrGf1* and *avrGf2* genes were cloned into pLAFR3, and conjugated in Xc-A306, transconjugants carrying *avrGf1* produced an HR by 96 h postinoculation in GF leaves, while a much faster HR was produced after 72 h by the transconjugant carrying *avrGf2* (Figure 2-9).

In order to determine if either XopAG gene (*avrGf1* and *avrGf2*) plays an important role in pathogenicity and fitness of Xc-A306, bacterial populations were quantified over time in KL. There was no significant difference in populations indicating that genes *avrGf1* and *avrGf2* are not critical for growth in leaf tissue. (Figure 2-10A). Bacterial populations were markedly lower in GF leaves infiltrated with Xc-A306:*avrGf2* compared to Xc-A306:*avrGf1* (Figure 2-10B). In electrolyte leakage experiments, electrolyte leakage reached a maximum after 72 h in leaf disks infiltrated with Xc-

A306:*avrGf2*, than in leaf disks infiltrated with Xc-A306:*avrGf1* which reached its highest electrolyte leakage after 96 h. In electrolyte leakage experiments, there was a difference in the extent and speed of tissue damage between Xc-306 transconjugants carrying *avrGf1* or *avrGf2* clones in GF (Figure 2-10C).

Phylogenetic Analysis between *avrGf2* Gene and Members of the XopAG Effector Family

Two different Neighbor-joining trees were constructed and then bootstrap analysis was performed for the XopAG family effectors, and also for other related T3Es from non-*Xanthomonas* species such as *Ralstonia solanacearum*, *Pseudomonas syringae*, *Rhizobium etli* and *Acidovorax citrulli*. The first tree was constructed using nucleotide sequences (Figure 2-11), and the second was constructed using amino acid sequences (Figure 2-12). In both comparisons *avrGf1* and *avrGf2* are always separated into two different clades, forming groups with different XopAG effectors.

Discussion

A novel XopAG effector in strain Xfa-C, *AvrGf2* is responsible for elicitation of a fast HR in citrus. This avirulence gene limits Xfa-C host range in citrus species. This was confirmed by electrolyte leakage and population dynamics in GF and KL. Verification was achieved by mutagenesis of the gene in the Xfa-C strain, which resulted in a compatible reaction in GF (Figure 2-1), however the absence of *avrGf2* in a constructed strain of Xfa-C did not induce a significant fitness change in the natural KL host.

AvrGf2 was shown to elicit a much more rapid HR than *AvrGf1*. This was verified by differences observed in electrolyte leakage and population dynamics performed in KL and GF. The expression of effector protein *AvrGf1* and *AvrGf2*, in Xc-A306 strain resulted in different phenotypes following infiltration into GF leaves. The transconjugant

Xc-A306:*avrGf2* elicited a faster HR and lower populations than Xc-A306:*avrGf1* in GF. There was no observable effect on virulence when transconjugant Xc-A strains containing either gene, *avrGf1* or *avrGf2*, were inoculated into KL (Figure 2-10). In contrast to what was observed, after infiltration of Xfa-CΔ*avrGf2* in GF, the presence of either of these two XopAG effectors (*avrGf1* and *avrGf2*) in strain Xc-A306 did not appear to affect its bacterial fitness in KL (Gochez et al., 2012).

Phylogenetic analysis using both *avrGf1* and *avrGf2* and other XopAG sequences recovered from Genbank, placed *avrGf1* and *avrGf2* in two different clades (Figure 2-11). Although AvrGf2 had greater sequence identity with AvrGf1 at the amino acid level, AvrGf2 had greater amino acid sequence identity with other described effectors, such as the HopG1 effector present in *Xc vasculorum*, *Xc musacearum* (87% identity), and *Ps tomato* DC3000 (47% identity) (Figure 2-12) indicating that both XopAG effectors, *avrGf1* and *avrGf2*, present greater amino acid similarities with different plant pathogens that do not affect citrus.

Only Xfa-C possesses a functional copy of the AvrGf2. Based on comparative analysis, Xfa-B strains contain a transposon insertion (IS 1479 transposase; EFF45537.1) in the *avrGf2* gene in a similar chromosomal region as Xfa-C. The non-functional effector present in Xfa-B is conserved in a pathogenicity island within the genome. Regardless of the presence of an inactive copy of *avrGf2* in Xfa-B, a high degree of nucleotide similarity exists with *avrGf2* sequence in Xfa-C strains (Moreira et al., 2010a, Moreira et al., 2010b). Confirmation that the avirulence gene in Xfa-B strains is disrupted helps to explain why Xfa-B has a broader host range than Xfa-C. The possibility of interaction of Xfa-B with other bacteria of the same niche and phylloplane

also may explain how several effectors described in Xc-A strains (like XopE2, XopN, XopP, XopAE) are also found in Xfa-B, and consequently why Xfa-B is more aggressive than Xfa-C (Gochez et al., 2008). It is also worth noting that strain Xfa-#93, isolated in Brazil from KL, produces symptoms in all citrus species and does not elicit an HR on any known citrus species. Based on biochemical tests the strain was originally characterized as Xfa-C. It was not possible to amplify any fragment of *avrGf2* gene, nor did an *avrGf2* probe hybridize with genomic DNA of Xfa-#93. The taxonomy of this strain still is undefined and requires further evaluation.

Previous work suggests that the Xc-A* strains are a group of different populations which are spread through Asia (Ngoc et al., 2009). In recent years, Escalon et al. (2013) demonstrated the presence of the *avrGf1** gene in strain Xc-A* JK2-10 (JX566667) isolated in 1988, and postulated that the limiting factor in host range of the Xc-A* strains is the presence of the gene *avrGf1**, which has 99% sequence identity (531/532 amino acids) with the previously described *avrGf1* gene from strain Xc-Aw. It is noteworthy that using Southern blot hybridization, the *avrGf1* gene was not identified in strains Xc-A* 290 or Xc-A* 406 used by Rybak et al. (2009).

In this comparison, the Xc-A* strain used (Xc-A*290, isolated in Saudi Arabia in 1988) (Table 2-1), produces a relatively slow HR, that was reported first by Rybak et al (2009). The visual comparison of the HR induced in GF leaves, and the population growth curves obtained in GF leaves for strain Xc-A*290 were different compared with the ones obtained for strains carrying *avrGf1* and *avrGf2* genes. Neither *avrGf1* (Rybak et al., 2009) nor *avrGf2* was found in strain Xc-A*290 using PCR or Southern hybridization methods. Although the genetics of strain Xc-A*290 is still not well

characterized, at first look this strain showed differences with Xc-A*JK2-10, and any other Xc-A* strains which were positive for the presence of *avrGf1* (Escalon et al., 2013).

In conclusion, XopAG-*avrGf2* is found only in Xfa-C strains, which produce an HR in certain Citrus species, a non-functional copy of this effector is present in Xfa-B strains, which suggests that Xfa-C is its progenitor. Furthermore compared with the previously characterized *avrGf1* gene, *avrGf2* elicited a faster type of HR in citrus.

Table 2-1. Bacterial strains, plasmid vectors, and plasmid constructs used in this study

Designation	Host (year, location of isolation)	Relevant characteristics	Source or reference
<i>Xanthomonas axonopodis</i> pv. <i>citri</i> strains.			
Xc-A306	Orange (<i>C. sinensis</i>) 1997, Paranavai, Parana, Brazil.	RifR	Rui Pereira Leite Jr. DPI (da Silva et al., 2002)
Xc-A306:pLAFR3		A306:pLFR3 empty (RifR; TetraR)	This work
Xc-A306: <i>avrGf2</i>		A306:pLFR3-351-88-36-1 (RifR; TetraR)	This work
Xc-A306: <i>avrGf1</i>		A306:pU799-3 (RifR; KanR)	This work
Xc-Aw	Alemow (<i>C. macrophylla</i>) 2000. Palm Beach, Wellington, Florida.	<i>Xc-A hrpB</i> fragment (100% identity). Wellington strain, pathogenic to KL and Alemow.	Xc-Aw 12879. DPI (Rybak et al., 2009)
Xc-A*290	Saudi Arabia. KL. 1988.	<i>Xc-A hrpB</i> fragment (100% identity). Elicit HR in tomato and slow-HR in GF; pathogenicity reaction in KL.	Xcc-A*290 DPI. Xc-A* 1974 (Rybak et al., 2009).
Xc-A*406	Southeast Asia.	<i>Xc-A hrpB</i> fragment (100% identity). Elicit HR in tomato; pathogenicity reaction in citrus.	Xcc-A*406G. DPI (Verniere et al., 1998).

KL: Key lime (*C. aurantifolia*). DPI, Division of Plant Industry of the Florida Department of Agriculture and Consumer Services, Gainesville, FL, USA.

Table 2-1 (continued).

Designation	Host (year, location of isolation)	Relevant characteristics	Source or reference
<i>Xanthomonas fuscans</i> pv <i>aurantifolii</i> strains.			
Type B			
Xfa-B16	Lemon (C. lemon) 1990, Concordia, Entre Rios, Argentina.	<i>X. f.</i> pv. <i>fuscans</i> <i>hrpB</i> fragment (99% identity). Pathogenic on citrus. HR in tomato.	Xc90-78-4-3 (B. I. Canteros, EEA INTA Bella Vista Collection)
Xfa-B69	Lemon (C. lemon) 1979, Bella Vista, Corrientes, Argentina.	<i>X. f.</i> pv. <i>fuscans</i> <i>hrpB</i> fragment (99% identity). Pathogenic on citrus. HR in tomato.	Strain 11122. J. W. Miller (Civerolo & Fan, 1982, Moreira et al., 2010c)
Xfa-B89	Lemon (C. lemon) 1981, Bella Vista, Corrientes, Argentina.	<i>X. f.</i> pv. <i>fuscans</i> <i>hrpB</i> fragment (99% identity). Pathogenic on citrus. HR not well defined in all tomato varieties.	Xcc-06-2975. Xcc 30 B (B. I. Canteros, EEA INTA Bella Vista Collection)
Xfa-B90	Lemon (C. lemon) 1978, Bella Vista, Corrientes, Argentina.	<i>X. f.</i> pv. <i>fuscans</i> <i>hrpB</i> fragment (99% identity). Pathogenic on citrus. HR not well defined in tomato.	Xcc-06-2993. Xcc 4 B (B. I. Canteros, EEA INTA Bella Vista Collection)

Table 2-1 (continued).

Designation	Host (year, location of isolation)	Relevant characteristics	Source or reference
<i>Xanthomonas fuscans</i> pv <i>aurantifolii</i> strains.			
Type C			
Xfa-C	KL, 1981, Sao Paulo, Brazil.	RifR; <i>X. f.</i> pv. <i>fuscans</i> <i>hrpB</i> fragment (99% identity); elicit HR in tomato and citrus except KL.	Type C Strain 10535 (IBSBF338) (Moreira et al., 2010c)
Xfa-C94	KL, 2000, Jose Bonifacio, Sao Paulo, Brazil.	<i>X. f.</i> pv. <i>fuscans</i> <i>hrpB</i> fragment (99% identity). Brown pigment production. Elicit HR in tomato and citrus except KL.	Xcc-08-3578. (IBSBF1479 FDC 535) (Nociti et al., 2006)
Xfa-C Δ avrGf2		Xfa-C knock out for gene <i>avrGf2</i> . RifR	This work
Xfa-C <i>avrGf2</i> :: <i>pavrGf2</i>		Xfa-C complementary strain. RifR; TetraR	This work
Xfa-#93	KL, 1997, Ubarana, Sao Paulo, Brazil.	<i>X. f.</i> pv. <i>fuscans</i> <i>hrpB</i> fragment (99% identity). Elicit HR in tomato and pathogenicity reaction in citrus.	Xcc-08-3577 (IBSBF 1350)

Table 2-1 (continued).

Designation	Host (year, location of isolation)	Relevant characteristics	Source or reference
<i>Xanthomonas fuscans</i> pv <i>aurantifolii</i> strains.			
<i>X. perforans</i>			
91-118	Tomato (1991, Florida)	Wild type. Pathogenic to tomato, RifR	(Jones et al., 2004)
Xp 1-7	Tomato (2006, Florida)	CuR	Stall, R. E.
<i>Xanthomonas vesicatoria</i> strains			
Xv1111	Tomato (1955, New Zealand)	ATCC 35937. CuR	ATCC
Xv BV5-4a	Tomato (1987, Bella Vista, ARG)	CuR.	Canteros, B. I.

Table 2-1 (continued).

Designation	Host (year, location of isolation)	Relevant characteristics	Source or reference
<i>Escherichia coli</i> strains.			
DH5 α		F-recA hsdR17(rk-mk+) Φ 80dLacZ	Bethesda Research Laboratories, Bethesda, MD, USA
HB101		F-recA	(Sambrook & Russell, 2001)
pU799-3		2.3-kb fragment containing <i>avrGf1</i> in pUFR034	(Rybak et al., 2009)
pL-351		pLFR3 (RifR; TetraR)	This work
pL-351-88-1		pLFR3 (RifR; TetraR) obtained from EcoRI religation of pL-351 (4402 bp).	This work
pGF13		pBluescript (AmpR): EcoRI fragment (2934 bp) from clon p351-88-1.	This work
pGF14		pBluescript (AmpR): EcoRI fragment (1474 bp) from clon p351-88-1.	This work
pGMTE-avrGf2-15B		pGEMT-easy (AmpR, Promega):2934 bp EcoRI fragment (containing <i>avrGf2</i>) from pL-351-88-1.	This work

Table 2-1 (continued).

Designation	Host (year, location of isolation)	Relevant characteristics	Source or reference
Plasmids			
pOK1		Suicide vector, pKNG101 derivative, Smr/Sucs	(Huguet et al., 1998)
pBluescript II SK(+)		Phagemid, pUC derivative, AmpR	Stratagene (La Jolla, CA, USA)
pGEMT Easy		AmpR	Promega Corp. (Madison, WI, USA)
pLAFR3		Tra–Mob+, RK2 replicon, tetR	(Staskawicz et al., 1987)
pUFR034		Inc W, Kmr, Mob+, lacZ α , Par+, cosmid	(DeFeyter et al., 1990)

Table 2-2. Primers utilized in the present work.

Name	Sequence (5'-3')	Length amplicon (bp); (strain)	Reference
RST65	GTCGTCGTTACGGCAAGGTGGTCG	420	Minsavage G. V.
RST69	TCGCCCAGCGTCATCAGGCCATC		
GF2Down-R	ACATGCATGCTAAGAAGTAGCCCCTGAAAAATC CACTC	4402; (Xfa-C)	This work
GF2Up-F	ACATGCATGCACGCATTACGAGCACCTCAACC		
JGF2F	GCGGTCAGGGCGGAGCAGTAAGG	2460; (Xfa-C)	This work
JGF2R	GAGTGCGCGTGTGTCGCGTTCCGG		
NPISF	CGCTCACAAGGTGCTAAGGAA	1064; (Xfa-B/C)	This work
NPISR	GGTTCACAGACGCACGCT		
BandC-F	AATGAAATCCTCTCAGGGCTCC	1395; (Xfa-C)	This work
BandC-R	CGCTTCTCCGCCATAAAACT	2551; (Xfa-B)	
Up-BC1-F	GGGCTCCCGTCTTTTTTCAA	135; (Xfa-B/C)	This work
Up-BC1-R	GTTGTCGTAGACATAAGCAGCACC		
Up-BC2-R	TTAGCACCTTGTGAGCGTCT		
Down-BC1F	TTTACGACAACGCCAGCAGT	146; (Xfa-B/C)	This work
Down-BC1R	TTCTCCGCCATAAAACTCCC		
avrGf1-R	CTGGTCGATGGCAAAGGCGGC*	365; (Xc-Aw)	*Modified from (Rybak et al., 2009)
avrGf1-F	CGCCGGTTTCTGTCCTGCACTTG		
avrGf1EV-F	ATGGCTCCGAGCATGCATTCGGC	1596; (Xc-Aw)	This work
avrGf1EV-R	GTCGCTGCTGGTCATTGACTTTTCT		
avrGf2EV-F	CGCGGATCCATGCGTGTTGCTAAACATAA	1524; (Xfa-C)	This work
avrGf2EV-R	CCGCTCGAGATTGCTCTTGGCCGCTCTAA		

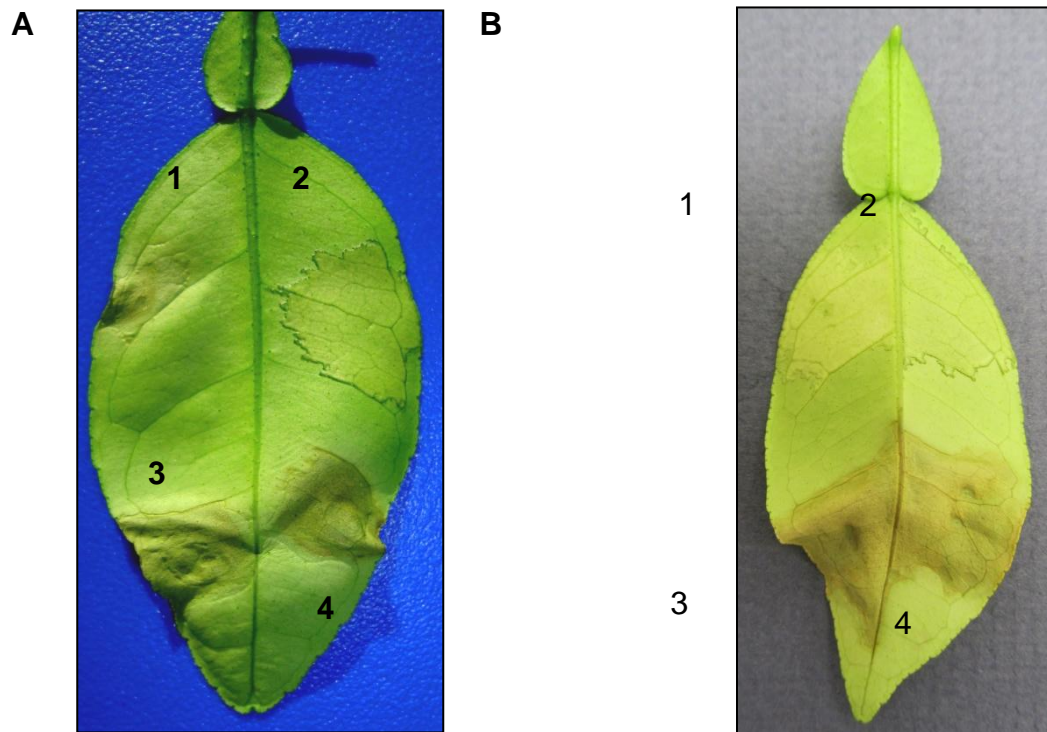


Figure 2-1. AvrGf2 expression in citrus canker producing strains results in elicitation of a hypersensitive reaction in Duncan grapefruit leaves. Duncan grapefruit leaves were infiltrated with bacterial suspensions adjusted to 5×10^8 CFU/ml. Bacterial suspensions in left picture are: A-1: *Xanthomonas fuscans* pv. *aurantifolii* type C (Xfa-C); A-2: *X. citri* type A306 (Xc-A306); A-3: Xc-A306:pL 351; A-4: Xc-A;pL 351-88-1. Bacterial suspensions in right picture are: B-1: Xc-A306; B-2: Xfa-C *avrGf2*⁻; B-3: Xfa-C *avrGf2*⁻:*avrGf2*; B-4: Xfa-C.

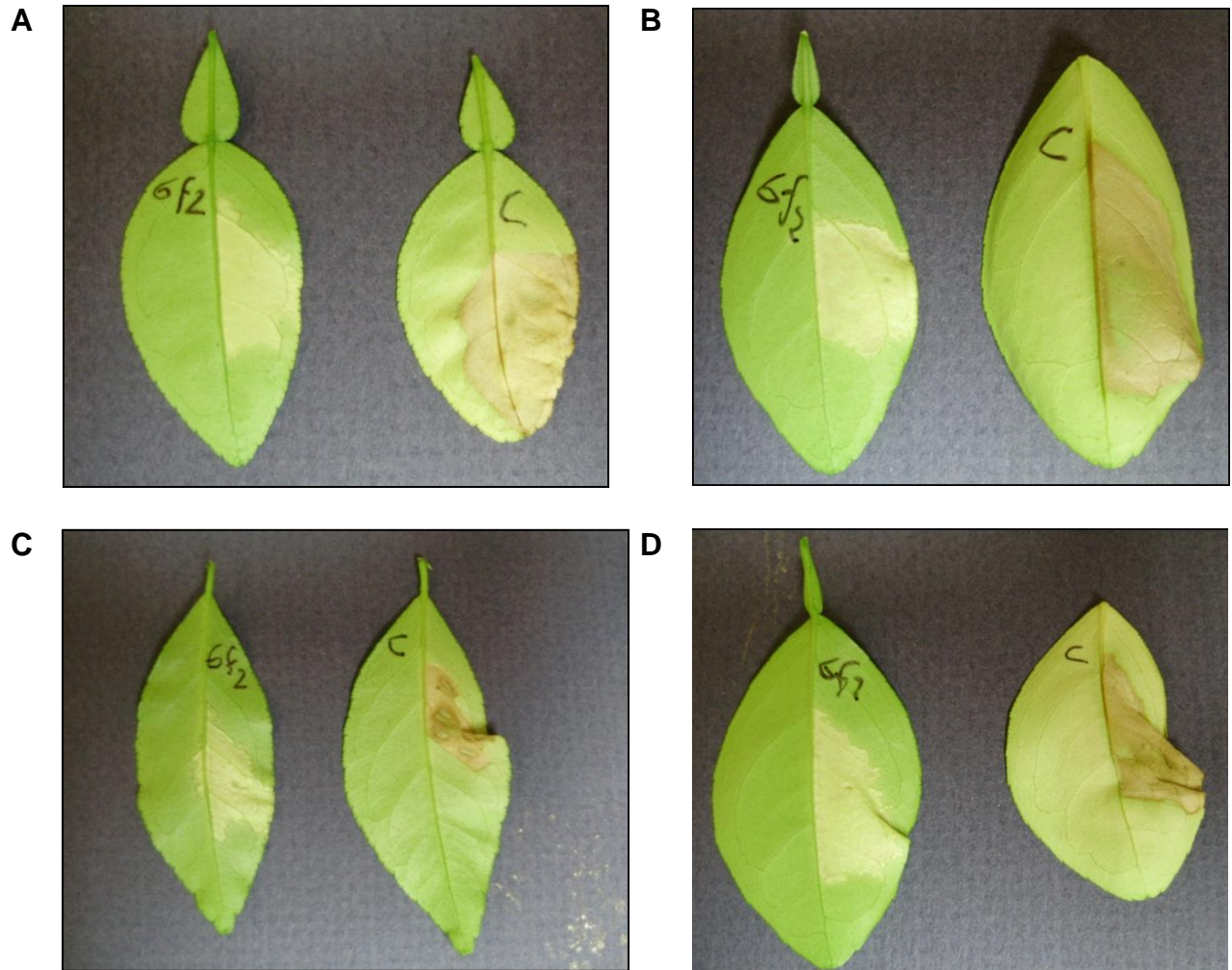


Figure 2-2. Disease reactions observed in leaves of Duncan grapefruit (A); Hamlin orange (B); Eureka lemon (C); and Satsuma mandarin (D) following infiltration with *Xanthomonas fuscans* pv. *aurantifolii* (Xfa) type C (hypersensitive reaction, right) or Xfa *avrGf2*⁻ (pathogenicity reaction, left). bacterial suspensions adjusted to 5×10^8 CFU/ml)

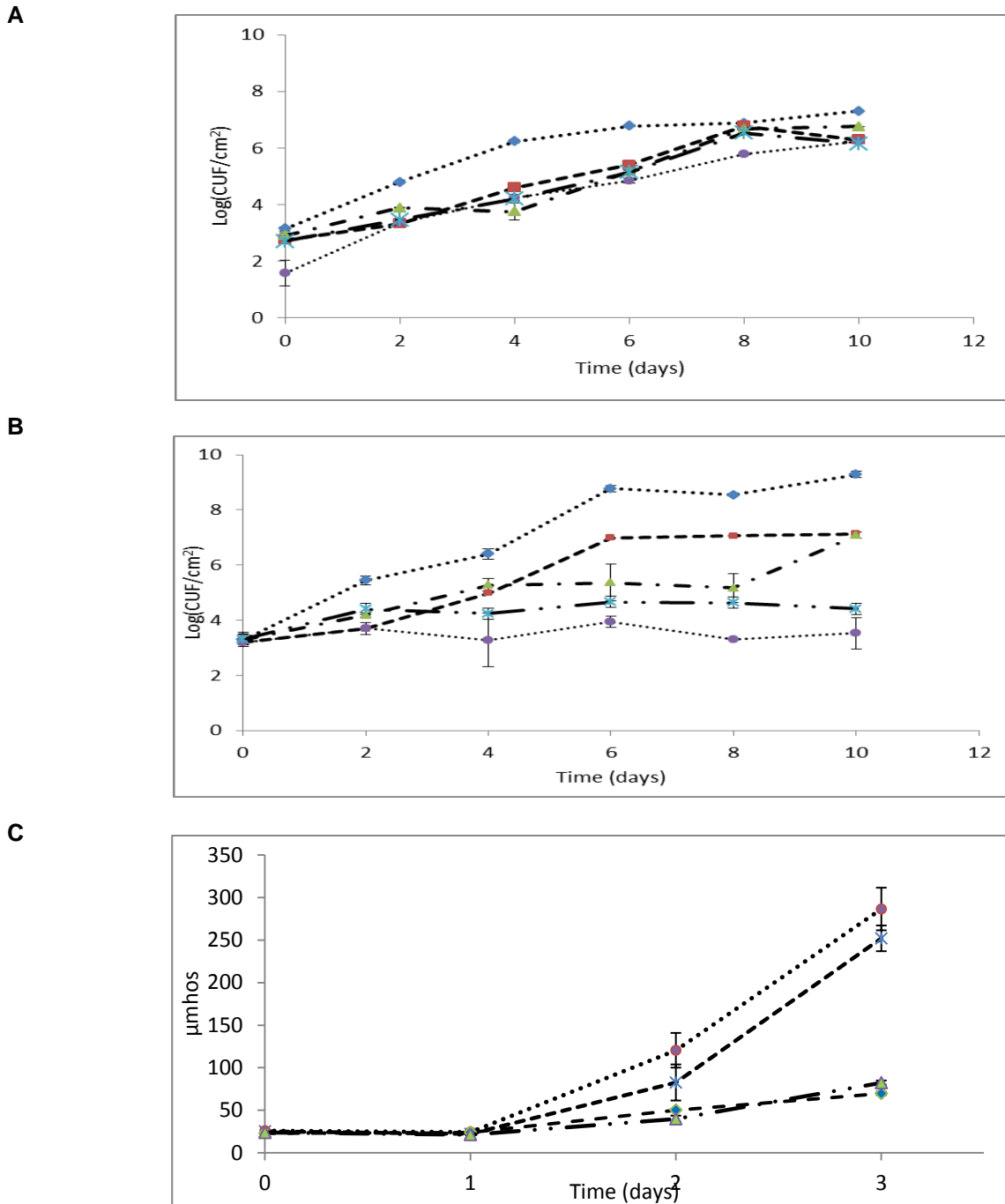


Figure 2-3. Population dynamics in Key lime (KL) (A), and Duncan grapefruit (DG) leaves (B) inoculated with bacterial suspensions adjusted to 5×10^5 CFU/ml. The bacteria that were infiltrated were *Xanthomonas citri* type A (Xc-A, blue diamond); *X. fuscans* pv *aurantifolii* Type B (Xfa-B, red square); Xfa type C (Xfa-C, green triangle); Xfa-C *avrGf2*⁻ (light blue star); and Xfa-C *avrGf2*⁺ (purple circle). Electrolyte leakage analysis of the same bacterial species in DG leaves (C) infiltrated with bacterial suspensions adjusted to 5×10^8 CFU/ml. Each point represents the mean from one experiment with three replicates. Vertical lines represent standard error of the mean.

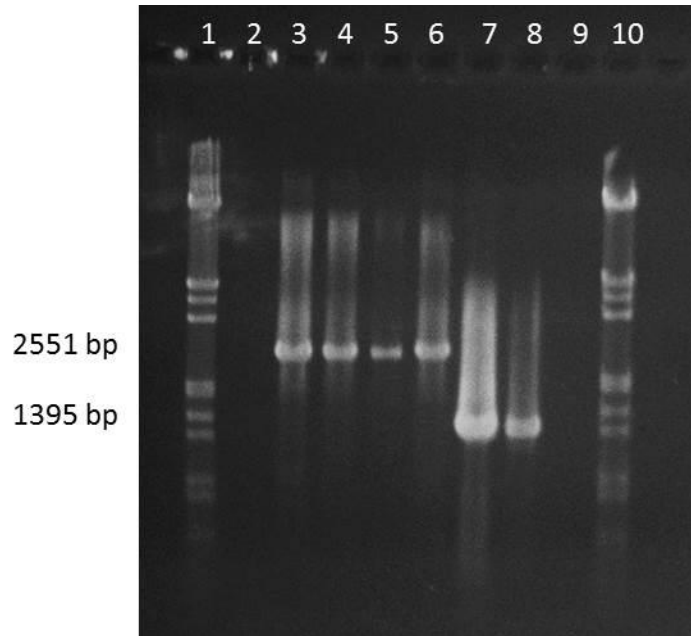


Figure 2-4. Xfa-B strains contain a transposon insertion in *avrGf2*. PCR products were amplified using primers BandC-F/R. Lanes 1 and 10: λ *HindIII-EcoRI* marker; lane 2: *Xanthomonas citri* Aw; lanes 3-6: *X. fuscans* pv *aurantifolii* (Xfa) type B (B69; B16; #89; #90 strains); lanes 7-9: Xfa-C (Xfa-C#94, and Xfa-#93 strains).

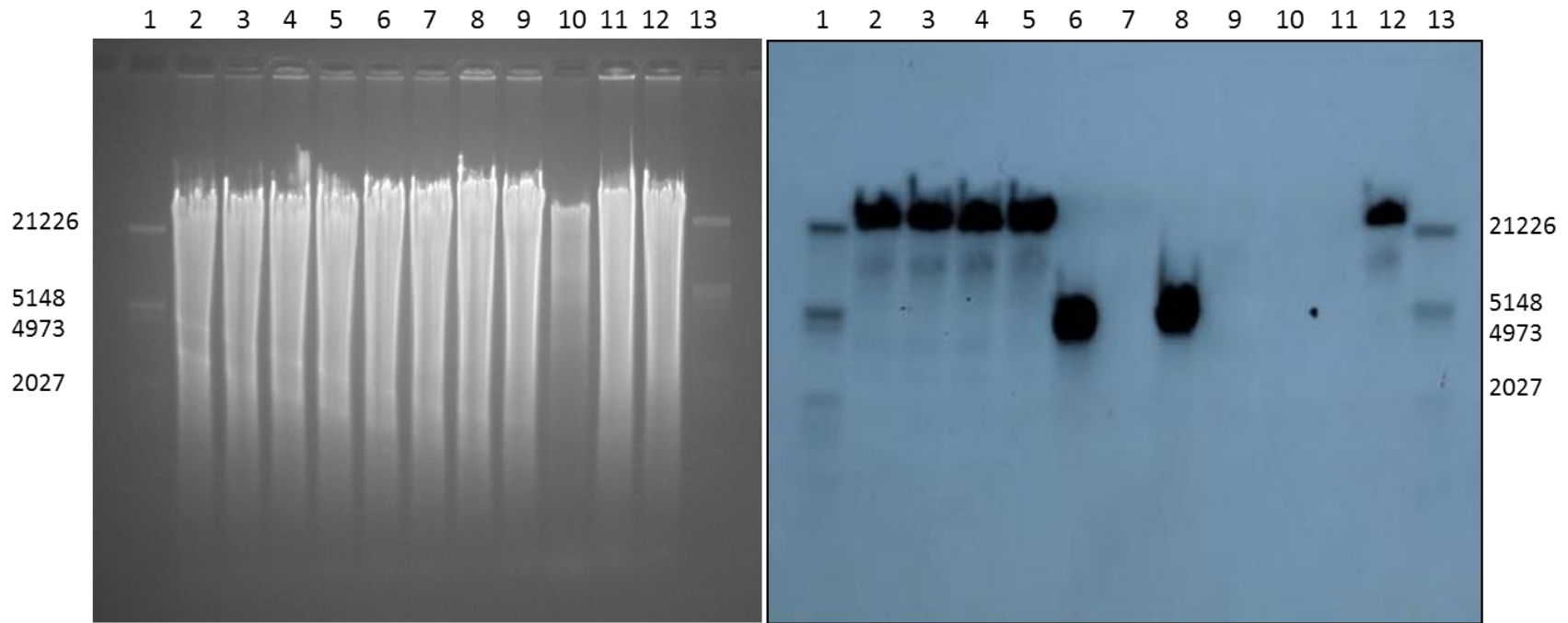


Figure 2-5. Hybridization of *avrGf2* with total genomic DNA of *Xanthomonas* strains digested with *EcoRI* (A). Lane 1 and 13= DNA Mol. Weight Marker III, 2= Xfa-B16, 3=Xfa-B69, 4=Xfa-B89, 5=Xfa-B90, 6=Xfa-C, 7=Xfa-C Δ *avrGf2*, 8=Xfa-C94, 9=Xfa-#93, 10=Xc-A306, 11=Xc-A*290, 12=Xfa-B16. Left panel= Ethidium bromide stained gel (agarose 0.7%). Right panel= Southern blot of gel in left. Number in left and right indicates size in kbp of DIG labeled marker only.

A

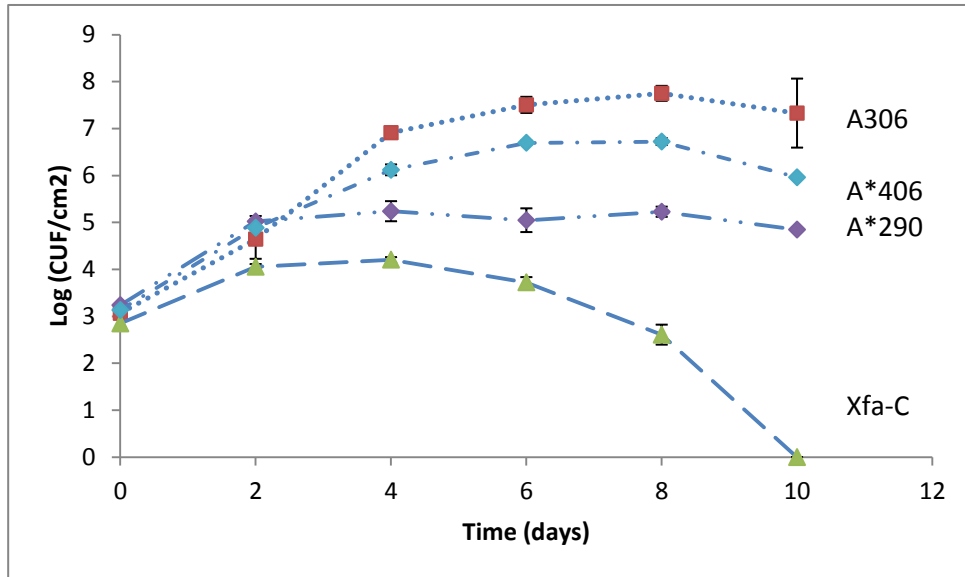


Figure 2-6. Population dynamics in Duncan grapefruit (DG) leaves following infiltration of bacterial suspensions adjusted to 5×10^5 CFU/ml. Bacterial strains infiltrated were *Xanthomonas citri* A306 (A306, red square); Xc-A*406 (light blue diamond); Xc-A*290 (purple diamond); and *X. fuscans* pv *aurantifolii* Type C (Xfa-C, green triangle). Each point represents the mean from one experiment with three replicates. Vertical lines represent standard error of the mean.

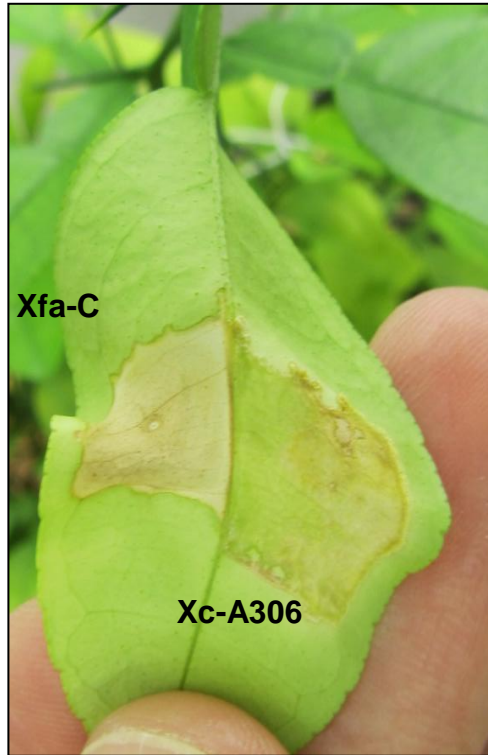
A**B**

Figure 2-7. Hypersensitive and susceptible reaction observed after 15 days in Duncan GF leaves infiltrated with bacterial suspension adjusted to 5×10^8 CFU/ml of *Xanthomonas fuscans* pv. *aurantifolii* type C (Xfa-C, A-left), *X. citri* A306 (Xc-A306, A-right); Xc-A*290 (B-left); and Xc-A*406 (B-right).

A**B**

Figure 2-8. Hypersensitive reaction observed after 5 days in Duncan grapefruit leaves infiltrated with bacterial suspension of *Xanthomonas fuscans* pv. *aurantifolii* (Xfa) type C (A left; B right) and *X. citri* A^w (A right; B left) adjusted to 5×10^8 CFU/ml. A and B panels represent the adaxial and abaxial surfaces of the leaf, respectively.



Figure 2-9. Expression of *avrGf1* and *avrGf2* in Xc-A results in elicitation of HR and reduces XccA growth in Duncan grapefruit leaves. Bacterial suspensions adjusted to 5×10^8 CFU/ml of wild-type Xc-A306 or transconjugants containing *avrGf1* or *avrGf2* were infiltrated into grapefruit. HR reaction was observed at 3, 4, and 6 DPI. Xc-A: Xc-A (*pLAFR3*); *avrGf1*: Xc-A (*pUFR034:avrGf1*); *avrGf2*: Xc-A (*pLAFR3:avrGf2*).

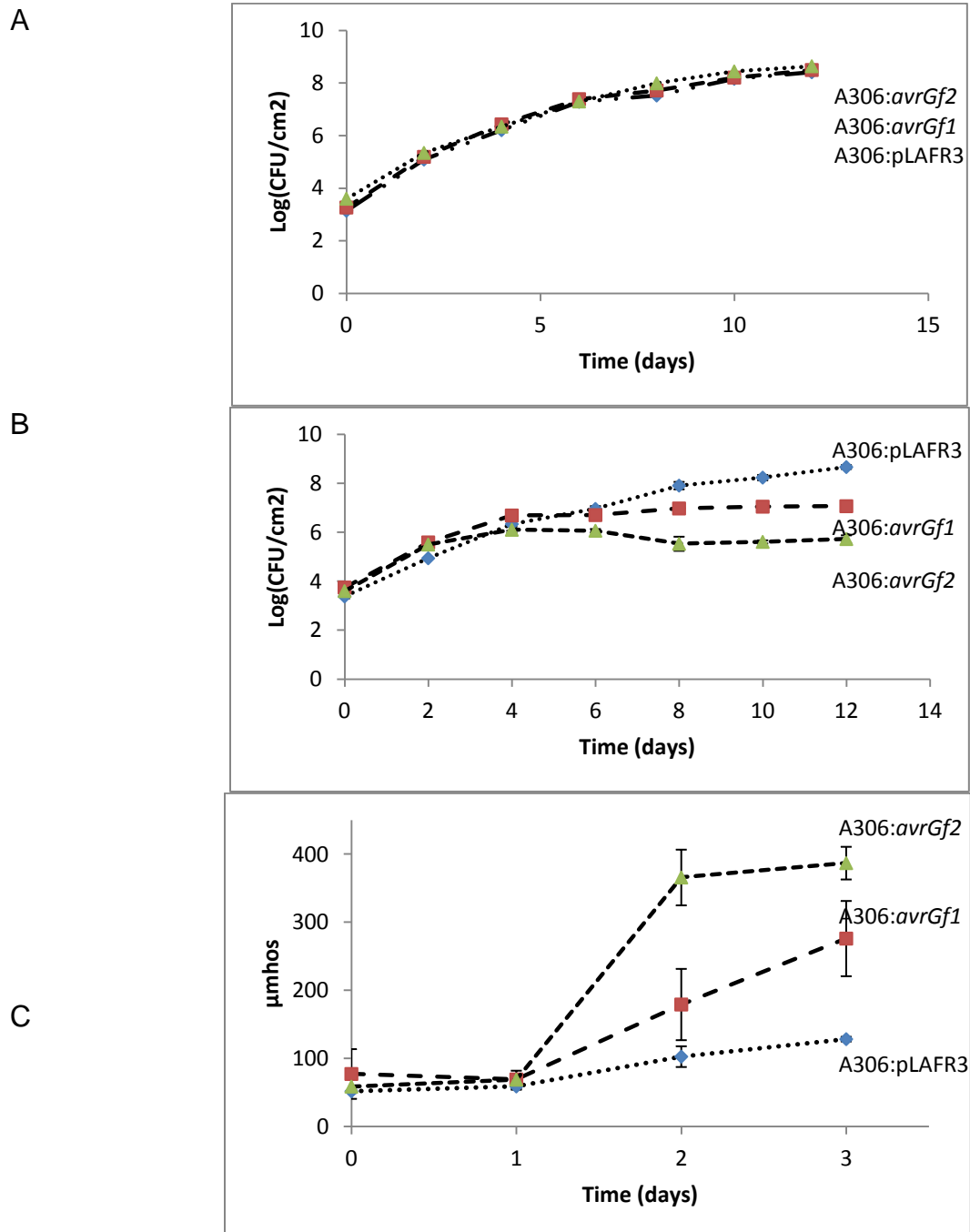


Figure 2-10. Population dynamics in Key lime (KL) (A), and Duncan grapefruit (DG) leaves (B) following infiltration with bacterial suspensions adjusted to 5×10^5 CFU/ml. Bacterial strains inoculated included *Xanthomonas citri* type A:pLAFR3 (*Xc-A306:pLAFR3*, blue diamond); *XcA306:avrGf1* (red square); *XcA306:avrGf2* (green triangle). Electrolyte leakage analysis in DG leaves (C) was determined following infiltration with bacterial suspensions adjusted to 5×10^8 CFU/ml using the same strains above. Each point represents the mean from two experiments, with three replicates. Vertical lines represent standard deviation of the mean.

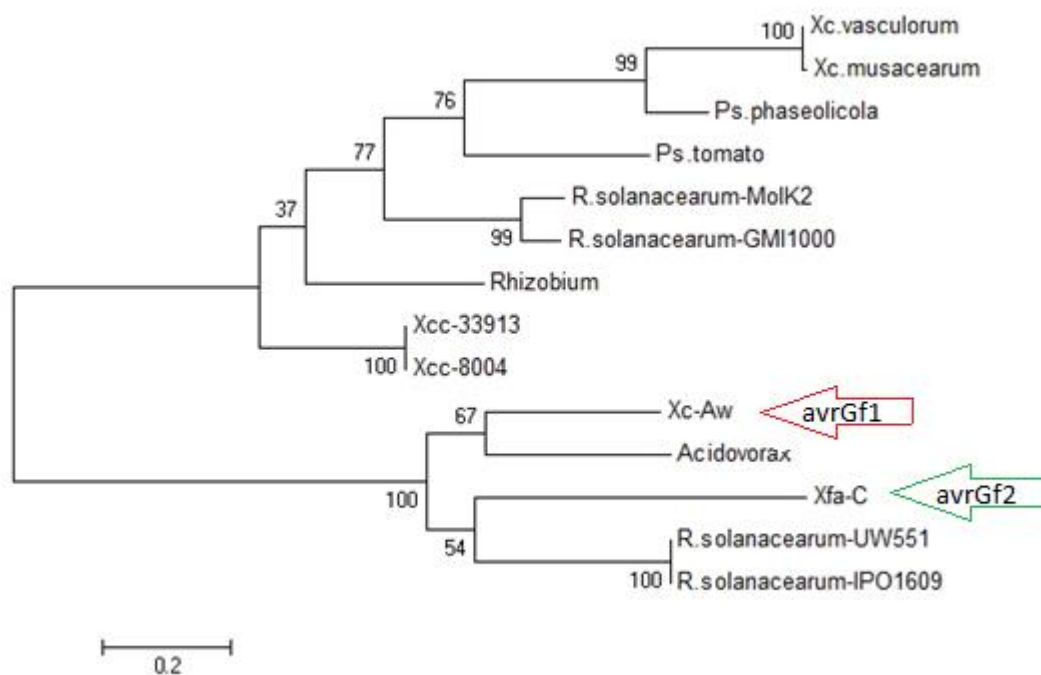


Figure 2-11. Neighbor-joining tree with a Bootstrap test of inferred phylogeny calculated using MEGA 5 for XopAG effector family genes and closely related nucleotide sequences recovered from Genbank: [*Xanthomonas fuscans* subsp. *aurantifolii* str. ICPB 10535 type III (T3) secretion effector *avrGf2* (green arrow)] [294664399:614-2140]; [*X. campestris* pv. *vasculorum* NCPPB702 T3 effector HopG1] [256574234:820-2187]; [*X. c.* pv. *musacearum* NCPPB4381 T3 effector HopG1] [256573118:4-1347]; [*Pseudomonas syringae* pv. *phaseolicola* 1448A T3 effector HopG1] [71733195:897416-898963]; [*P. s.* pv. *tomato* str. DC3000 T3 effector HopG1] [28867243:5353685-5355166]; [*Ralstonia solanacearum* UW551 Hypothetical Protein RRSL_00926] [83749121:7129-8658]; [*Rhizobium etli* CFN 42 hypothetical protein RHE_PA00116] [86359705:122542-124221]; [*X. axonopodis* pv. *citri* secretion effector *avrGf1* (red arrow)] [CDS of 82571049]; [*Xanthomonas campestris* pv. *campestris* str. ATCC 33913 AE008922.1] |:4294677-4296251|; [*Ralstonia solanacearum* strain IPO1609] [206591779:1787782-1789308]; [*Ralstonia solanacearum* strain MolK2] [385273552:951231-952757]; [*Ralstonia solanacearum* GMI1000] [30407128:422680-424218]; [*Acidovorax citrulli* AAC00-1 CP000512.1] |:308126-309682|; [*Xanthomonas campestris* pv. *campestris* str. 8004 CP000050.1] |:675258-676832|.

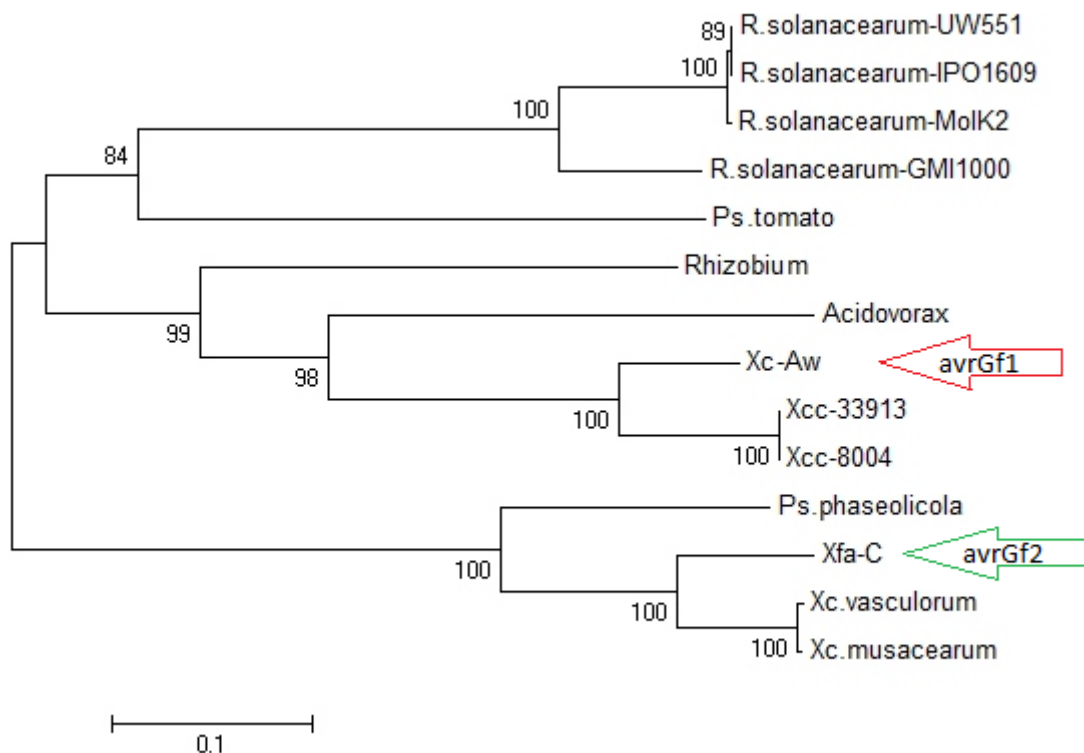


Figure 2-12. Neighbor-joining tree with a Bootstrap test of inferred phylogeny calculated using MEGA 5 for XopAG effector family genes and close related amino acid sequenced recovered from Genbank: [*Xanthomonas fuscans* subsp. *aurantifolia* str. ICPB 10535 type III (T3) secretion effector *avrGf2* (green arrow)] [294664399:614-2140]; [*X. campestris* pv. *vasculorum* NCPPB702 T3 effector HopG1] [256574234:820-2187]; [*X. c.* pv. *musacearum* NCPPB4381 T3 effector HopG1] [256573118:4-1347]; [*Pseudomonas syringae* pv. *phaseolicola* 1448A T3 effector HopG1] [71733195:897416-898963]; [*P. s.* pv. *tomato* str. DC3000 T3 effector HopG1] [28867243:5353685-5355166]; [*Ralstonia solanacearum* UW551 Hypothetical Protein RRSL_00926] [83749121:7129-8658]; [*Rhizobium etli* CFN 42 hypothetical protein RHE_PA00116] [86359705:122542-124221]; [*X. axonopodis* pv. *citri* secretion effector *avrGf1* (red arrow)] [CDS of 82571049]; [*Xanthomonas campestris* pv. *campestris* str. ATCC 33913 AE008922.1] |:4294677-4296251]; [*Ralstonia solanacearum* strain IPO1609] [206591779:1787782-1789308]; [*Ralstonia solanacearum* strain MoIK2] [385273552:951231-952757]; [*Ralstonia solanacearum* GMI1000] [30407128:422680-424218]; [*Acidovorax citrulli* AAC00-1 CP000512.1] |:308126-309682]; [*Xanthomonas campestris* pv. *campestris* str. 8004 CP000050.1] |:675258-676832].

CHAPTER 3

MOLECULAR CHARACTERIZATION OF AvrGf2, A XopAG EFFECTOR THAT IS REQUIRED FOR ELICITATION OF HR IN GRAPEFRUIT

Introduction

Citrus canker is one of the most important diseases of citrus. It is caused by two bacterial species, *Xanthomonas citri* (Xc-A) and *X. fuscans* pv. *aurantifolii* (Xfa) (Young et al., 2008, Bull et al., 2010). The former species is associated with Asiatic Citrus canker caused by A-group strains. It has become the primary pathogen where citrus canker occurs. *X. fuscans* pv. *aurantifolii* consists of B and C group strains (Xfa-B, and Xfa-C). The B group (Xfa-B) is less virulent but produces symptoms in all citrus species and was observed mainly on lemon (*Citrus limon*) in Argentina from 1929, but has not been found since 1991. In 1963, in São Paulo (Brazil), a new type of xanthomonad, which caused canker lesions only in Key lime (KL; *C. aurantifolia*) was isolated. This strain initially known as *X. citri* f. sp. *aurantifoliae* (Namekata & Oliveira, 1972), was designated as the C strain (Rosetti, 1977). In 1981, Stall, et al. (1981) reported that Xfa-C group strains produced an HR in GF leaves.

In 2000, citrus canker was observed affecting only Key lime, and Alemow (*C. macrophylla*) trees in Wellington (Palm Beach County, Southeastern Florida). The strains isolated from these trees were different from conventional Xc-A strains, eliciting an HR in grapefruit (GF, *C. paradisi*). As a result the strains were designated Xc-Aw (Sun et al., 2004). One gene in Xc-Aw strains, *avrGf1*, was identified as responsible for elicitation of an HR in grapefruit (Rybak et al., 2009). Another XopAG type III effector (T3E), *avrGf2*, was found in Xfa-C strains. The presence of *avrGf2* in xanthomonads

produces an HR in Citrus all species, except KL. Compared with the previously characterized gene *avrGf1*, *avrGf2* elicited a faster type of HR in citrus (see Chapter 2).

The presence of the *hrp* gene cluster in xanthomonads delineates the pathogenic *Xanthomonas* strains from the non-pathogenic or saprophytic ones (Stall and Minsavage, 1990). In most *Xanthomonas* species characterized as plant pathogens, the *hrp/hrc* core region, which encodes proteins that form the type 3 secretion system (T3SS) or injectisome, (24 genes) is highly conserved (Lindgren et al., 1988, Arlat et al., 1991). A wide number of bacterial outer membrane proteins are exported by a T3SS, and these are usually classified as effectors in pathogenic processes (Ryan et al., 2011). The most studied family of proteins exported by T3SS in xanthomonads is referred to as Transcription Activator Like Effectors (TALEs). The C-terminal region contains a Nuclear Localization Signal (NLS) in these effectors, and an activation domain that controls specific host gene expression, as well a central repeat domain which defines the targeted genes in the host (Bogdanove et al., 2010). The first T3Es described were the *Yop* (*Yersinia* outer proteins) genes identified in the human pathogen *Yersinia pestis* (Portnoy et al., 1981, Cornelis et al., 1989). Almost all the Gram-negative plant pathogens have T3Es. These genes have particular designations depending on the bacterial species and include Hop genes (Hrp-dependent outer proteins) in the genus *Pseudomonas* (Collmer et al., 2000), Pop genes in *Ralstonia* (Poueymiro et al., 2009), and Xop (*Xanthomonas* outer proteins) genes in *Xanthomonas*. In (2000), Zhu et al. (2000) isolated and identified the Xop gene, *hpa1* from *X. oryzae*. Noel, et al. (2002) characterized XopA and XopD genes from *X. vesicatoria*, with nucleotide sequences similar to *Hpa1* and *PsvA* from *P. syringae*. This

discovery showed that Xop genes are a highly conserved group between plant pathogens in different genera (Gophna et al., 2003, Rohmer et al., 2004, Hajri et al., 2009). Based on functional protein assays, sequence and structural similarities, a united nomenclature for all the T3Es was proposed by White et al. (2009), in which all the effectors were placed in 39 Xop groups.

Several T3Es target plant cell organelles to suppress defense response (Jelenska et al., 2007, Block & Alfano, 2011, Figueiredo et al., 2011, Block et al., 2010). The chloroplast plays an important role in plant defense (Vellosillo et al., 2010, Ishiga et al., 2012), mediating expression of reactive oxygen species (ROS) (Doyle et al., 2010). However, some T3Es suppress this type of oxidative burst in order to avoid elicitation of an HR (Rodríguez-Herva et al., 2012). A member of the *XopAG* effector class, *HopPtoG*, isolated from *P. syringae* DC3000, was reported as a suppressor of the gene *PR1a* in tobacco, which regulates programmed cell death (Jamir et al., 2004). *AvrGf1* and *AvrGf2* from *Xc-Aw* and *Xfa-C* respectively, which elicit HRs in citrus, are closely related to *HopPtoG*, such as *HopPtoW*, that was isolated from *P. syringae* (Rohmer et al., 2004). Based on results from artificial neural-network algorithm analyses including PCLR, ChloroP and LOCtree, several other T3Es were also predicted to have N terminus regions carrying chloroplast-target signals (Jelenska et al., 2007, Guttman et al., 2002, Schein et al., 2001). Some of these predicted signals were confirmed using *in situ* methods such as fluorescence microscopy of tagged proteins (Figueiredo et al., 2011).

The goal of this work was to determine the importance of conserved structural domains shared in the XopAG effectors *avrGf1* and *avrGf2*, and their importance in HR elicitation in citrus.

Material and Methods

Bacterial Strains and Media

Strains utilized in this work are listed in Table 2-1. Strains of Xfa (B and C) and Xc-Aw were stored in sterile tap-water and were grown on nutrient agar (NA) medium. Rifampicin resistant strains were obtained by plating 10^9 colony-forming-units (CFU)/ml on NA containing 50 µg/ml of rifampicin and selecting individual colonies that grew on the amended medium. *Escherichia coli* (Ec) strains were maintained on Luria-Bertani (LB) medium (Sambrook et al., 1989), and for long term storage bacterial cells were suspended in nutrient broth (Difco™) containing 30% glycerol, and placed in a -80°C freezer. Conjugations were performed on nutrient yeast glycerol agar (NYGA) (Daniels et al., 1984). The media were amended, when necessary, with one or more of various antibiotics at the following concentrations: rifampicin, 50 µg/ml; tetracycline, 10 µg/ml; and, kanamycin, 40 µg/ml.

Growth of Plants and Inoculum Preparation

Duncan grapefruit, Key lime, Valencia orange, and Eureka lemon were grown in steamed peat-vermiculite mix in 20 cm (diameter) pots in a greenhouse at 20-35°C. Plants were regularly fertilized with a slow-release fertilizer (Osmocote®).

Bacterial cultures for plant inoculations were grown on nutrient agar for 18 h at 28°C. The bacterial cells were suspended in sterile tap water and suspensions were adjusted to an optical density (O.D.) of 600 nm = 0.3 ($2-5 \times 10^8$ colony-forming unit (CFU) per ml) with a spectrophotometer (Spectronic 20). For population dynamics

experiments bacterial suspensions were serially diluted in sterile tap water to 5×10^5 CFU/ml (Klement et al., 1990).

Bacterial Growth Curves and Electrolyte Leakage Experiments

For quantifying internal population growth in KL and GF leaves bacterial suspensions adjusted to 1×10^5 CFU/ml were infiltrated into the leaf mesophyll with a hypodermic needle and syringe as previously described (Hibberd et al., 1987a). Every 48 h for 14 days following infiltration three leaf disks of 0.5 cm^2 were sampled using a previously described technique (Stall & Cook, 1966, Hibberd et al., 1987b). Disks were crushed separately in 0.5 ml of sterilized tap-water and 10^{-1} to 10^{-6} dilutions were plated on NA to count the CFU. Plants were maintained in a growth room at 25-30°C.

For electrolyte leakage experiments conductivity was determined using a previously described technique (Cook & Stall, 1968, Hibberd et al., 1987b). Leaves were infiltrated with 10^8 CFU/ml. Six 0.5 cm^2 leaf disks were placed in 3 ml of distilled water in each assay. Experiments were repeated at least two times and the data were combined. Three replicates per treatment were used, with each replicate consisting of different leaves on the same plant. Plants were maintained in a growth chamber at 28°C or 24°C.

Aminoacid Sequence Comparison of XopAG Effectors

The translated amino acid sequences of avirulence genes *avrGf1* and *avrGf2* were compared using BLASTx with other members of the xopAG effector family, which were recovered from the online database <http://www.xanthomonas.org/t3e.html> and Genbank. In order to identify conserved motifs in the AvrGf1 and AvrGf2, as well other members of the XopAG effector family, several translated amino acid sequences from different plant pathogenic bacteria were analyzed via Clustal W (EMBL-EBI), PCRL

software (Schein et al., 2001), and MEME Suite (Bailey et al., 2006) using default parameters in the output options.

Swapping of the C Terminal Domains from *avrGf1* to *avrGf2* Gene

Taking advantage of a *BglIII* restriction site present in position 1144 on *avrGf2*, a hybrid protein with the N-terminal region of AvrGf2, and the C-terminal region of AvrGf1, which contained two putative motifs previously identified using MEME program was constructed (Fig. 3-2). First, a 375 bp *BglIII-EcoRI* PCR product, which contains the C-terminal part of the gene, *avrGf1*, was amplified from Xc-Aw12789 genomic DNA by PCR using primers SWAP-F (5'-CGCGATCTATGGCTAAGCAGAAGAACATGGAA-3'), and SWAP-R (5'-CGCAGATCTTAGTCGCTGCTGGTCATTGACTTT-3'). The PCR fragment was digested with *BglIII* and *EcoRI* enzymes, and purified using the phenol-chloroform Na-acetate precipitation method (Sambrook et al., 1989). Next, the gene *avrGf2* contained in a *EcoRI* fragment cloned from the Xfa-C library in the construct pGEMT-*avrGf2*-15B (Table 2-1), was digested with *BglIII* enzyme (Promega), purified, mixed with an aliquot of the previously digested 375bp PCR amplicon in a proportion of 3:1 (pGEMT-*avrGf2*-15B: *BglIII-EcoRI* PCR product), and ligated using T4 ligase (Promega) to obtain the construct pGEMT:*NavrGf2-CavrGf1*, and transformed into *E. coli* DH5 α . A clone, *NavrGf2-CavrGf1*, containing the C-terminal fragment of *avrGf1* in pGEMT:*avrGf2* was confirmed by Sanger sequencing. The construct pGEMT:*NavrGf2-CavrGf1* was digested using *EcoRI* (Promega) restriction enzyme, and religated into pLAFR3, a *Xanthomonas* compatible plasmid. The new construct was transformed into *E. coli* DH5 α and mobilized into recipient Xc-A-306 by triparental mating for subsequent infiltration into GF and KL leaves, for characterization by determining population dynamics and electrolyte leakage.

Mutational Analysis of *avrGf2* 'CLNA' Motif

Using MEME, a highly conserved domain (CLNAXYD) (Figure 3-3) was identified in several XopAG family effectors described in the online database <http://www.xanthomonas.org/t3e.html>. Given that this domain was highly conserved in this effector family, a mutation for the conserved site *avrGf2*-C⁴⁴⁹LNAXYD was created in *avrGf2* to determine its importance in the effector for eliciting an HR in grapefruit. Conserved residues Leu⁴⁴⁹-Asp (L⁴⁴⁹N) of *avrGf2* were mutated to Ala and Ser (A⁴⁴⁹S) by a PCR-mutagenesis approach (Potnis et al., 2012) using primers: CLNA-CASA-F (5'-GCGCTAGCGCTGTTTACGACAACGCCA-3') and CLNA-CASA-R (5'-GCGCTAGCGCATCCAACACTACGGCAACA-3'). Both primers contain *NheI* overhangs at the 5' end for use with pGEMT-Easy:*avrGf2* construct as template. The target for this specific mutagenesis was the central amino acids (L⁴⁴⁹N) of the motif, 'C⁴⁴⁸LNA', to create 'C⁴⁴⁸ASA.' After purification of the PCR product, using a Qiagen (Valencia, CA, USA.) spin kit, the amplicons were digested with *NheI* (Promega). The products were religated and transformed into *E. coli* DH5 α . The presence of the mutation was confirmed by Sanger sequencing and the mutant gene construct was moved into pLAFR3 vector, a *Xanthomonas*-compatible plasmid, mobilized into a recipient strain, Xc-A-306, by triparental mating, with subsequent infiltration into GF and KL leaves for characterization of plant reaction (i.e., population growth and electrolyte leakage using) as described by Gochez, et al. (2008, 2012).

Mutation of a Cyclophilin Binding Site in *avrGf2*, and Phenotype Characterization of Mutants

Catalytic residues of a cyclophilin binding site in *avrGf2* were mutated to alanine (A) and/or serine (S) by a PCR-site direct mutagenesis approach (Potnis et al., 2012)

The target of this specific mutagenesis was the G³⁵⁷ in 'G³⁵⁷PLL' to be mutated to 'A³⁵⁷ASL' using the primers: AASL-F (5' GCGCTAGCCCGCTTCTCCACGAGCTT 3') and AASL-R (5' GCGCTAGCGACGCTGGTATTACGCCG 3'). After amplification and purification of the PCR product, using Qiagen (Valencia, CA, USA.) spin kit, the amplicons were digested with *NheI* enzyme (Promega). The product was religated and transformed into *E. coli* DH5 α , and Sanger sequencing confirmed the insert. The construct was then moved into the *Xanthomonas*-compatible plasmid pLAFR3, mobilized into the recipient strain, Xc-A-306, by triparental mating, and subsequently infiltrated into GF and KL leaves for characterization of plant reactions (i.e., population growth and electrolyte leakage).

The same experimental design was used to create a single mutation in the 'G³⁵⁷PLL' site of gene *avrGf2*, changing the amino acid Gly to Ser by PCR and maintaining the amino acid proline, which could have structural importance in the 3D structure of the *avr* gene (Coaker et al., 2006). For these experiment primers SPLL-F (5'-GCGCTAGCCCGCTTCTCCACGAGCTT-3') and SPLL-R (5'-GCGCTAGCGACGCTGGTATTACGCCG-3') were used to create the mutant as described above (Chapter 2).

Determination of the Interaction between a Citrus Cyclophilin and XopAG Effectors Using a Yeast Two Hybrid Approach

A yeast two-hybrid experiment was performed using a constitutively expressed *GF-Cyp* gene cloned from GF cDNA. The *GF-Cyp* gene, that had 100% match at the nucleotide level with the previously identified *Cs-Cyp* gene (Campos et al., 2013), was cloned using pDBLeu (GAL4 DB; bait; +Leu) (Invitrogen®). Both XopAG genes, *avrGf1* and *avrGf2*, were amplified from total genomic bacterial DNA using PCR, and cloned

into pPC86 (GAL4 AD; prey, +Trp) (Invitrogen®). Each construct (pDBLeu-*GF-Cyp*, pPC86-*avrGf1*, and pPC86-*avrGf2*) was mobilized into *E.coli* DH5α strain, and the plasmid was extracted using a conventional miniprep method (Sambrook et al., 1989).

The constructs were verified by DNA sequencing and used as bait/prey in a two-hybrid assay. Bait (pDBLeu –Cyclophilin) and preys ((pPC86- *avrGf1*) or (pPC86-*avrGf2*)) were cotransformed into *Saccharomyces cerevisiae* strain CG 1945 (*MATa*, *ura3-52*, *his3-200*, *ade2-101*, *lys2-801*, *trp1-901*, *leu2-3, 112*, *gal4-542*, *gal80-538*, *cyhr2*, *LYS2 : : GAL1UAS-GAL1TATA-HIS3*, *URA3 : : GAL4 17-mers(x3)-CYC1TATA-lacZ*). The cells were grown for 5 days at 30°C on Synthetic Drop-out Medium (ClonTech Lab. Inc.) lacking tryptophan (-Trp), leucine (-Leu) and histidine (-His) in containing 5 mM 3-aminotriazole (3AT). Gene accession information, *avrGf1*= DQ275469.1; *GF-Cyp*= GQ853548.1 ; *avrGf2*= KM30332.

Determination of the Interaction between a Citrus Cyclophilin and AvrGf2 Using a Transient Silencing Approach *in planta*

To demonstrate the importance of the presence of constitutively expressed Cyp in GF for elicitation of HR, a transient *GF-Cyp* silencing experiment in GF was performed to determine if variation in expression level of *GF-Cyp in planta* affected elicitation of HR. A 200 bp cDNA region of the 5'-terminal region of the *GF-Cyp* gene was amplified using primers Cyclo-Eco-F (5'-CCGGAATTCATGCCAAACCCCAAAGTGTT-3'), and Cyclo-Eco-R (5'-CCGGAATTCGAATCCGGGGATCACACGGT -3'), digested using *EcoRI* restriction enzyme (Promega), and cloned into the entry vector pENTR3C (Gateway). The RNAi construct was made using pHellsgate12 through recombination using Gateway® LR Clonase II Enzyme mix (Invitrogen, Grand Island, NY, USA). The *GF-Cyp*-RNAi

constructs were transformed in *Agrobacterium tumefaciens* strain CV301 (GV3101). Suspensions of GV3101 adjusted to 5×10^6 CFU/ml containing the RNAi construct (GV3101:pHell-GF-Cyp) were infiltrated into young GF leaves, and samples were taken every 24 h for 6 days and frozen in liquid nitrogen. Total mRNA was isolated using a Trizol (Sigma, St Louis, MO, USA) protocol as recommended by the manufacturer, and treated with DNA-free Dnase (Ambion, Austin, TX, USA) to remove any contaminating DNA; finally QRT-PCR was performed with the samples using a Bio-Rad CFX96 Touch™ Real-Time PCR Detection System to quantify the expression level of the target gene *GF-Cyp* compared to the constitutively expressed gene, EF1, using primers EF1alpha-F (5'-GTAACCAAGTCTGCTGCCAAG-3') and EF1alpha-R (5'-GACCCAAACACCCAACACATT-3'). The cycle threshold values (Ct-GF-Cyp) obtained using a Bio-Rad CFX Manager 3.0 software were normalized and compared with the average Ct-EF1 value (Ct-cycloN_n=[Ct-EF1_n]/[Ct-GF-Cyp_n], where *n* corresponded to number of the day sampled). The relative expression level change (fold change) for every day sampled *n* (Ct-GF-CypF_n) was obtained after comparison of the average Ct-GF-CypN_n values obtained vs Ct-GF-CypN₀ ($\Delta\Delta C_T$ -GF-CypF_n= ΔC_T -GF-CypN₀- ΔC_T -GF-Cyp_n). A general statistical analysis of the normalized $\Delta\Delta C_T$ values (mean, standard and error deviation, confidence interval, and t-Student comparison) was calculated using JMP® software (SAS Institute).

In order to evaluate the possible interactions of *AvrGf2* effector with *GF-Cyp* in GF leaves, a co-infiltration experiment was performed to assess and quantify bacterial populations and electrolyte leakage as follows: young GF leaves were separately infiltrated with a suspension of 5×10^6 CFU/ml of GV3101:pHellsGate and

GV3101:pHellsGate-*GF-Cyp*; immediately after infiltration half of the leaves were separately co-infiltrated with 5×10^5 CFU/ml of suspensions of Xc-A306:pLAFR3 or Xc-A306:*avrGf2* at 0 DAI (no-silence effect), and the other half at 4 days after infiltration (DAI). Bacterial populations were determined for 12 days as described previously using the set of leaves infiltrated with *Xanthomonas* at 0 and 4 DAI. In order to characterize electrolyte leakage in *GF-Cyp* silenced leaves, several leaves were infiltrated with a bacterial suspension adjusted to 5×10^6 CFU/ml for GV3101:pHellsGate, and also for GV3101:pHellsGate-*GF-Cyp* at 0 DAI. At 4 DAI leaves were infiltrated with suspensions adjusted to 5×10^8 CFU/ml of Xc-A306:pLAFR3 or Xc-A306:*avrGf2* I. Two electrolyte leakage experiments were performed over a 4-day period as described before. The area under the curve (AUC) was calculated using the formula described in Madden et al (2007), and the AUC values were compared using proc ANOVA (SAS Institute).

Results

The XopAG-effectors AvrGf1 and AvrGf2 Share Related Functional Features

Both avirulence genes, *avrGf1* (1599 bp) and *avrGf2* (1527 bp), produced HR in citrus. Using the discontinuous megablast nucleotide BLAST algorithm for alignment comparison, both avirulence genes share low sequence similarity at the nucleotide level, except for a small region in the last 200 nucleotides of the genes that shows a high level of identity (68%). The alignment of translated proteins AvrGf1 (533 aa) and AvrGf2 (509 aa) using ClustalW and BLASTp algorithms determined that AvrGf2 had a low degree of homology (45% amino acid identity) with the previously identified citrus XopAG effector, AvrGf1 present in Xc-Aw strains (Fig. 3-1). Again, higher identities were observed between AvrGf2 and AvrGf1 in the C terminal part of the effector proteins. The translated nucleotide sequences of *avrGf1* and *avrGf2* were aligned using

ClustalW and found to contain putative chloroplast localization signals in the effectors, when analyzed using the bioinformatics tool, PCLR Chloroplast Localization Prediction (Schein et al., 2001). A chloroplast localization signal was predicted for AvrGF1 in its first 87 amino acids, and for AvrGF2 in its first 69 amino acids (with predicted values of 0.857 and 0.937 respectively) (Figure 3-1).

The C-terminal Part of XopAG-AvrGf2 Effector is Essential for Elicitation of HR in Citrus

Using MEME Suite software (Bailey et al., 2006), three common C-terminal motifs were identified in XopAG AvrGf1 and AvrGf2 effectors (Figure 3-2.A). Previous work demonstrated that elimination of the C terminal region of AvrGf1 resulted in the effector lacking the ability to elicit an HR (Figueiredo et al., 2011). In the MEME result, the same region truncated in a study by Figueiredo et al. (2011) corresponded to the last two putative motifs identified by MEME Suite (Figure 3-2).

AvrGf2 was shown to elicit a faster HR in citrus than AvrGf1 (Chapter 2). Given that only the C terminal parts of both effectors have a high degree of similarity, the first experimental approach was to determine if the C terminal portion of the effector could be swapped and still elicit an HR. Therefore the N-terminal portion of *avrGf2* was replaced with the corresponding N-terminal portion of *avrGf1* to create the hybrid protein N-AvrGf2:C-AvrGf1 (1508 nucleotides). The hybrid effector gene *N-avrGf2:C-avrGf1* was cloned in the *Xanthomonas* compatible vector pLAFR3, conjugated in Xc-A 306 by triparental mating, and infiltrated at 10^8 CFU/ml into GF leaves. No difference was observed between the strain Xc-A306 that carried the construct N-AvrGf2:C-AvrGf1, and strain Xc-A306:pLAFR3 which did not produce an HR. In a second approach, the highly conserved domain (CLNaxYD) was identified in several XopAG family effectors using

MEME (Figure 3-3). Following mutation of the first amino acids in the motif CLNAXYd (AvrGf2-C⁴⁴⁹LNA for AvrGf2-C⁴⁴⁹ASA), a construct that contains the mutant effector AvrGf2-CASA was cloned in pLAFR3 vector, and expressed in Xc A306 by triparental mating. A bacterial suspension of Xc-A306:*avrGf2*-CASA was adjusted to 5x10⁸ CFU/ml, and infiltrated into GF leaves. This construct did not elicit HR compared to the wild type gene expressed in Xc-A306:*avrGf2* strain (Figure 3-4).

The XopAG AvrGf2 Effector Contains a Cyclophilin Binding Site that Determines the Elicitation of HR in Citrus

Based on the amino acid sequence of the effector AvrGf2, a putative ‘cyclophilin binding motif’ (GPxL) (Block & Alfano, 2011) was identified, which was present at amino acid position 356 (AvrGf2-G³⁵⁶PLL). The site ‘GPxL’ was also identified in all XopAG effector family members previously described in the phylogenetic analysis Chapter (Figure 2-12). A pGEMT:*avrGf2* construct was used as a template for site directed PCR mutagenesis of the GPLL site in *avrGf2* (Potnis et al., 2012). The mutant gene *avrGf2*-‘A³⁵⁶ASL’ when cloned in pLAFR3 plasmid and transformed into Xc-A306 (Xc-A306-AASL) did not elicit an HR in GF leaves (Figure 3-5). The next step in this analysis was to determine if a single mutation of the Gly³⁵⁶ amino acid in the motif ‘GPLL’, would affect HR elicitation. We did not want to alter the proline as it is reported to be important in maintaining the structure of proteins and could be important in the final folding of the effector once delivered to the plant (Coaker et al., 2006). Therefore, the Gly was changed to S to create AvrGf2-S³⁵⁶PLL (Xc-A306-SPLL). After infiltration of the Xc-A306-SPLL mutant, a slower type of HR was elicited compared with the HR induced by Xc-A306:*avrGf2* strain (Figure 3-5).

Growth of Xc-A306, transconjugant carrying *avrGf2* and transconjugants carrying mutations in '*avrGf2*-GPLL' were examined by determining bacterial populations in inoculated leaf tissue. Internal populations of the wild-type strain Xc-A306:pLAFR3 increased up to 10^8 CFU/cm² by 10 days post inoculation (Figure 3-6A). Strain Xc-A306 carrying the *avrGf2*-AASL clone reached close to 10^8 CFU/cm² and then growth ceased to increase and stayed at the same level afterwards, whereas mutant Xc-A306:*avrGf2*-SPLL grew up to 10^6 CFU/cm² (Figure 3-6A). In summary, a strain carrying *avrGf2* gene grew significantly less compared to Xc-A306 transconjugants carrying the mutant versions of *avrGf2* (-AASL and -SPLL). Both mutants exhibited more growth *in planta* compared to Xc-A306 transconjugants carrying *avrGf2*. Although mutant -SPLL showed reduced growth compared to Xc-A306 and mutant -AASL strains, the populations reached for mutant -SPLL were higher than the population measured for Xc-A306:*avrGf2* strain (Figure 3-6A).

In electrolyte leakage experiments, leaf tissue infiltrated with Xc-A306:*avrGf2* reached a maximum increase in conductivity 3 days after infiltration (when an HR was observed), while a maximum loss in electrolytes in tissue infiltrated with Xc-A306:*avrGf1* did not occur until day 6. Leaf tissue infiltrated with the mutant Xc-A306-SPLL had similar values as Xc-A306 and Xc-A306-AASL (no HR) until day 4 after inoculation, and 6 days after infiltration the electrolyte leakage values increased in the SPLL mutant inoculated leaf, but not in the wild type or AASL mutant inoculations (Figure 3-6B).

A Constitutively Expressed Cyclophilin in Grapefruit Interacts with AvrGf1 and AvrGf2

The yeast two-hybrid experiments between GF-Cyp, and T3E *avrGf1* or *avrGf2* confirmed the interaction between both avirulence gene proteins and the plant cyclophilin protein. The combination of GF-Cyp and avirulence genes (*avrGf1* and *avrGf2*) in a double carrier strain, allowed growth of the yeast on SD media lacking His, Trp, and Leu (Figure 3-7).

In the transient silencing experiment, normal expression values for gene GF-Cyp were registered at the time of inoculation (0 DAI) and 1 DAI using QRT-PCR quantification (Table 3-1), whereas at 2 DAI a reduction in expression of *GF-Cyp* in GF leaves was observed (Figure 3-8). There was a difference in the extent and speed of tissue damage between *avrGf2* clones in silenced and non-silenced conditions (Figure 3-9). Infiltration of GF leaves with *Agrobacterium* GV3101 (non-silence *GF-Cyp*, Agro) and GV3101:sGF-Cyp (silenced *GF-Cyp*, sCyp) and subsequent infiltration of Xc-A306 and Xc-A306:*avrGf2* resulted in a different phenotype for the GV3101:sGF-Cyp leaves infiltrated with Xc-A306:*avrGf2* in 4 DAI, compared with the values obtained 3 DAI (Figure 3-9). The growth of Xc-A306 and Xc-A306:*avrGf2* strains was examined by quantifying bacterial populations (CFU/cm²) in inoculated GF-Cyp silenced leaves (sCyp), and GF-Cyp non-silenced leaves (Agro), following infiltration 0 and 4 DAI with the *Agrobacterium* strains. There were no obvious differences in the bacterial growth curves obtained in silenced or non-silenced leaves (Figure 3-10-A and 3-10-B respectively). The electrolyte leakage data for the pathogenicity reaction observed after infiltration of strain Xc-A306 in silenced and non-silenced GF leaves showed significant differences compared to the HR produced after infiltration of Xc-A306:*avrGf2* in GF

leaves. However, GF-Cyp (Agro) non-silenced tissue inoculated with Xc-A306 carrying *avrGf2* increased electrolyte leakage significantly, showing a peak at 48 hr compared to the same strain infiltrated in GF-Cyp (sCyp) silenced tissue, which showed a peak after 72 h for strain Xc-A306 infiltrated in Agro or sCyp leaves (Figure 3-11).

Discussion

Although nucleotide identity between *avrGf1* and *avrGf2* genes was low, the translated sequences of these genes had slightly higher identity, which was also observed in all other members of the XopAG Class effector group. Both citrus avirulence genes, *avrGf1* and *avrGf2*, contained predicted chloroplast localization signals, of which AvrGf1 was confirmed by Figueiredo et al. (2011). This has not been determined in other XopAG members. It is also notable that all the XopAG effector family members contain two conserved C-terminal motifs with highly-conserved amino acids. No difference was observed between the strain (Xc-A306) that carried the construct N-Avrgf2:C-AvrGf1, and the negative control (Xc-A306:pLAFR3), indicating a possible non-functionality of the hybrid protein, which may have been due to, among other factors, incorrect folding of the effector or even a lack of translation of the transcript. One of these contained the motif, CLNAXYd (CLNA for CASA), which when expressed in Xc and infiltrated into GF resulted in no HR. It is interesting to note that only two point mutations were necessary to disrupt the ability of the effector to produce HR in the host. This highly conserved domain (CLNAXYD) is observed in all XopAG family members analyzed (nine bacterial species) (Figure 3-3), and the same motif was observed in all the XopAG effectors from the bacterial species included in the phylogenetic analysis (Figure 2-12). There is no reference about the functionality of this CLNAXYD motif in online databases (<http://www.genome.jp/tools/motif/>). Recently, 3D-

structures of several injectisome proteins, chaperones, and effectors (Phan et al., 2005, Davis et al., 2008, Potnis et al., 2012) have been determined using crystallography and NMR spectroscopy (Tampakaki et al., 2010). Currently, we have been unable to develop models concerning the 3D structures of any XopAG class effector (J. Hurlbert, unpublished data). It would be interesting to determine the importance of the highly conserved sequence in the C-terminal region, which includes the CLNaxYD motif in AvrGf2, and characterize its possible function in HR elicitation. Further analyses are necessary to confirm the correct expression of the mutant effector AvrGf2-CASA in bacteria, and also to confirm its translocation into the host.

A highly conserved cyclophilin (Cyp) binding domain (GPxL) (Figure 3-1) was identified in AvrGf1 and AvrGf2, and also in several XopAG family effectors described in the online database <http://www.xanthomonas.org/t3e.html>. Given that this domain is highly conserved in this effector family, two mutations for the conserved site *avrGf2*-G⁴⁴⁹PLL (-AASL, and -SPLL) were created in *avrGf2* to determine their functionality in eliciting an HR in GF. Although mutations 'AASL' abolished the HR caused by the wild type AvrGf2, the resistance reaction elicited by mutant 'SPLL' was different from the HR elicited by effectors AvrGf1 and AvrGf2. The infiltration of the Xc-A:*avrGf1* strain causes a slower HR (after 96 h) compared with strain Xc-A:*avrGf2* (72 h).

The yeast two-hybrid assay showed an interaction between a constitutively expressed cyclophilin in grapefruit and XopAG -*avrGf1* or *avrGf2* (Figure 3-7). A close relationship between the activation of some bacterial effectors and Cyp has already been previously confirmed (Coaker et al., 2005, Aumüller et al., 2010). Coaker *et al.* (2006) demonstrated that a single mutation in the Cyp binding site (GPxL motif) in

effector AvrRpt2 from *P. syringae* would affect for protease activity *in vitro*. Block *et al.* (2009) reported that another T3E, *HopG1* from *P. syringae*, a related member of the *XopAG* effector class, also contains this putative Cyp binding site (GPxL motif), and that the effector suppresses pathogen-associated molecular pattern (PAMP)-triggered immunity (PTI). Interestingly, Jamir *et al.* (2004), also demonstrated that HopPtoG from *P. syringae* DC3000 suppresses HR elicitation in tobacco; specifically mediating suppression of the *PR1a* gene. The yeast two-hybrid results support the idea of a protein-protein interaction between *XopAG* effectors and GF-Cyp. Using the Cs-Cyp 3D protein structure determined by Campos *et al.* (2013), the native AvrGf2-GPLL site was predicted to bind GF-Cyp as a substrate in molecular docking simulations; also, in experiments where peptides encoding the ‘GPLL’, ‘AASL’, and ‘SPLL’ domains were used, preliminary isothermal titration calorimetry experiments confirm strong interaction between the ‘GPLL’ peptide, as well as interaction of the “SPLL” peptide with purified GF-Cyp, but no interaction between the “AASL” peptide and GF-Cyp could be defined (J. Hurlbert, unpublished).

Cyclophilins (Cyps) are widely reported in prokaryotes and eukaryotes (Wang & Heitman, 2005). These proteins exhibit a characteristic peptidyl prolyl isomerase that catalyzes *cis-trans* isomerization of proline imidic peptide bonds, and as a result accelerates protein folding (Schmid, 1995). This family shares a conserved protein structure, but a diversity of functions in the cell (Stamnes *et al.*, 1992, Heitman *et al.*, 1992); the most well defined function is related to immunosuppression (Göthel & Marahiel, 1999). Numerous Cyps have been characterized *in planta* (He *et al.*, 2004), and different numbers of genes of these proteins were identified in several species

(Gupta et al., 2002). Using QRT-PCR a constitutively expressed *Cyp* was cloned from a cDNA library of Sweet orange (*C. sinensis* cultivar Pera, *Cs-Cyp*: Genbank accession number GQ853548.1) (Domingues et al., 2012). That gene was identical to two other constitutively expressed Citrus *Cyp* genes previously cloned from the hybrid *C. cv.* Shiranuhi [(*C. reticulata* × *C. sinensis*) × *C. aurantium*] *Cyp* (*Sh-Cyp*; EF122402), and *C. cv.* Clementine [*C. reticulata* × *C. sinensis*] hypothetical protein CICLE (*CC-Cyp*; XM_006423544). Recently (Domingues et al., 2012), the tridimensional structure of *Cs-Cyp* was determined using X-ray diffraction of different *Cs-Cyp* complexes to identify possible catalytic domains. A transgenic sweet orange line, which was down-regulated for *Cs-Cyp* showed more susceptibility to citrus canker, and it was determined that *Cs-Cyp* is involved in the elicitation of the citrus canker symptoms. In this work, a transient approach using *Agrobacterium* was used to silence GF-*Cyp* in Duncan GF leaves. The down-regulation of the GF-*Cyp* gene was corroborated using QRT-PCR. Even after a GF-*Cyp* transient down-regulation, a basal level of *Cyp* was still expressed in GF leaves (Figure 3-8). A delay in the HR elicitation for *avrGf2* in leaves with reduced GF-*Cyp* expression was observed (Figure 3-9).

Domingues et al (2012) demonstrated that *Cs-Cyp* protein is present in the nucleus of the cell. Several studies have reported the presence of *Cyp* also in the chloroplast, where it may participate in different roles in the lumen and thylakoid (Romano et al., 2004, Fu et al., 2007, Dominguez-Solis et al., 2008). The silencing of GF-*Cyp* gene in citrus should allow the determination of these protein-protein interactions and confirm if they have a role in the resistance process (Domingues et al., 2012).

The expression of *GF-Cyp* was only down-regulated in GF leaves in transient *GF-Cyp* knock-down leaves after 4 days of the infiltration with *Agrobacterium*. Lower electrolytes leakage values were observed for the *GF-Cyp* silenced leaves compared with the non-silenced leaves. Here, a slight change in bacterial populations and electrolyte leakage values was observed after silencing of *GF-Cyp* gene; these results did not completely match with previous studies, (Domingues et al., 2012) or even with what was expected here: a non-elicitation of HR after infiltration of the transiently silenced leaves with strain Xc-A306:*avrGf2*. Substantial differences were not observed between the population dynamics of *GF-Cyp* silenced and non-silenced leaves infiltrated with Xc-A306 (Figure 3-10). The observed delayed HR elicited by *avrGf2* in leaves with reduced *GF-Cyp* expression (Figure 3-9) is supported by the reduction in electrolyte leakage values induced by strain Xc-A306:*avrGf2* in *GF-Cyp* silenced leaves (Figure 3-11), which was significantly different than the HR by Xc-A306:*avrGf2* strain in non-silenced GF leaves (Table 3-2). Interestingly, a similar situation was observed after infiltration of GF leaves with the mutant strain Xc-A306:*avrGf2*-SPLL, which elicited a slow HR compared with strain Xc-A306:*avrGf2*. In this case, and based on preliminary molecular simulations (J. Hurlbert, unpublished) a possible explanation would be that after the mutant effector enters the plant cell in the *cis*-state and is still recognized by the plant Cyp, resulting in the protein being isomerized to its *trans*-state at a lower rate compared to the wild type effector AvrGf2. The recognition of the *trans* 'isomer, (i.e., "SPLL') version of the effector by the plant cyclophilin as the inducer of the resistance reaction was demonstrated by the increased electrolyte leakage and bacterial population differences registered in GF leaves (Figure 3-6).

In conclusion, the two avirulence genes, *avrGf1* and *avrGf2*, both members of the XopAG family, have 45% identity at the amino acid level and both contain chloroplast localization signals. Their dissimilar nucleotide sequences suggest that these effectors arose through convergent evolutionary processes. Based on amino acid sequence comparisons, two C-terminal motifs were identified in AvrGf1 and AvrGf2 effectors and also in several XopAG related members described from *Xanthomonas* spp., *Pseudomonas* spp., *Acidovorax citrulli*, and *Ralstonia solanacearum*. A putative C-terminal domain contains a conserved site CLNAXYD, and its presence was determined to be essential for HR elicitation. A cyclophilin binding site (GPxL), also conserved in all the XopAG class effector family members was determined to be essential for HR elicitation although slight modification delayed the HR.

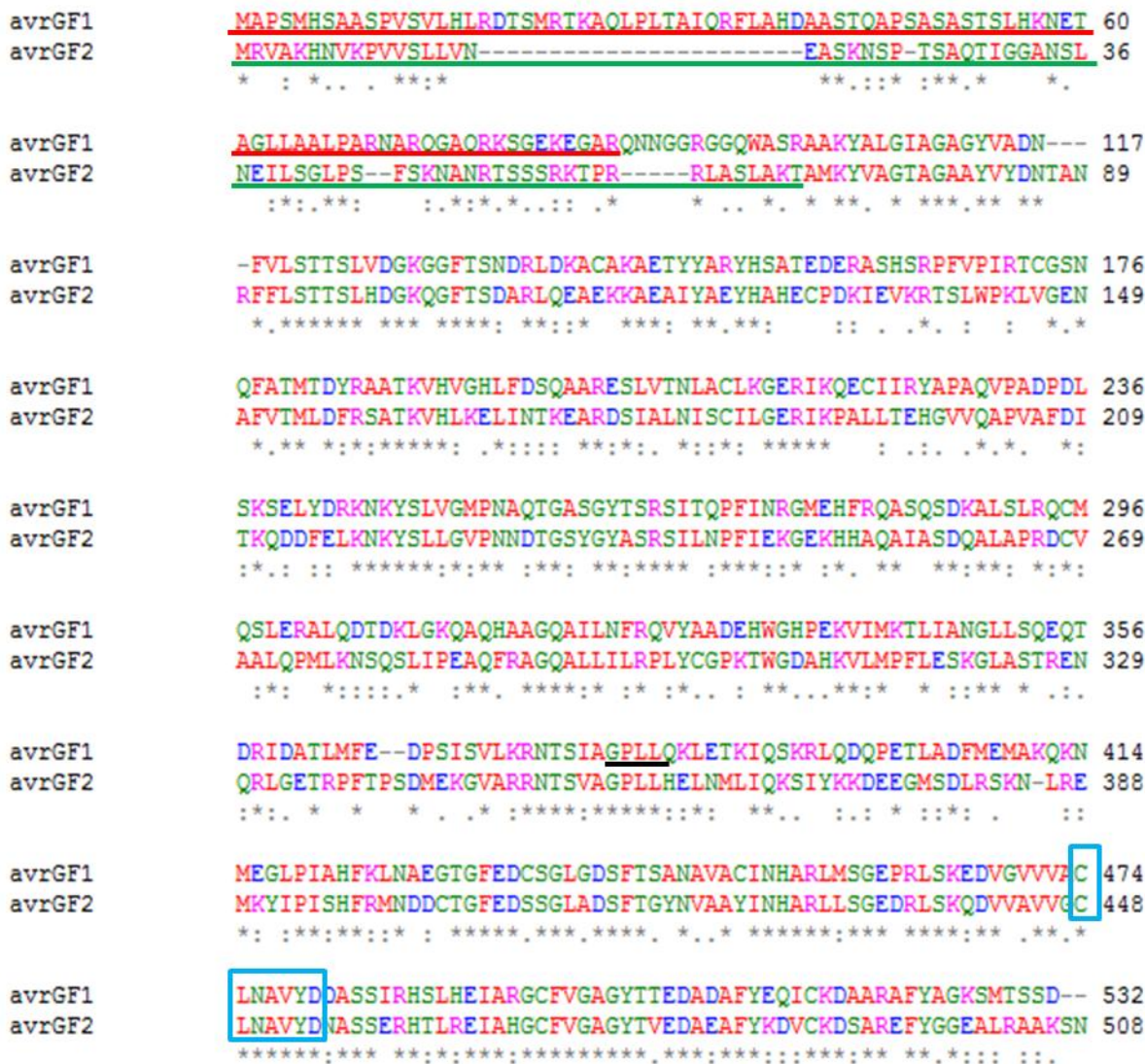


Figure 3-1. Clustal W multiple sequence alignment of translated proteins AvrGf1 (from XC-Aw) and AvrGf2 (from Xfa-C). The comparison showed 45% identity (226/498), with 62% positives values. Both proteins contain chloroplast localization signals, AvrGF1 in its first 87 (red underline), and AvrGF2 in its first 69 amino acids (green underline) with probability values of 0.857 and 0.937, respectively (PCRL standard limit value=0.45). A cyclophilin binding site 'GPxL' (black underline), and a putative conserved domain CLNAXYD (blue box) were identified in both sequences.

A



B

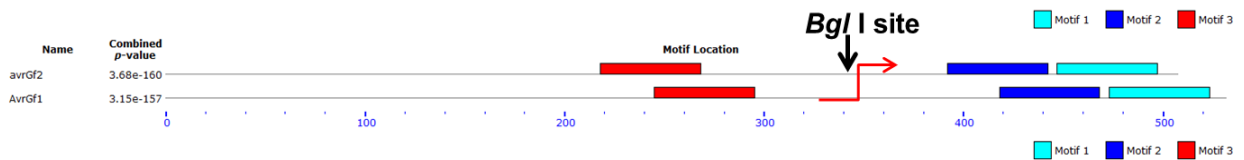
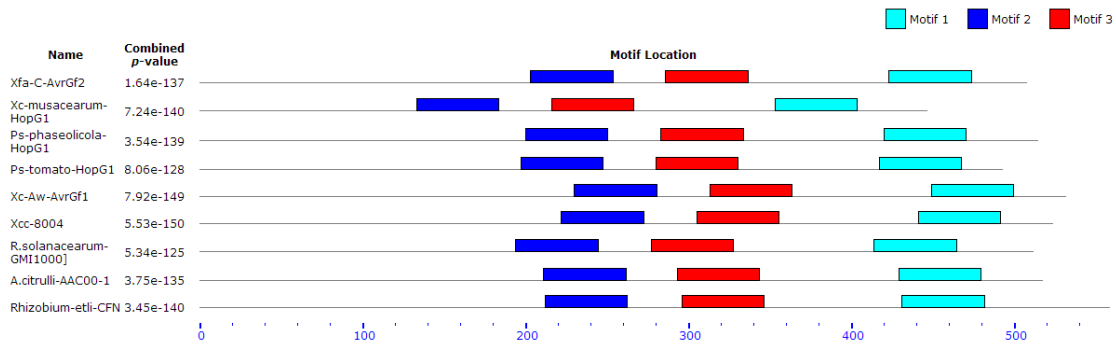
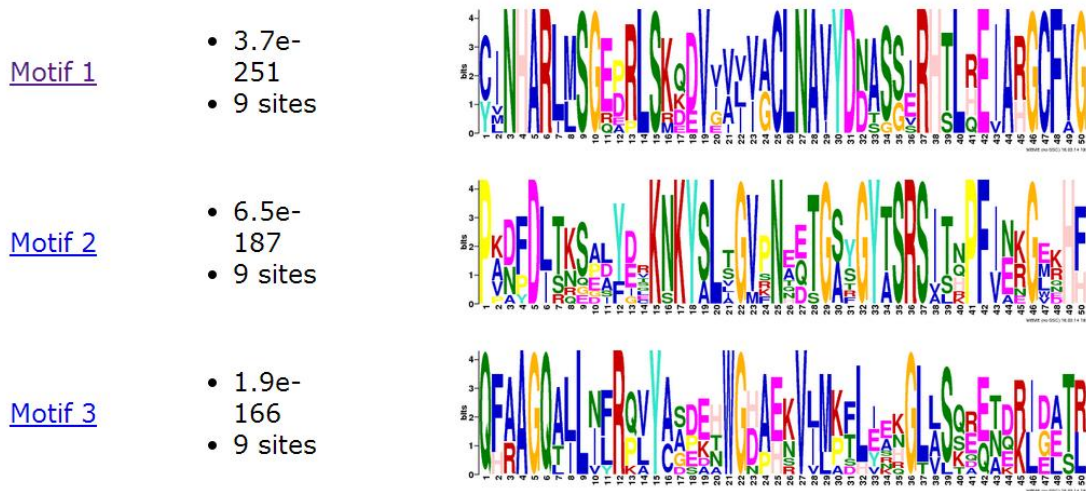


Figure 3-2. (A) Three C-terminal domains were predicted in AvrGf1 and AvrGf2 using MEME Suite. (B) To determine if the motifs were responsible for the difference in HR timing between AvrGf1 and AvrGf2, *avrGf2* was digested using *Bgl I* and religated with a PCR fragment corresponding to the latter two C-terminal motifs (motif 1 and 2) from *avrGf1*, creating the hybrid protein *NAvrGf2::C³⁸³AvrGf1* that was cloned into pLAFR3. The hybrid protein expressed in Xc-A306 looks non-functional 6 days after infiltration in GF (No HR was observed).

A



B



C

Name	Start	p-value	Sites
Xcc-8004	442	2.08e-60	DSFTSANAVA CIN ARLMSG EP RLSKQ DV GVV V ACLN AV Y DD ASS VR SL HE I AR GC FC VG AGYTT ED ADV
Xc-Aw-AvrGf1	450	4.42e-59	DSFTSANAVA CIN ARLMSG EP RLSK ED VGVV V ACLN AV Y DD ASS IR SL HE I AR GC FC VG AGYTT ED ADA
Xc-musacearum-HopG1	354	3.06e-57	DSFTGYNVSA YIN ARLLSG ED RLSKQ DV V V AV IG CLN AV Y DN ASS ER TL RE IA IG CF VG AGYTT VE DAEA
Xfa-C-AvrGf2	424	5.59e-57	DSFTGYNVAA YIN ARLLSG ED RLSKQ DV V V AV IG CLN AV Y DN ASS ER TL RE IA IG CF VG AGYTT VE DAEA
Ps-phaseolicola-HopG1	421	1.26e-55	DSFTGYNVSA YIN ARLLSG ED RLSK QD V V AV IG CLN AV Y DN ASS ER TL RE IA IG CF VG AGYTT VE DAED
A.citrulli-AAC00-1	430	5.54e-54	DSFTAANAVA CIN ARLMSG EP RLSMQ DV E V LIACLN AV Y DD ASS RS TL Q E IA RG CF AG AGYTT IE DADA
Rhizobium-etli-CFN	432	2.89e-53	DSFTCANAVA CMN ARLMSG Q ARLS KE V IV IVACLN AV Y DD T SS IR TL HE VA RG CF VG AGYTT VE DADA
Ps-tomato-HopG1	418	5.30e-53	DSFTALNATS CVN ARIMS GE PP LS K DD V V IL IG CLN AV Y DN SS G IR SL RE IA RG CF VG AGFT VQ DGDD
R.solanacearum-GMI1000]	415	2.94e-51	DSFTSLNATA CLN ARLMSG RE RLSR DE V IV LIACLN AV Y DN AG G IR TL Q E IA RG CF VG AGYTT VA EADD

Figure 3-3. (A) Three C-terminal domains were predicted in nine XopAG effectors (from five different bacterial genera) using MEME Suite. (B) For all the XopAG effectors included in this comparison, the 'CLNAXYD' site is highly conserved in Motif 1. (C) Motif 1 sequence comparison alignment for Xfa-C-AvrGf2 [*Xanthomonas fuscans* subsp. *aurantifolii* str. ICPB 10535 type III (T3) secretion effector *avrGf2*]; Xc-musacearum-HopG1 [*X. campestris* pv. *musacearum* NCPPB4381 T3 effector HopG1]; PS-phaseolicola-HopG1 [*Pseudomonas syringae* pv. *phaseolicola* 1448A T3 effector HopG1]; Ps-tomato-HopG1 [*P. s.* pv. *tomato* str. DC3000 T3 effector HopG1]; *Rhizobium-etli*-CFN [*Rhizobium etli* CFN 42 hypothetical protein RHE_PA00116]; Xc-Aw-avrGf1 [*X. axonopodis* pv. *citri* secretion effector *avrGf1*]; R.solanacearum-GMI1000 [*Ralstonia solanacearum* GMI1000]; A.citrulli-AAC00 [*Acidovorax citrulli* AAC00-1 CP000512.1]; and Xcc-8004 [*X. campestris* pv. *campestris* str. 8004 CP000050.1].



Figure 3-4. The effect of site directed mutagenesis of CLNA motif in *avrGf2* gene on elicitation of an HR. The construct (pGEMTE:*avrGf2*.C⁴⁴⁸ASA was mutated using a PCR mutagenesis approach. The pLAFR3 vector carrying different constructs was conjugated by triparental mating into Xc-A306 strain, and infiltrated at 5×10^8 CFU/ml into grapefruit leaves. The strain designatons are: Xc-A= Xc-A306:pLAFR3; Xc-A:*avrGf2*= Xc-A306:*avrGf2*; or Xc-A:CASA (1 and 2)= Xc-A306:*avrGf2*-CASA in grapefruit leaves.

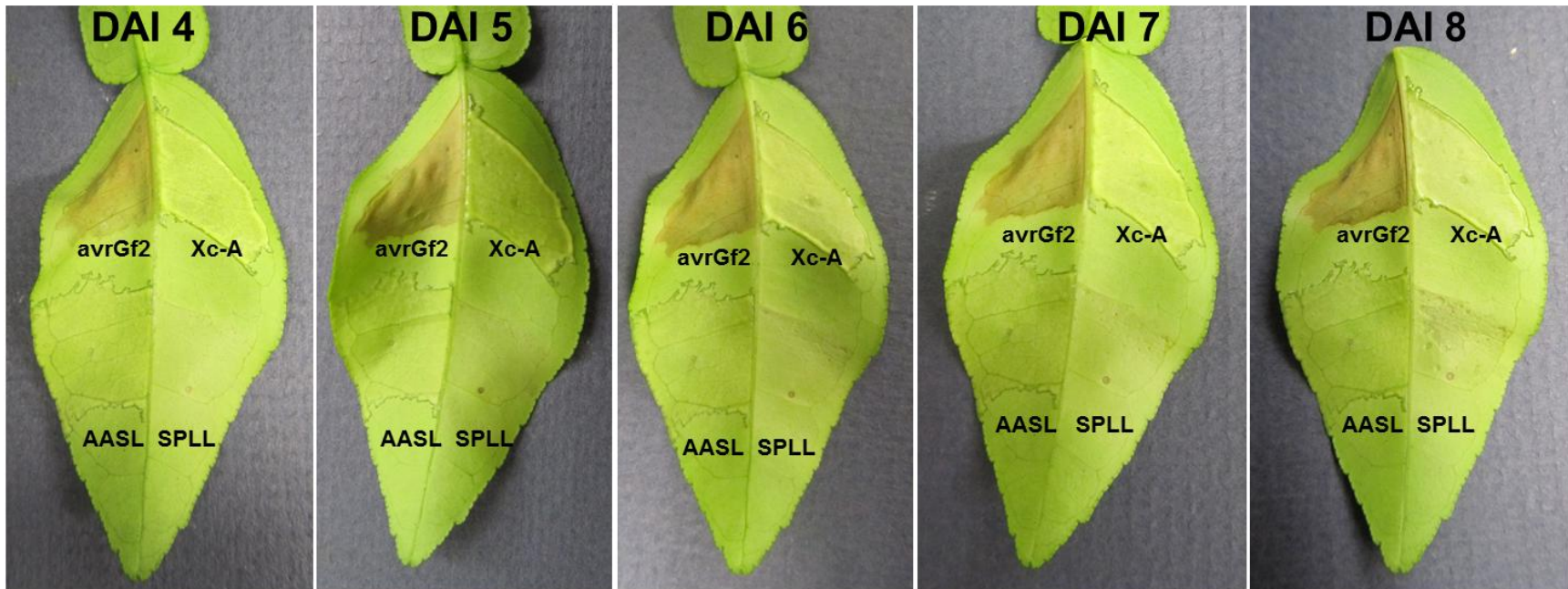
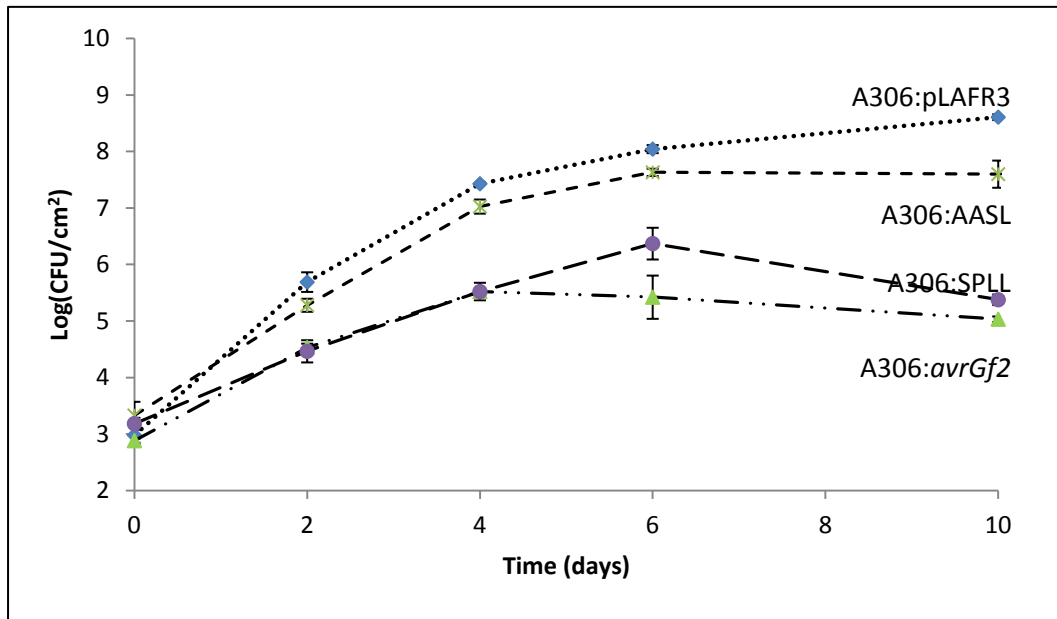


Figure 3-5. The effect of site directed mutagenesis of GPxL motif in *avrGf2* gene on elicitation of an HR. The construct (pGEMTE:*avrGf2*.A³⁵⁶ASL, and pGEMTE:*avrGf2*.S³⁵⁶PLL) was mutated using a PCR mutagenesis approach. The pLAFR3 vector carrying different constructs was conjugated by triparental mating into Xc-A306 strain. The following strains were infiltrated into GF leaves at 5×10^8 CFU/ml: Xc-A= Xc-A306:pLAFR3; *avrGf2*= Xc-A306:*avrGf2*; AASL= Xc-A306:*avrGf2*-A³⁵⁶ASL; and SPLL= Xc-A306:*avrGf2*-S³⁵⁶PLL.

A



B

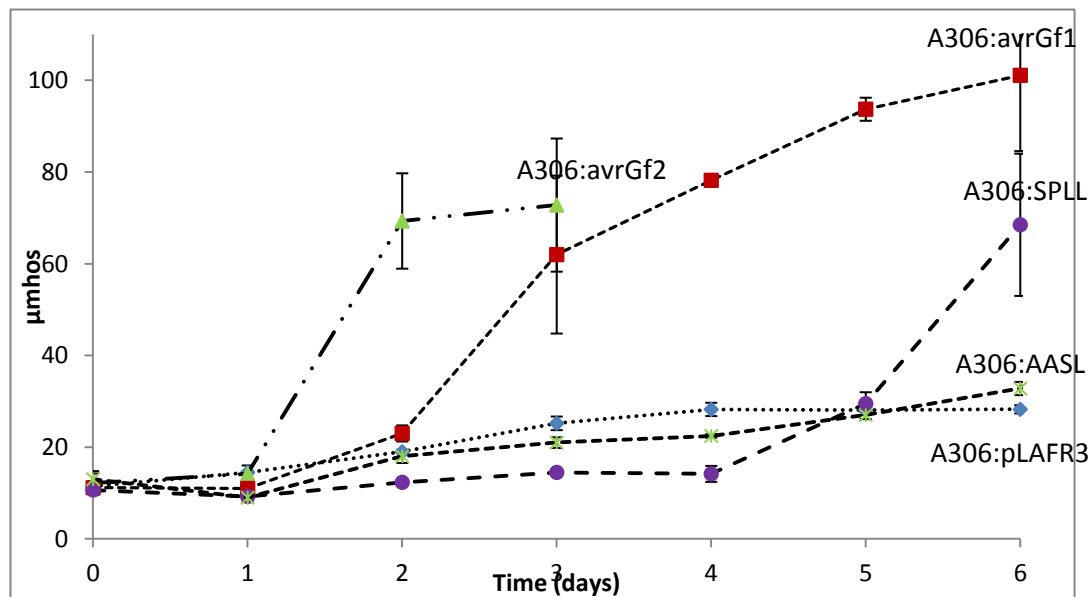


Figure 3-6. (A) The effect of GPxL motif and mutation derivatives in *avrGf2*. on bacterial growth in Duncan grapefruit (GF). The following strains were infiltrated in grapefruit leaves at 5×10^5 CFU/ml: A306:pLAFR3 (*Xcc-A306:pLAFR3*, blue diamond); *avrGf2* (*Xcc-A306:avrGf2*, green triangle); A306:AASL (*XccA306:avrGf2-A³⁵⁶ASL*, green star); and A306:SPLL (*XccA306:avrGf2-S³⁵⁶PLL*, purple circle). (B) Electrolyte leakage analysis in DG leaves infiltrated with 5×10^8 CFU/ml using the same strains and including A306:*avrGf1* (*Xcc-A306:avrGf1*, red square). Each point represents the mean of one experiment with three replicate measurements. Vertical lines represent standard deviation of each mean.

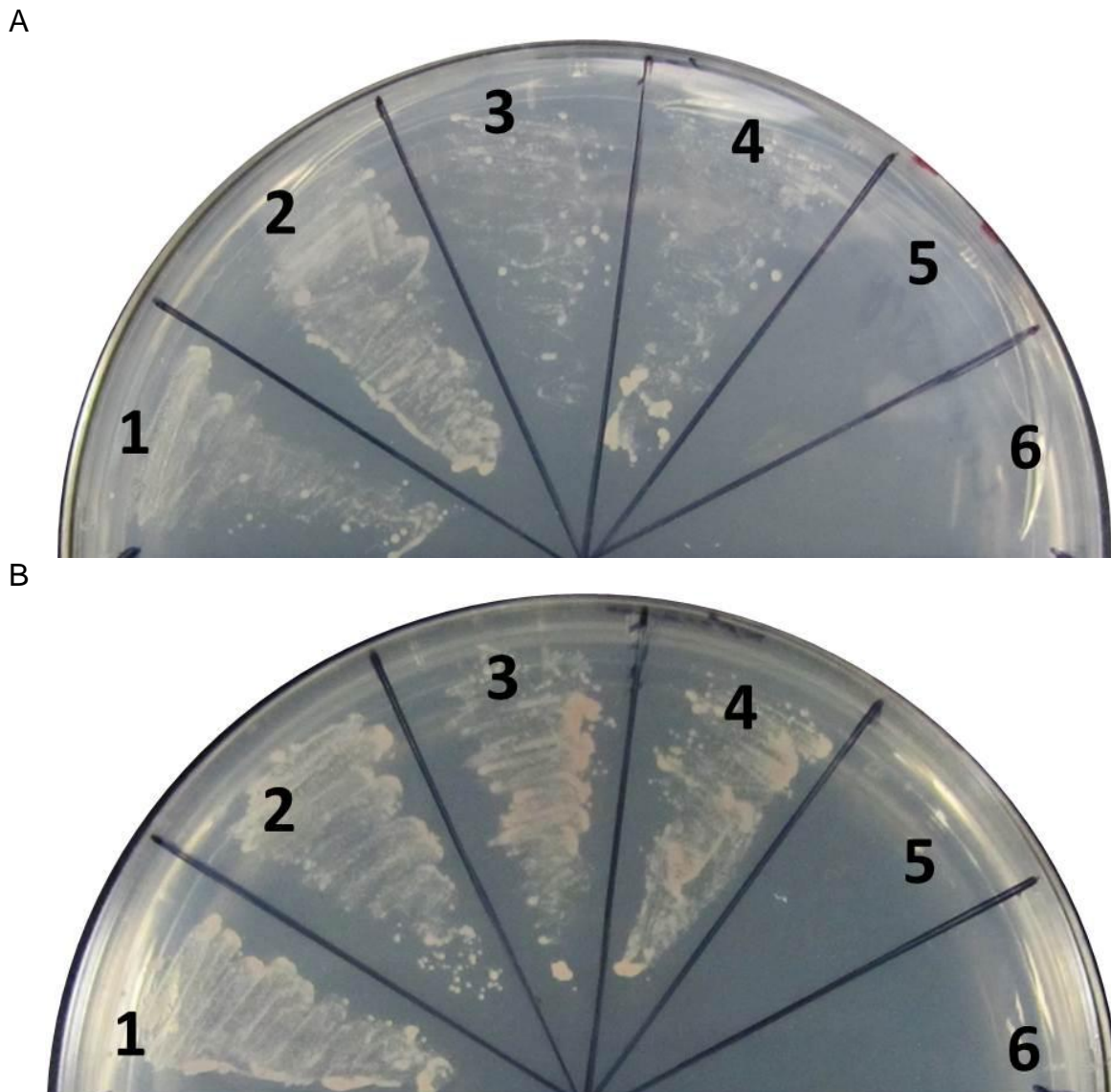


Figure 3-7. Yeast two-hybrid assay showing the interaction between the *Citrus paradisi* cyclophilin (GF-Cyp) and XopAG *avrGf1* and *avrGf2*. (A) Yeast cells co-transformed with the individual Bait vector pDBLeu –GF-Cyp and Prey vector pPC86- *avrGf1*(1–4) show an interaction. Yeast cells co-transformed with Bait vector pDBLeu –Empty and Prey vector pPC86- Empty (5–6) served as controls and show no growth. (B) Yeast cells co-transformed with the individual Bait vector pDBLeu –GF-Cyp and Prey vector pPC86- *avrGf2*(1–4) show interaction. Yeast cells co-transformed with Bait vector pDBLeu –Empty and Prey vector pPC86- Empty (5–6) served as controls and show no growth.

Table 3-1. Comparison of *GF-Cyp* gene expression in grapefruit leaves in a transient gene silencing experiment using *Agrobacterium tumefaciens* and QRT-PCR.

DAI ^a	n	Mean $\Delta\Delta C_T^b$	SD	SE	95% Confidence Interval	p ^c	Fold change ^d
0	5	1.06534	0.42176	0.18862	0.5417; 1.589		
1	6	1.50498	1.22319	0.49937	0.2213; 2.7886	0.2742	0.439639
2	6	0.63925	0.90977	0.37141	-0.3155; 1.594	0.2890	0.426091
3	6	0.19975	0.28135	0.11486	-0.0955; 0.495	0.0359*	0.865593
4	5	0.36267	0.30415	0.13602	-0.015; 0.7403	0.0984	0.702673
5	5	0.34373	0.36409	0.16282	-0.1083; 0.7958	0.0900	0.721615
6	6	0.01602	0.01851	0.00756	-0.0034; 0.0354	0.0122*	1.049324

^aDays after infiltration (DAI). ^bThe mean $\Delta\Delta C_T$ was normalized based on the value of the constitutively expressed gene *EF1* ($\Delta\Delta C_T$ -EF1), to obtain the relative expression level change for every day sampled ^ct-Student test comparison using 0 DAI as standard expression value. Values are significantly different when p is <0.05. ^dThe fold change in expression was calculated using 0 DAI value as standard expression value.

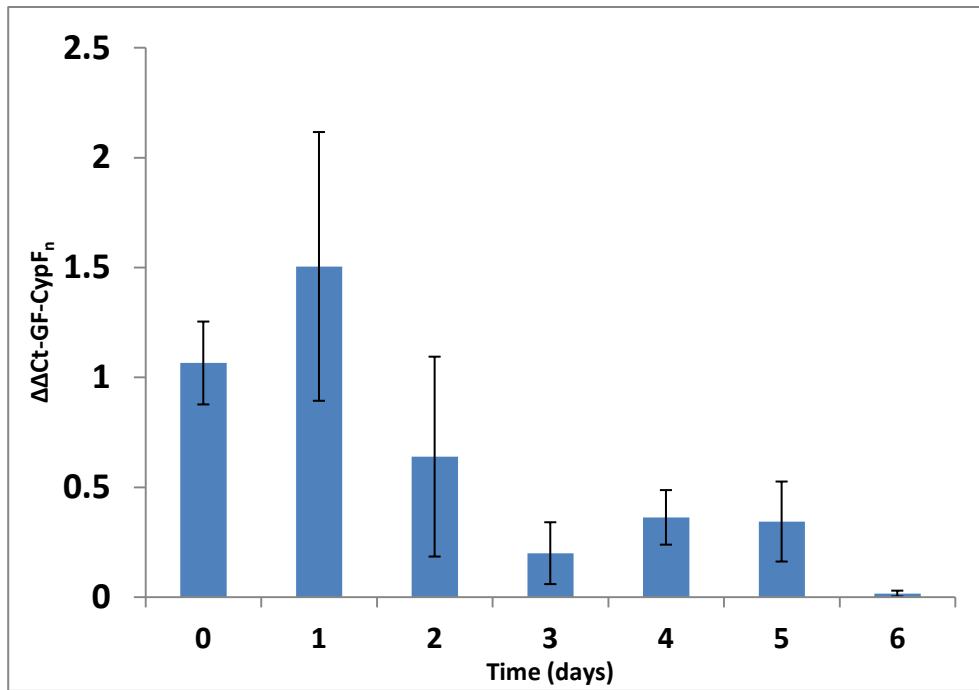


Figure 3-8. Quantification of the expression of *GF-Cyp* in a transient gene silencing experiment using *Agrobacterium tumefaciens* in GF leaves. The expression level of the target gene *GF-Cyp* (Ct-*GF-Cyp*) was normalized based on the value of the constitutively expressed gene *EF1* (Ct-*EF1*), to obtain the relative expression level change for every day sampled ($\Delta\Delta\text{Ct-GF-Cyp}_{Fn}$). The bars represent the average and standard error results of two different quantification experiments, with three replicates each.

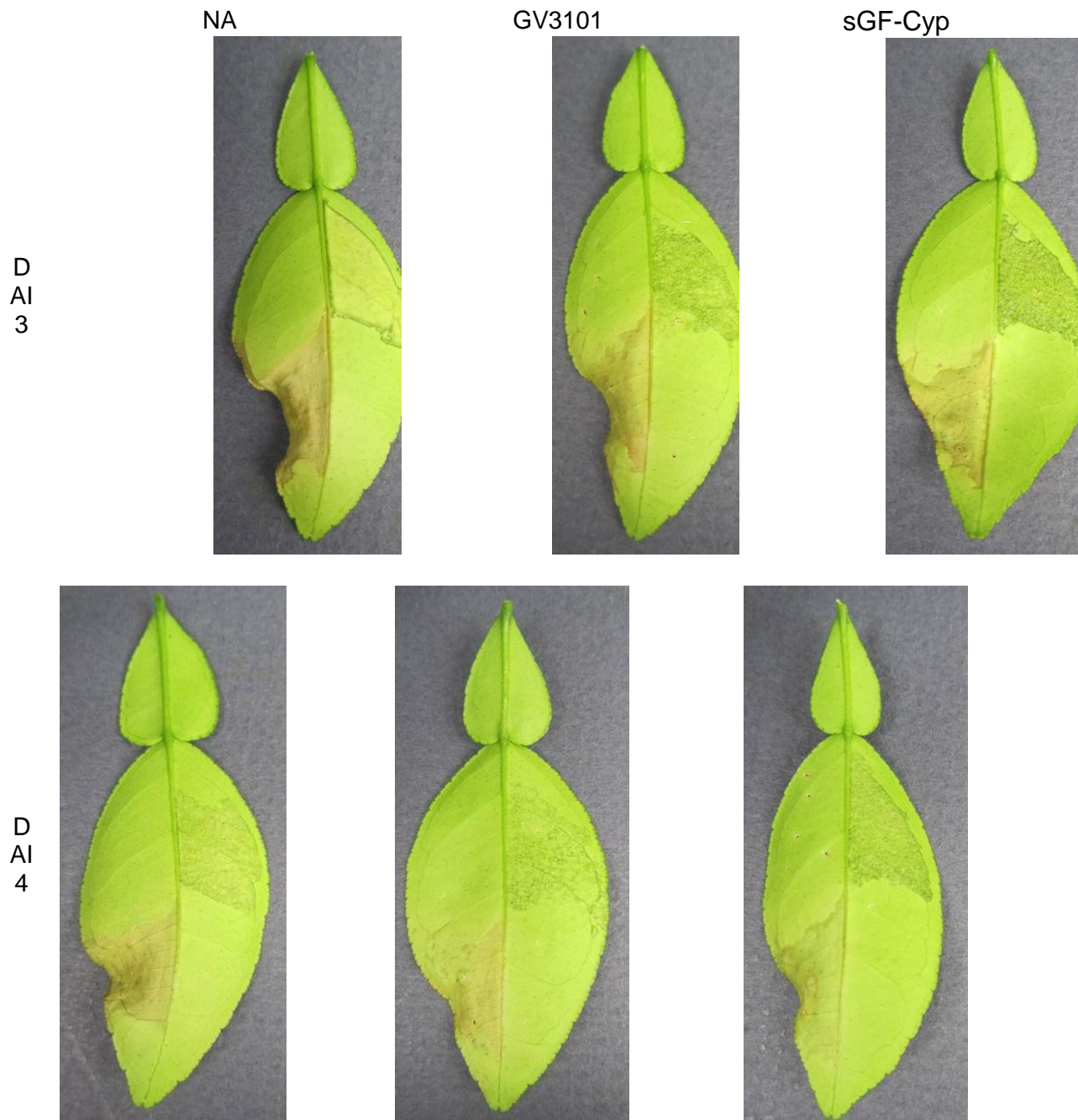
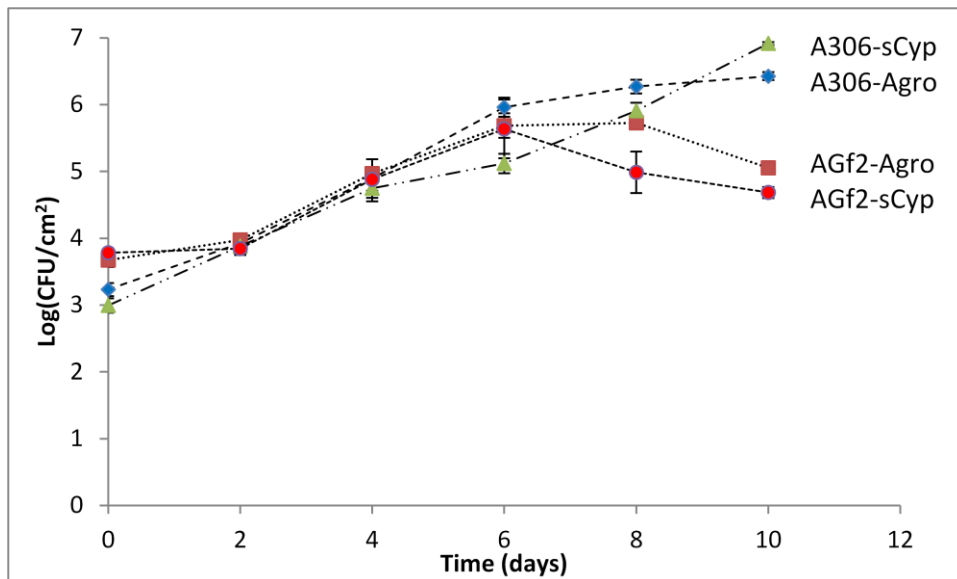


Figure 3-9. Transient silencing experiment in young Duncan grapefruit (GF) leaves infiltrated separately with a suspension of *Agrobacterium tumefaciens* strains GV3101:pHellsGate (GV3101) and GV3101:pHell-GF-Cyp (sGF-Cyp) adjusted to 5×10^6 CFU/ml at day 0, and then infiltrated at 0 and 6 days later with bacterial suspensions of Xc-A306:pLAFR3 (upper right part of the leaf), and Xc-A306:avrG/2 (lower left part) adjusted to 5×10^8 CFU/ml. Leaves not infiltrated with *Agrobacterium* (NA) were used as a second control.

A



B

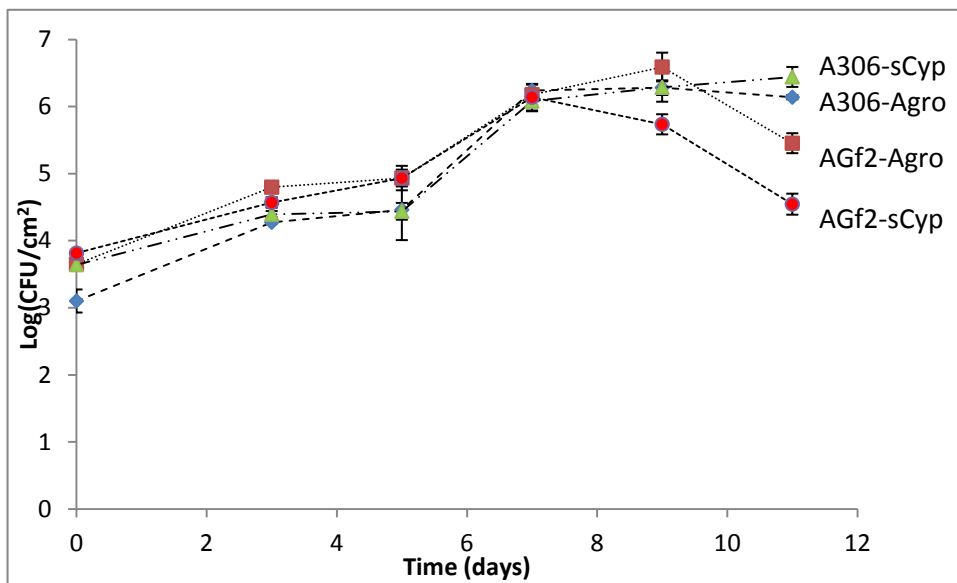


Figure 3-10. Transient silencing experiment in young Duncan grapefruit (GF) leaves infiltrated separately with suspensions of *Agrobacterium tumefaciens* strain GV3101:pHellsGate empty (Agro) and GV3101:pHell-GF-Cyp (sCyp) at day 0 (DAI0) adjusted to 5×10^6 CFU/ml. Half of the leaves was re-infiltrated at DAI0 (A) and the other half at DAI4 (B) with 5×10^5 CFU/ml suspensions of Xc-A306:pLAFR3 (A306), and Xc-A306:*avrGf2* (AGf2). Each point represents the mean of one experiment with three replicate measurements. Vertical lines represent standard error of the mean.

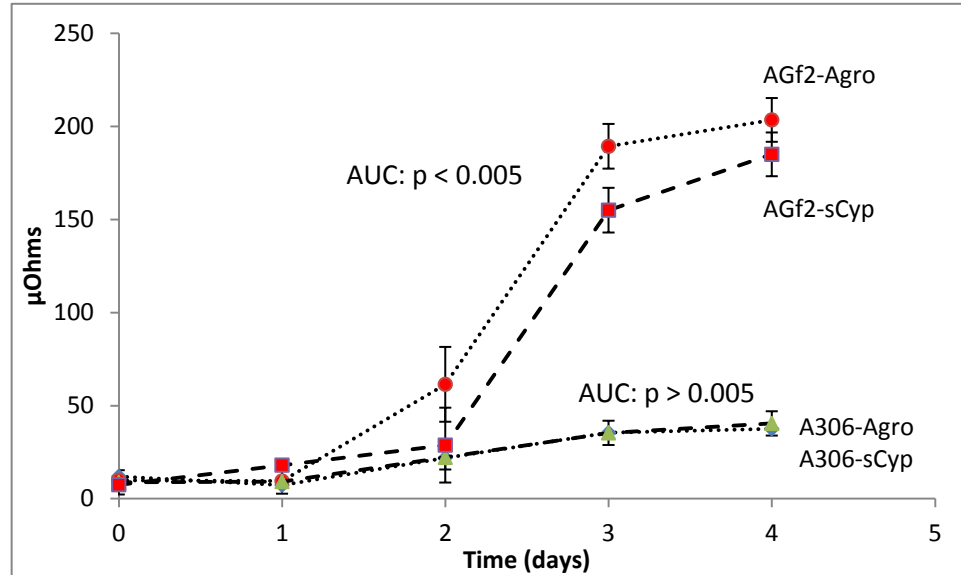


Figure 3-11. Electrolyte leakage in transient silenced young Duncan grapefruit (GF) leaves separately infiltrated with suspensions of 5×10^6 CFU/ml of *Agrobacterium tumefaciens* strain GV3101:pHellsGate empty (Agro) or GV3101:pHell-GF-Cyp (sCyp) at day 0 (DAI0) and then infiltrated at DAI 4 with 5×10^8 CFU/ml suspensions of Xc-A306:pLAFR3 (A306) or Xc-A306:*avrGf2* (AGf2). Each time point represents the mean from two experiments with three replicate measurements each. Vertical lines represent standard error of the mean.

Table 3-2. Comparison of the areas under the curve (AUC) of the electrolyte leakage analysis data performed in transient silenced young Duncan grapefruit (GF) leaves separately infiltrated with suspensions of 5×10^6 CFU/ml of *Agrobacterium tumefaciens* strain GV3101:pHellsGate empty (Agro) or GV3101:pHell-GF-Cyp (sCyp) at day 0 (DAI0) and then infiltrated at DAI 4 with 5×10^8 CFU/ml suspensions of Xc-A306:pLAFR3 (A306) or Xc-A306:*avrGf2* (AGf2). Values represent the mean and standard deviation (SD) from two experiments with three replicate measurements each.

Strain	AUC		F	p
	Mean	SD		
A306-Agro	140.3333	8.8454	0.436	0.524
A306-sCyp	144.7917	13.9729		
AGf2-Agro	598.8167	66.0800	9.202	0.013***
AGf2-sCyp	491.375	56.2181		

CHAPTER 4

SEQUENCING OF THE COPPER RESISTANT *Xanthomonas citri* STRAIN A44. EFFECTOR PROFILE AND PLASMID ARRANGEMENT

Introduction

Copper is a potent bactericide that works by damaging bacterial membranes and proteins (Cooksey, 1990a). Bacterial spot was identified in the U.S. in 1922 and relied extensively on copper bactericides and later on antibiotics for disease control. With the development of *X. vesicatoria* (Xv) strains with resistance to streptomycin in tomato and pepper fields in Florida, growers relied mostly on Cu compounds combined with ethylene bis dithiocarbamates to control the disease (Stall, 1964).

In 1983, Marcó and Stall (1983) reported copper resistant (CuR) strains of Xv (pepper race 2) from pepper fields in Florida. This was the first report of copper resistance in plant pathogenic bacteria. In that work, a collection of several Xv strains collected since 1960 in different Florida locations were tested for viability in suspensions of Cu compounds and several of the strains isolated in 1968 were already CuR. Interestingly, the Xv strain ATCC35937 (Xv1111), isolated in New Zealand from tomato in 1955 by Douglas W. Dye, and used as a taxonomic reference in several studies, was shown to be CuR (Potnis et al., 2011). In 1987, Canteros & Minsavage identified CuR *X. vesicatoria* strains from bacterial spot symptoms in plants of tomato in Bella Vista, Corrientes, Argentina (Canteros, 1990).

In 1994, Canteros isolated the first CuR strain of *X. citri* type A (Xc-A) from symptomatic lemon trees (cv. Eureka) in Bella Vista, Corrientes, Argentina (Canteros, 1996). CuR strains of Xc-A have only been isolated in the northeastern region of Argentina. More recently, Xc-A CuR strains were identified in two other provinces in

Northeast Argentine (Formosa and Entre Rios) (Canteros et al., 2013). In 2003, the CuR strain, Xcc03-1638-1-1 #44 (Xc-A44), was isolated from a citrus canker lesion on grapefruit (GF) leaves in the EEA INTA Bella Vista. This strain was sent to the University of Florida (IFAS) for molecular characterization (Behlau et al., 2011).

Two different types of CuR plasmids (pCuR) have been described in Gram-negative bacteria. One of them is represented by a large plasmid (approx.. 200 Kbp), similar to the ones found in Xc-A, *X. perforans* (Xp) and Xv. The other type comprises several smaller size plasmids, similar to the ones identified in *Pseudomonas* and also in other *Xanthomonas* species (with sizes ranging from 35 to 100 Kbp).

The megaplasmids that mediate CuR in Xc-A and Xv have sequence homology with the *cop* operon characterized in smaller copper plasmids present in *Pseudomonas*. This homology, demonstrated by hybridization experiments with DNA probes based on the *P. tomato* copper resistance plasmid, may indicate a common origin for both types of plasmids (Canteros et al., 2004).

The *cop* genes from *P. syringae* were located in a 4.5 kb specific region of the plasmid pPT23 (Cooksey, 1990a). Within this region lies the *copABCD* operon. Genes in this operon are organized, and oriented in the same direction and with sequence homology to the CuR *pco* (plasmid copper) operon present in *E. coli*.

Different arrangements of the CuR genes were characterized in Xc-A44 (*copLABMGCDF*) and *X. citrumelonis* (*copLABMGF*). Both types of *cop* operons have highly conserved nucleotide sequences ($\geq 92\%$), and have been identified in other

bacterial species, such as *Stenotrophomonas maltophilia* K279a and *X. vesicatoria* strain 7882 (Behlau et al., 2011).

The most significant landmark in the characterization of Xc-A was the complete genome sequencing of strain Xc-A306 (da Silva et al., 2002). The genome of this strain, isolated in 1997 in the southern region of Brazil in the state of Parana (Rui Pereira Leite Jr, personal communication), consists of a bacterial chromosome that encodes approx. 4489 genes on a 5.27 megabase pair (Mbp) chromosome, and two plasmids, pXAC64 and pXAC33 which are 64.9 and 33.7 kilobase pairs (Kbp), respectively (da Silva et al., 2002). Many bacterial outer-proteins are exported by the type III secretion system (T3SS). Many of these type III effectors (T3E) are involved in pathogenic processes (Ryan et al., 2011). There are two types of proteins exported by T3SS; one of these protein types is composed of the transcription activator like effectors (TALEs), which control specific host gene expression (Bogdanove et al., 2010); the other protein type is a diverse group of effectors which share no similarities with TALEs but are also exported using the T3SS. Based on functional protein assays, sequence and structural comparisons, a united nomenclature for all the Xop effectors was proposed by White et al. (2009), in which all the effectors were classified into 39 groups which are listed and maintained updated in the online database <http://www.xanthomonas.org/t3e.html>.

A comparative genomic study was conducted in the copper resistant Xc strain, Xc-A44 (Behlau et al., 2011) through characterization of chromosomal and plasmid rearrangements, compared to the copper sensitivity (CuS) strain Xc-A306. In order to gain a better understanding of the ecological and evolutionary relationships between

those isolates, both strains were compared for differences in pathogenicity and also in arrangement of copper resistant plasmids relative to other xanthomonads.

Material and Methods

Bacterial Strains Media and Inoculum Preparation

Strains utilized in this work are listed in Table 2-1. Strain Xc-A44 was stored in sterile tap-water and was subcultured on nutrient agar (NA) medium. Rifampicin resistant strains were obtained by plating 10^9 colony-forming-units (CFU)/ml on NA containing 50 $\mu\text{g/ml}$ of rifampicin. Xc-A44, and *Escherichia coli* (Ec) strains were maintained on Luria-Bertani (LB) medium (Sambrook et al., 1989), and also stored in nutrient broth (Difco™) containing with 30% glycerol, in a -80°C freezer. Conjugations were performed on nutrient yeast glycerol agar (NYGA) (Daniels et al., 1984). The media were amended, when necessary, with antibiotics at the following concentrations: rifampicin, 50 $\mu\text{g/ml}$; tetracycline, 10 $\mu\text{g/ml}$; and kanamycin, 40 $\mu\text{g/ml}$.

Bacterial cultures for plant inoculations were grown on nutrient agar for 18 h at 28°C . Bacterial cells were suspended in sterile tap water and the bacterial suspension was adjusted to an optical density (O.D.) 600 nm = 0.3 ($2-5 \times 10^8$ colony-forming unit (CFU) per ml) with a spectrophotometer (Spectronic 20). Bacterial suspensions were diluted to a concentration of 5×10^5 in sterile tap water for population dynamics studies (Klement et al., 1990).

Growth of Plants

Citrus plants, Duncan GF (*C. paradisi* Macf), were grown in steamed peat-vermiculite mix in 20 cm (diameter) pots in a greenhouse at 20-35°C. Plants were regularly fertilized with a slow-release fertilizer (Osmocote®).

Bacterial Population Dynamics *in planta*

Bacterial multiplication in leaves was determined following infiltration with a hypodermic needle and syringe of a bacterial suspension, adjusted to 1×10^4 CFU/ml, into the leaf mesophyll. Infiltrated tissue was sampled at regular intervals, and the internal bacterial populations were determined as described previously (Stall & Cook, 1966, Hibberd et al., 1987b). Plant shoots with leaves of approximately the same age were infiltrated with each strain. The infectivity titration was performed during a 14-day period. Every 48 h three 0.5 cm^2 disks were sampled from leaves infiltrated with each strain in both KL and GF. Each disk was crushed in 0.5 ml of sterilized tap-water, then the suspensions were serially diluted and plated on NA to count the CFU. Plants were maintained in a greenhouse at 25-30°C.

Infectivity Titration

Duncan GF seedlings were selected when new shoots were about 1 cm long. Leaves were inoculated at approximately 21 days after the beginning of shoot development. Inoculum was adjusted to about 5×10^3 CFU/ml and the actual bacterial populations were determined by plating 50 μl of suspension on each of two nutrient agar plates. The inoculum concentration was determined from the average number of colonies that developed. Grapefruit seedlings were kept at 28°C and under 12 h of light and 12 h of darkness.

The number of lesions (NL) was determined by manually counting lesion number in the infiltrated area of the leaf (Marshall, 1968) for each side of the leaf. The experiment included infiltrating each side of 6 leaves with Xc-A44 (CuR) and Xc-A306 (CuS) strains, to minimize a possible 'age of leaf' effect at the moment of lesion assessment. Given that the bacterial titer was different (8.5×10^3 CFU/ml of Xc-A306 CuS; and 6.5×10^3 CFU/ml of Xc-A44 CuR), the 'Number of Lesions' obtained (NL) for each strain ($NL_{Xc-A306}$ and NL_{Xc-A44}) was corrected to 5×10^3 CFU/ml to get an NL adjusted value (NLA) using the formula $[NLA = (NL_{\text{strain}} \times 5000) / (CFU/ml_{\text{strain}})]$. The analysis of the variance (ANOVA) of variable NLA was performed using SAS Software with default values.

Isolation of Plasmid DNA

Transfer of plasmid copper resistance genes from CuR to CuS strains was substantiated through plasmid profiling. Bacterial strains were grown overnight in 4 mL of nutrient broth (NB) at 28°C under agitation at 250 rpm using a KS10 orbital shaker (BEA-Enprotech Corp., Hyde Park, MA). Bacterial cell suspensions were then standardized to an OD of 0.3 A at 600 nm using a spectrophotometer (Spectronic 20, Baush & Lomb, Inc.). Plasmid DNA was extracted following the method of Kado and Liu (1981) with modifications (Minsavage et al., 1990b). Detection of plasmids was performed by electrophoresis as described previously (Minsavage et al., 1990b). After extraction, 28 µL of individual plasmid preparations were run in a 0.5% agarose gel, stained with ethidium bromide ($0.5 \mu\text{g mL}^{-1}$) for 30 min and photographed using a UV transilluminator and Quantity One software (Bio-Rad Universal Hood II, Hercules, CA). Plasmids of *Pantoea stewartii* SW2 (syn. *Erwinia stewartii*) were used as molecular size markers (Coplin et al., 1981).

Southern hybridization experiments were performed on positively charged nylon membranes and the DIG-High Prime DNA Labeling and detection kit, according to the manufacturer's instructions (Roche). Genomic DNA extractions were made using the CTAB- DNA isolation method (Sambrook et al., 1989). DNA preparations were digested with *EcoRI* endonuclease (Promega). The digested DNA was electrophoresed in 0.8% agarose gel, using as a size reference marker DIG labeled 0.12-21.2 Kbp DNA Molecular Weight Marker III (Roche).

Cosmid Cloning and Genome Finishing

The genomic library of Xc-A44 was constructed in the vector, pLAFR-3 (Ditta et al., 1980, Friedman et al., 1982, Staskawicz et al., 1984, Staskawicz et al., 1987), following digestion with the restriction enzyme *SauIII* (NEB). Individual clones were maintained in Ec DH5 α (BRL). Subcloning, plasmid alkaline lysis, and agarose gel electrophoresis were essentially as described by Sambrook et al. (1989). Specific clones from the Xc-A44 library were digested with restriction enzymes, religated, and sequenced using Sanger method (ICBR, UF).

PCR Analysis

Primers were synthesized by Sigma-Aldrich (Sigma-Aldrich Co., St. Louis, MO). Amplification of target genes from all bacteria was performed using a DNA thermal cycler (Bio-Rad-MyCyclerTM) and the Taq polymerase kit (Promega, Madison, WI). For extraction of template DNA, strains were individually grown overnight on NA, suspended in sterile deionized water (DI), boiled for 20 min, cooled on ice for 5 min, shaken thoroughly using a vortex mixer (Genie2), centrifuged at 15,000 rpm for 5 min and placed on ice until the supernatant was used in the PCR reaction mixture. Each PCR reaction mixture, prepared in 25 μ L total volume, consisted of 11.4 μ L of sterile water, 5

μL of 5 × PCR buffer, 1.5 μL of 25 mM MgCl₂, 4 μL deoxyribonucleoside triphosphates (0.8 mM each dATP, dTTP, dGTP, and dCTP), 0.5 μL of each primer (stock concentration, 25 pmol μL⁻¹), 2 μL of template, and 0.2 μL (5 U/μl) of Taq DNA polymerase. PCR reactions were initially incubated at 95°C for 5 min. This was followed by 30 PCR cycles which were run under the following conditions: denaturation at 95°C for 30 s, primer annealing for 30 s at 5°C below the minimum primer T_m, calculated for each primer based on the following formula: $T_m = [81.5 + (41 * (\%GC/100)) - 21.6 - (500 / (\text{length}))]$, and DNA extension at 72°C for 45 s in each cycle. After the last cycle, PCR tubes were incubated for 10 min at 72°C and then placed at 4°C. In every reaction, a positive control was included depending on the set of primers. PCR reaction mixtures were analyzed by 1% agarose gel electrophoresis (Bio-Rad Laboratories, Hercules, CA) with Tris-acetate-EDTA (TAE) buffer system. A λ-*EcoRI-HindIII* DNA marker (Promega, Madison, WI) was used as the standard molecular size marker for PCR product sizing. Reaction products were visualized by staining the gel with ethidium bromide (0.5 μg mL⁻¹) for 20 min and then photographed using a UV transilluminator and Quantity One software (Bio-Rad Universal Hood II, Hercules, CA).

Genome Sequencing and Alignment

Whole-genome sequencing of strain Xc-A44 was performed using two high-throughput sequencing techniques, 454 pyrosequencing and Illumina GAllx sequencing at Yale Center for Genomic Analysis. The raw sequencing reads were further analyzed using CLC Genomics Workbench v6.0 (CLC Bio, Aarhus, Denmark). The reads were trimmed, compared and overlapped to create contigs. The Xc-A44 contigs obtained were mapped against the chromosome of the reference strain Xc-A306 (GenBank accession number AE008923.1).

Using primers specific for the nuclear localization signal of TALEs, several clones from the Xc-A44 library were identified as *pthA* carriers (*pthA* clones). Each *pthA* clone was digested with enzymes, and the end terminal fragments of each insert were subcloned, and sequenced to be compared with the plasmids sequences from the reference strain Xc-A306: pXAC33 and pXAC64 (Genbank accession AE008924.1; and AE008925.1 respectively). Also, each *pthA* gene was restricted, subcloned and sequenced.

The Xc-A44 contigs were compared using the draft genomes of *X. vesicatoria* Maraité, ATCC 35937 (Xv1111; IMG/ERproject ID: Gi08344), and *X. perforans* 1-7 (Xp1-7) (Horvath et al., 2012), as references to create a scaffold for the CuR plasmid. After all the gaps were closed in Xc-A44 pCuR, the nucleotide sequence for every plasmid was annotated using the gene calling method at Integrated Microbial Genomes-Expert Review (IMG/ER) system (IMG Submission ID:12077). The bacterial genome sequences were compared and aligned using BLAST (Altschul et al., 1997) and Progressive Mauve 2.0 software with default values. The graphic representations of the sequences were made using BLAST Ring Image Generator (Sourceforge), and CGView Server (Stothard Research Group).

Gap Closure and Assembly Validation

Genome assembly yielded several virtual gaps. PCR primers were designed and Sanger sequences of these PCR products were used to close the gaps between the scaffolds using several cosmid libraries generated using pLAF3 vector, with inserts ranging from 20 to 25 kb in size. The genome finishing process was performed using a combination of bioinformatics software mentioned above, PCR walking by Sanger

sequencing from the genomic library, and comparative genomics using the sequences from other bacterial genomes uploaded in Genbank, and IMG-ER (JGI).

Effector Analysis

The candidate T3SS effectors in the Xc-A44 genome were identified using tBLASTn (Altschul et al., 1997) analysis and Pfam domain (Finn et al., 2008) searches. For tBLASTn analysis, all known plant and animal pathogen effectors were used to query with an e-value threshold ≤ 0.00001 . Pfam domains were searched for possible domains found in known effectors in the predicted set of ORFs of draft genome sequences. Candidate effectors were classified according to the nomenclature and classification scheme for effectors in xanthomonads described by White et al. (White et al., 2009).

Results

Pathogenicity Assessment for CuR Strain Xc-A44

Both the analysis of populations and the infectivity titration of Xc-A44 (CuR) and Xc-A306 (CuS) strains in infiltrated GF leaves showed no differences (Figure 4-1). Although no significant differences were observed in infectivity titration experiment, GF leaves were infiltrated to determine if Xc-A44 virulence is similar to Xc-A306 based on citrus canker development of individual pustules. Following infiltration the number of lesions was counted per cm^2 on leaves infiltrated with Xc-A44 and Xc-A306 strains. The number of lesions was normalized to 5×10^3 CFU/ml based on a calculation of the exact inoculum concentration by plating on NA. There were no significant differences ($p: 0.1855$; $\alpha=0.05$) observed for the number of lesions between strains Xc-A44 and Xc-A306 (Figure 4-2).

Genome Alignment and Assessment of Genes Related to Virulence between Xc-A44 and Xc-A306

Following genome assembly, a chromosome molecule for the Xc-A44 strain was obtained. The BLASTn alignment comparison for the nucleotide sequences of Xc-A44 chromosome versus the reference strain Xc-A306 (AE008923.1) showed a high level of similarity between both strains (>99%). This level of similarity is represented in the dot matrix plot shown in Figure 4-3A. No genome rearrangements were observed between the Xc-A44 and the Xc-A306 chromosome. The degree of similarity between both chromosomes can be visualized also in the graphic representation of the MAUVE alignment, where no inversions or translocations were detected (Figure 4-3B). In both graphics it is possible to observe a few gaps corresponding to putative deletions on the Xc-A44 or the Xc-A306 chromosome.

The T3E assessment performed between strains Xc-A44 and Xc-A306 showed no differences in respect to the number of T3Es present, as well as a high level of effector identity at the amino acid level (100%) with strain Xc-A306. Moreover, for each effector, the differences observed at the nucleotide sequence level were synonymous substitutions, because the translated sequence of the effector genes identified among Xc-A44 and Xc-A306 chromosomes were identical (i. e. *xopC*; *xopF2*; *xopP*, *xopAK*; *hpa2* genes) (Table 4-1). No T3E was found in Xc-A44 chromosome that was not present in Xc-A306.

The *pthA* TALE Genes are Carried in the Pathogenicity Plasmid pXc123

Xc-A44 has a unique plasmid arrangement relative to xc-A306 (Figure 4-7). The TALEs are present in a unique plasmid designated pXc123 (size 123 Kb) in strain Xc-A44 (Figure 4-4). Homology was observed among the TALEs carried in pXc123 in Xc-

A44 strain, relative to the TALEs described in pXAC33 and pXAC63 in Xc-A306 strain. The presence of TALEs was identified in several clones of the Xc-A44 library using specific primers for the nuclear localization signal (NLS) located in the terminal part of the *pthA* gene. The *pthA2*, *pthA3* and *pthA4* genes characterized in Xc-A44 showed a high degree of identity with the corresponding *pthA2*, *pthA3* and *pthA4* genes present in strain Xc-A306 (Table 4-1). The equivalent *pthA1* gene from Xc-A44 (*pthA1-44*) is larger than *pthA1* from Xc-A306 (*pthA1-306*), and consequently the translated Xc-A44 PthA-1 (PthA1-44) protein has a larger number of repeats in the central domain of the effector (21.5 repeats) relative to the 16.5 repeats present in Xc-A306 PthA1 (PthA1-306).

Interestingly, two different clones from the Xc-A44 library carried a copy of *pthA4-44* (clones 'NLS-8' and '5-4-2'). The presence of a *pthA4-44* homolog in each clone (p'NLS8' and p'5-4-2') was demonstrated after conjugation of the clones 'NLS8' and '5-4-2' into Xp 91-118 and Xc-A306 Δ *pthA4* (pustule minus). In the first case both transconjugant strains: Xp 91-118:'NLS8' and Xp 91-118:'5-4-2' elicited an HR in tomato leaflets. In the second case the transconjugant strains Xc-A306 Δ *pthA4*:'NLS8' and Xc-A306 Δ *pthA4*:'5-4-2' restored pustule formation (Figure 4-5). It was determined that p'NLS8' contained two *pthA* genes: *pthA2-44* and *pthA4-44* (closely related in sequence with *pthA2* and *pthA4* genes from Xc-A306) (Table 4-1). The sequences at the 3' end of the insert in p'NLS8' show sequence identity with pXAC33 and pXAC64. Using PCR walking with specific primers and Sanger sequencing, the central region of the sequence inserted p 'NLS8' shares identity with *ISxac2* and *ISxac3* genes, among other transposon genes described in pXAC33 and pXAC64.

The Xc-A44 library clone '5-4-2' carried only one *pthA* gene (*pthA4-44*). Both ends of the insert in p'5-4-2' show homology with pXAC64. No region in the insert has homology with pXAC33'. Another clone, 'NLS3', also contains two *pthA* genes: *pthA1-44* and *pthA2-44*, both of which were confirmed by sequencing in the laboratory of Dr. Thomas Lahaye (Ludwig Maximilian University of Munich, Germany). The terminal end of the insert in plasmid 'NLS3' showed sequence identity only with pXAC33. One more clone, '12-5-2', contained *pthA3-44*. The sequencing of the terminal ends of the insert in p'12-5-2' only showed sequence identity with pXAC64 (Figure 4-6). Based on the analysis of the Xc-A44 library clones 'NLS8', 'NLS3', '12-5-2', and '5-4-2', and the comparison of several contigs generated from the 454 and Illumina reads, a backbone for pXc123 is postulated to explain the location and orientation of the five TALEs, and its overall structure (Figure 4-6).

Comparison of Strain A44 Copper Resistance Plasmid with Other Xanthomonads

A plasmid profile comparison was performed among strains Xc-A, *X. vesicatoria* (Xv1111; Xv BV5-4a) (Minsavage et al., 1990a), and Xp1-7 (Table 2-1). All the Xc-A strains isolated inform the Bella Vista region showed similar plasmid sizes, which were larger than pCuRs in strains Xp1-7, Xv1111, and Xv BV5-4a (isolated also from the Bella Vista region). The strain Xc-A79 (isolated from a different region of Argentina) contained the largest pCuR (Figure 4-7).

Using the sequences published by Behlau et al. (2011), the *cop* genes were found on a contig from the Xc-A44 genomic dataset. In the comparison of the Xc-A44 contig, which contains the *cop* operon, with the draft genome of strain Xv1111, high sequence identity (>99%) was identified with one of the Xv1111 scaffolds that included the *cop* genes and also its flanking region. Based on the sequence comparison of both

datasets, contig scaffolds were created for Xc-A44pCuR and Xv1111pCuR. The gaps observed in both plasmids were closed using different approaches. For Xc-A44pCuR, the terminal end of specific clones from a genomic Xc-A44 library were sequenced and then used to find new contigs in the 454 and Illumina dataset. For Xv1111 pCuR sequence determination, the draft version of its genome (uploaded into the IMG database) was compared with Xc-A44 pCuR and all the gaps observed were closed using PCR and Sanger sequencing.

In all cases, the junctions between contigs were confirmed using PCR and Sanger sequencing. High sequence identity and gene homology were observed after comparison of plasmids Xv1111pCuR and Xc-A44pCuR (Figure 4-8A; Table 4-2). Several rearrangements were observed between the plasmids (Figure 4-8B). The plasmid Xc-A44 pCuR has two sequence insertions, both with transposon identities. The first insertion (designated region '00052', 12230 bp, matches primarily with the 454 Contig_00052) shows 100% sequence identity with Xc-A44 chromosome. The second insertion (designated region '00056', 26132 bp, from 454 Contig_00056) shows low sequence identity with the Xc-A44 chromosome (Figure 4-10). Both insertions also appear on Xc-A306 chromosome as regions '3399205- 3411434' (Table 4-3), and '4624091- 4651419', except for two *ISxac2* genes (XAC3943 and XAC3944), not present in the Xc-A44 genome (Figure 4-10; Table 4-4). Compared to Xv1111 pCuR, which does not have regions '00052' and '00056', both plasmids contain several mismatches and inversions. Despite these differences, the percent homology between Xc-A44-pCuR and Xv1111pCuR was high (>94.9% identity) (Fig. 4-9). The Xc-A44pCuR, which confers CuR in Xc-A44 strain, contains the *cop* operon (10.3 Kbp)

(Behlau et al., 2011). The Xc-A44 *cop* operon shows high sequence identity with the *cop* genes present in strains Xv1111 (90.62%) and Xp1-7 (94.48%) (Figure 4-9).

Discussion

The pathogenicity assessment revealed no differences between strains Xc-A44 and Xc-A306. These results in part can be explained based on both strains sharing the same genetic repertoire of chromosomal effectors. The only differences in T3Es in strain Xc-A44 compared to strain Xc-A306 was found in the TALEs where variation was observed in sequence and the number of the TALEs. Plasmid Xc-A44p123 contains five TALEs of which two *pthA4* homologs are present. It is interesting that even though both strains, Xc-A44 and Xc-A306, were isolated in different years and countries; all the chromosomal T3Es analyzed were identical at the amino acid level. In, 2005, Carvalho et al. (2005) postulated that, regardless of the common origin of the citrus canker outbreak in the late 1950' in Brazil, today two different lineages of Xc-A strains could be differentiated in South America. One with less genetic diversity, which encompasses strains from the central part of Brazil (Sao Paulo region) and Bolivia, and a more variable group of strains present in the southeastern region of South America (where Xc-A306 and Xc-A44 strains were isolated).

In a detailed study by Jaciani et al. (2012), T3Es were characterized in several Xc strains from Brazil and support the previously proposed idea of low genetic variability for the strains isolated in the central part of Brazil, as well as a more rich genetic diversity for the strains isolated in the southern region of this country, where citrus canker have has had less pressure due to eradication programs and chemical control. Both strains, Xc-A44 and Xc-A306, although they have differences in their plasmid profile structure, and variances in the number and sizes of its *pthA* genes, do not show

pathogenicity differences, and also share a high level of genetic identity regarding its chromosomes (>99% similarity) and T3E composition.

The pCuRs found in Xc, Xp, and Xv are transmissible between bacteria of the same species and also among those species. The sizes of the megaplasmids are variable, albeit at values close to 200 kb (Canteros, 1990) (Figure 4-7).

The strain Xc-A44 contains two different plasmids (Figure 4-4 and 4-7). The first one is a pathogenicity-associated plasmid (Xc-A44p123; approx. size 123 Kbp), which contains all of the *pthA* genes (denoted here *pthA44* genes) necessary for typical citrus canker symptoms. The second one is a plasmid that allows the bacterium to grow in presence of Cu (Xc-A44pCuR; approx. size 250 Kbp).

The Xc-A44p123 is a pathogenicity-associated plasmid, which contains the *pthA4* homologs necessary to produce typical citrus canker symptoms. By comparing with the reference genome of strain Xc-A306, the sequence of Xc-A44 p123 could be explained by a recombination event between plasmid pXAC33 and pXAC64 from Xc-A306 (Figure 4-7). The presence of regions rich in transposons allows the possibility for recombination between plasmids, as was described in *X. a. pv. glycines*, where several plasmid variants, which are based on a non-described plasmid prototype, share transposase, integrase and resolvase genes (Kim et al., 2006).; these types of genes also are present in Xc-A44p123, pXAC33 and pXAC64

The variable plasmid configuration observed in Xc-A strains was previously reported by Amuthan & Mahadeban (1994), and Carvalho et al. (2005). In this analysis, some of the strains simultaneously contain plasmids with sizes similar to pXAC33,

pXAC64, and Xc-A123, and even dissimilar profiles which did not match any of the sizes described above (Figure 4-7). The reason(s) why so many variants of the pathogenicity plasmids exist are undetermined. Recently, it was determined in specific strains of *Pseudomonas syringae* pv. *phaseolicola* (Neale et al., 2013) and *X. a.* pv. *malvacearum* (Narra et al., 2013), that *in planta* effects induce changes in its plasmid profile structure, through loss and rearrangement of plasmids after infiltration, or exposure of the pathogen to host leaf extracts.

The presence of two dissimilar plasmids, 'pNLS8' and 'p5-4-2', in the Xc-A44 library suggests the presence of two homologs of *pthA4* genes in strain Xc-A44. Both *pthA4* homologs, *pthA44-4.1* and *pthA44-4.2*, confer pustule formation, and indicate that five copies of TALEs are present in plasmid Xc-A44p123. Specific cosmid library 'pNLS8' shows other remarkable features such as: the presence of two *pthA* genes with sequences related to *pthA4*, which are located on separate plasmids in strain Xc-A306, homology with pXAC33 and pXAC64 sequences in each terminal end of the clone insert, and a central region which has homology with transposon genes *ISxac2* and *ISxac3*. This finding strongly supports the idea of a transposon region that permitted the recombination of Xc-A plasmids, as well the opportunity of diverse plasmids fusions events. The presence of Xc-A strains with different numbers of TALEs was reported by Lin et al. (2013) where they found strains with 3 to 6 *pthA* homologs genes. In *P. s.* pv. *syringae* (Pss) a possible explanation for the diversity in sizes of copper resistance plasmids observed in several isolates was proposed after the demonstration of the co-integration of Pss-pPT23D (35 Kpb; allows CuR), with Pssp-PS6 (a plasmid present in CuS strains). The obtained CuR tranconjugants showed plasmids of 60 kbp and 100

kpb size, similar to the ones found in CuR strains of *Xc juglandis* and *X. vesicatoria* previously isolated (Cooksey, 1990a).

Based on the analysis of several clones from the Xc-A44 library and also numerous contigs that show homology with the sequences obtained from the clone characterization, a draft model for Xc-A44p123 was generated in order to explain how the TALEs are ordered in the plasmid, and also provide a possible structure for Xc-A44p123 (Figure 4-6). To confirm the sequence of the proposed Xc-A44p123 molecule, it will be necessary to screen more clones from the Xc-A44 library using specific primers, which recognize regions between the *pthA* clones described here. After subcloning and sequencing these clones, a new version of the Xc-A44p123 needs to be generated, and its sequence will need to be corroborated using a combination of the 454 and Illumina contigs databases. Also, single molecule real time (SMRT) sequencing of an enriched Xc-A44 plasmid fraction will minimize errors generated at the moment of concatenated sequences in a final scaffold.

The second plasmid present in Xc-A44, which confers CuR (pCuR; approx. size 250 Kb), contains the *cop* operon (10.3 Kb), and other regions that are also present in other CuR bacteria (Xv1111) but in a different order (Figure 4-9-10; Table 4-2). The size of the CuR plasmids found in Xc-A strains was not always the same, and also were different compared with the size of the pCuR observed in Xv. Xeu and Xp strains (Figure 4-7). Given that strain Xv1111 was isolated decades before strain Xc-A44 and does not have the duplicate sequences present in Xc-A44pCuR, it is very likely that an insertion event occurred after the acquisition of the plasmid for the Xc-A strains (Figure

4-11). The integration of plasmids into genomes, as well the identification of conjugative transposon is well documented in bacteria (Mark Osborn & Böltner, 2002). Interestingly, the plasmid pCuR from Xc-A44 has two insertions, one that appears to be a duplication from Xc-A44 bacterial chromosome, and the other that is absent from the Xc-A44 chromosome. Both occur in the Xc-A306 chromosome (Figure 4-10). Both duplications show transposon identities and are not present on any contig of the CuR strain Xp1-7 genome, or Xv1111pCuR, for which sequence (200 Kbp) was also determined. Most of the genes described in regions '00052' and '00056' of Xc-A44pCuR are related to bacterial endonucleases, recombinases, integrases, and transposases (Table 4-3 – 4-4) as well as several undescribed protein genes. Some of the transposases present in Xc-A44pCuR, such as IS1389 and ISxac, were previously described in *Xanthomonas spp.*, and represent families of transposons disseminated in several *Xanthomonas* genomes (Gómez et al., 1999).

In this work, it was determined that strain Xc-A44 has similar pathogenicity and T3E profile as strain Xc-A306, although they have different plasmid arrangements. The first plasmid difference is associated with the pathogenicity plasmid, which has an approx. size of 123 Kbp. Plasmid Xc-A44p123 has differences in the sequence and number of its TALEs, like two functional copies of *pthA44-4* gene, and nucleotide sequences that resemble a recombination of plasmids pXAC33 and pXAC64 from strain Xc-A306. The second plasmid rearrangement occurs on the 250 Kbp pCuR, which has two sequence insertions with Xc-A44 and Xc-A306 chromosome homology. The duplications found in Xc-A44pCuR have sequence similarities with transposon genes

previously identified in several *Xanthomonas* species, but were never found in the plasmid which mediates CuR.

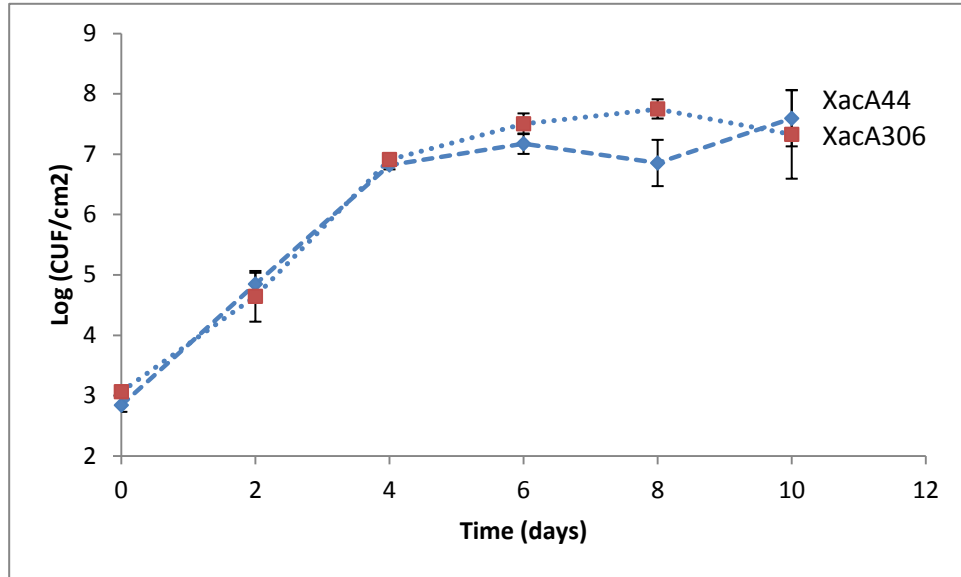
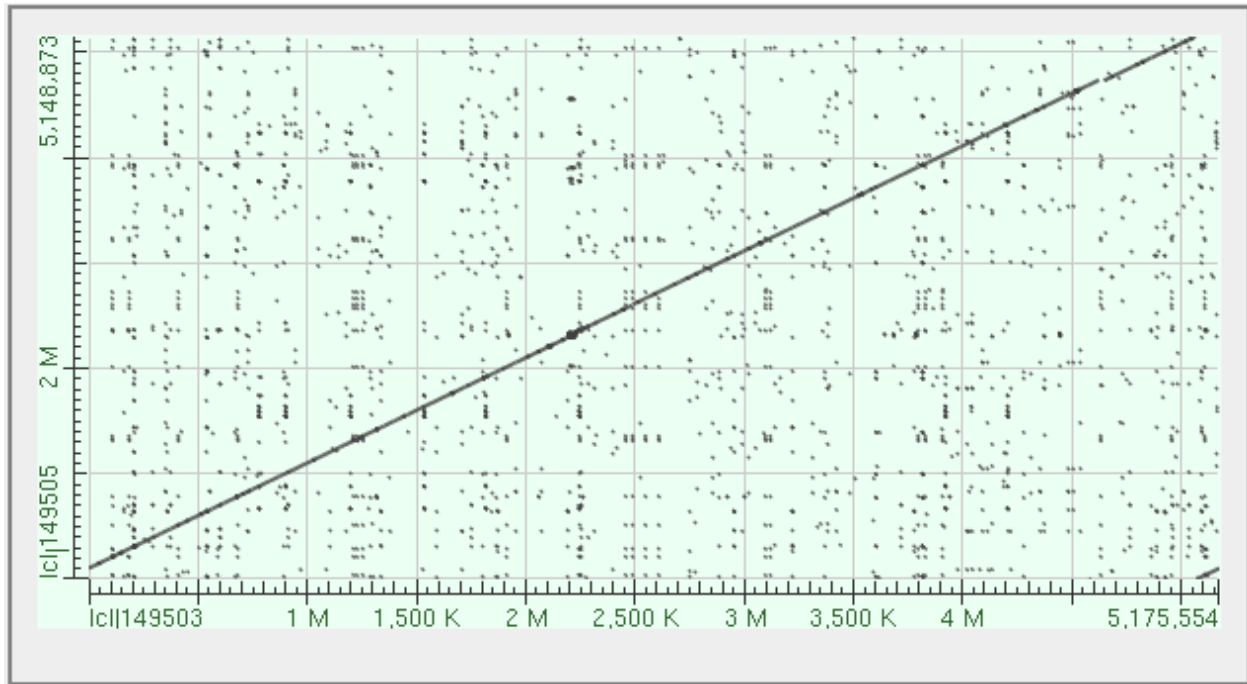


Figure 4-1. Population dynamics in Duncan grapefruit (DG) leaves following infiltration with 5×10^5 CFU/ml of *Xanthomonas citri* type A CuS (Xc-A306, red square) and CuR (Xc-A44, blue diamond). Each point represents the mean of three replications. Vertical lines represent standard error of the mean.



Figure 4-2. Citrus canker lesion development on Duncan grapefruit leaves following infiltration with a suspension of *Xanthomonas citri* Xc-A306 CuS adjusted to 8.5×10^3 CFU/ml (left side of leaf); or Xc-A44 CuR adjusted to 6.5×10^3 CFU/ml (right side of leaf).

A



B

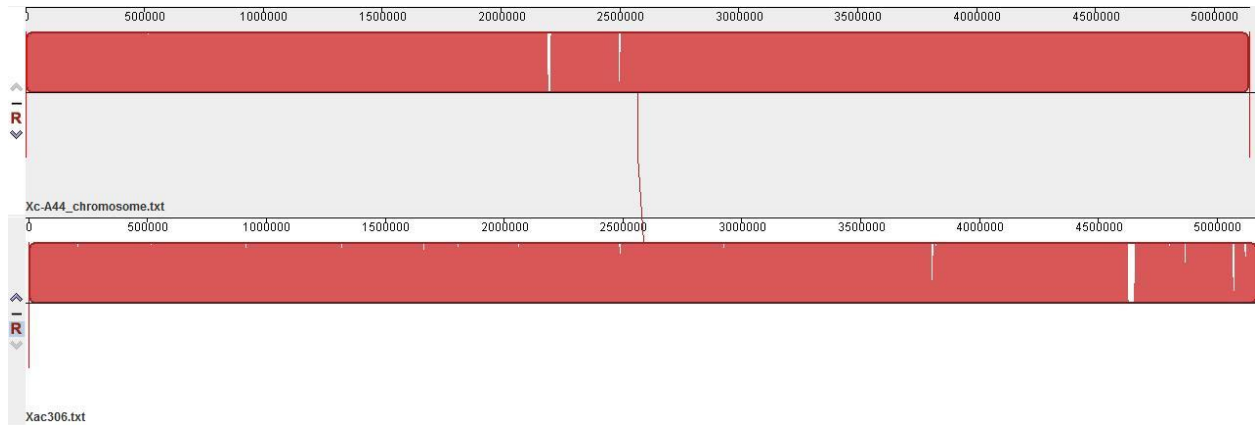


Figure 4-3. (A) BLAST Dot Matrix representation of alignment based on chromosomal sequence comparison between Xc-A306 (X axis) and Xc-A44 (Y axis). (B) Chromosomal rearrangement representation for Xc-A306 (above) and Xc-A44 (below) sequences using MAUVE. Conserved regions are colored and low identity unique regions are in white.

Table 4-1. Putative Type III effectors (T3E) present in the Xc-306 and Xc-A44 plasmids.

Effector family	Xc-306 designation. Locus tag (plasmid location) (size in aa) Number of repeats	Xc-A44 designation (size aa) Number of repeats	Pfam: functional/structural domain	BLASTp: Identities (%); Positives (%)	Related proteins. (References)
AvrBs3	PthA1 XACa0022- (pXAC33) (1126) 16.5	PthA1-44 (1296) 21.5		N-terminal region: 855/891 (96%); 867/891 (97%); C-terminal region: 812/905 (90%); 831/905 (91%)	
	PthA2 XACa0039- (pXAC33) (1096) 15.5	PthA2-44 (1096) 15.5		1043/1047 (99%); 1046/1047 (99%)	
	PthA3 XACb0015- (pXAC64) (1096) 15.5	PthA3-44 (1096) 15.5	Transcriptional activator, nuclear localization	1045/1047 (99%); 1046/1047 (99%)	PthA (Swarup et al., 1992)
	PthA4 XACb0065- (pXAC64) (1163) 17.5	PthA4-44.1 PthA4-44.2 (1163) 17.5		1164/1164 (100%)	
XopE2	XACb0011 (380)	no specific designation	Putative transglutaminase	379/380 (99%); (100%)	XopE2 found in Xfa type-C strain, avrXacE3, avrXccE1 (Moreira et al., 2010c)

aa= aminoacids

Table 4-1 (continued).

Effector family	Xc-306 designation. Locus tag (size in aa)	Xc-A44 position	Pfam: functional/structural domain	BLASTp: Identities (%); Positives (%)	Related proteins. (References)
AvrBs2	XAC0076 (714)	(194907..197048)	Glycerophosphoryl diester phosphodiesterase	714/714 (100%)	AvrBs2 from <i>X. campestris pv. vesicatoria</i> (Kearney & Staskawicz, 1990)
XopA	XAC0416 (137)	(589648..590061)	Harpin, maybe not a T3E	137 (100%)	Hpa1/HpaG (Noel et al., 2002)
XopC	XAC1210 Ψ (170)	(1485987..1485478)	Haloacid dehalogenase-like hydrolase	169/170 (99%); (100%)	(Occhialini et al., 2005)
	XAC1209 Ψ (81)	(1485299..1485057)		81/81 (100%)	
XopE1	XAC0286 (401)	(443379..442177)	Putative transglutaminase	401/401 (100%)	AvrXacE1, XopE1 from <i>X. campestris pv. vesicatoria</i> , (avrXacE1, hopX, avrPphE) (Thieme et al., 2007)
XopE3	XAC3224 (356)	(3914585..3913518)	Putative transglutaminase	356/356 (100%)	AvrXacE2, (avrXacE2, hopX, avrPphE) (Dunger et al., 2008)
XopF2	XAC2785 Ψ (245)	(3382060..3381323)		245/246 (99%); (100%)	XopF2 (Gurlebeck et al., 2006)
XopI	XAC0754 (452)	(997415..998770)	F-box protein	452/452 (100%)	<i>X. campestris pv. vesicatoria</i> (Thieme et al., 2007)
XopK	XAC3085 (688)	(3740040..3737977)		688/688 (100%)	Identified in Xoo (Furutani et al., 2009)

Some of the effectors appear to be pseudogenes (indicated by a Ψ).

Table 4-1 (continued).

Effector family	Xc-306 designation. Locus tag (size in aa)	Xc-A44 position	Pfam: functional/structural domain	BLASTp: Identities (%); Positives (%)	Related proteins (References)
XopL	XAC3090 (497)	(3743764..3745254)	LRR protein	497/497 (100%)	(Dunger et al., 2008)
XopN	XAC2786 (733)	(3382241..3384439)	ARM/HEAT repeat	733/733; (100%)	HopAU1 (Kim et al., 2009)
XopP	XAC1208 (723)	(1482812..1484980)		722/723 (99%); 100%	(Roden et al., 2004)
XopQ	XAC4333 (464)	(50729..49338)	Inosine uridine nucleoside Nribohydrolase	464/464 (100%)	HopQ1 (Roden et al., 2004)
XopR	XAC0277 (410)	(434940..433711)		410/410 (100%)	Identified in Xoo (Furutani et al., 2009)
XopV	XAC0601 (331)	(808795..807803)		331/331 (100%)	Identified in Xoo (Furutani et al., 2009)
XopX	XAC0543 (748)	(739402..737159)		748/748 (100%)	HolPsyAE (Metz et al., 2005)
XopZ	XAC2009 (1290)	(2463299..2459430)		1289/1290 (99%); 100%	XopZ1; HopAS, AWR (Furutani et al., 2009)
XopAD	XAC4213 (2883)	(5056720..5048072)	SKWP repeat protein	2883/2883 (100%)	RSc3401, Skwp from <i>Ralstonia</i> (Guidot et al., 2007)
XopAE	XAC0393 (646)	(567019..565379)	LRR protein	646/646 (100%)	HpaF/G/PopC (Noel et al., 2002)

Table 4-1 (continued).

Effector family	Xc-306 designation. Locus tag (size in aa)	Xc-A44 position	Pfam: functional/structural domain	BLASTp: Identities (%); Positives (%)	Related proteins (References)
XopAI	XAC3230 (296)	(3918462..3919349)	ADP-ribosyltransferase	296/296 (100%)	HopO1 (HopPtoO, HopPtoS), HopA11 (HolPtoAI) (Thieme et al., 2007)
XopAK	XAC3666 (220)	(4456639..4457298)	conserved hypothetical protein	219/220 (99%), 220/220 (100%)	(Petnicki-Ocwieja et al., 2002)
Hpa2	XAC0417 (138)	(590582..590995)	MitE	137/138 (99%); (100%)	(da Silva et al., 2002)
HrpW	XAC2922 (303)	(3544451..3545359)	Pectate lyase, may not be T3E	303/303 (100%)	(Park et al., 2006)

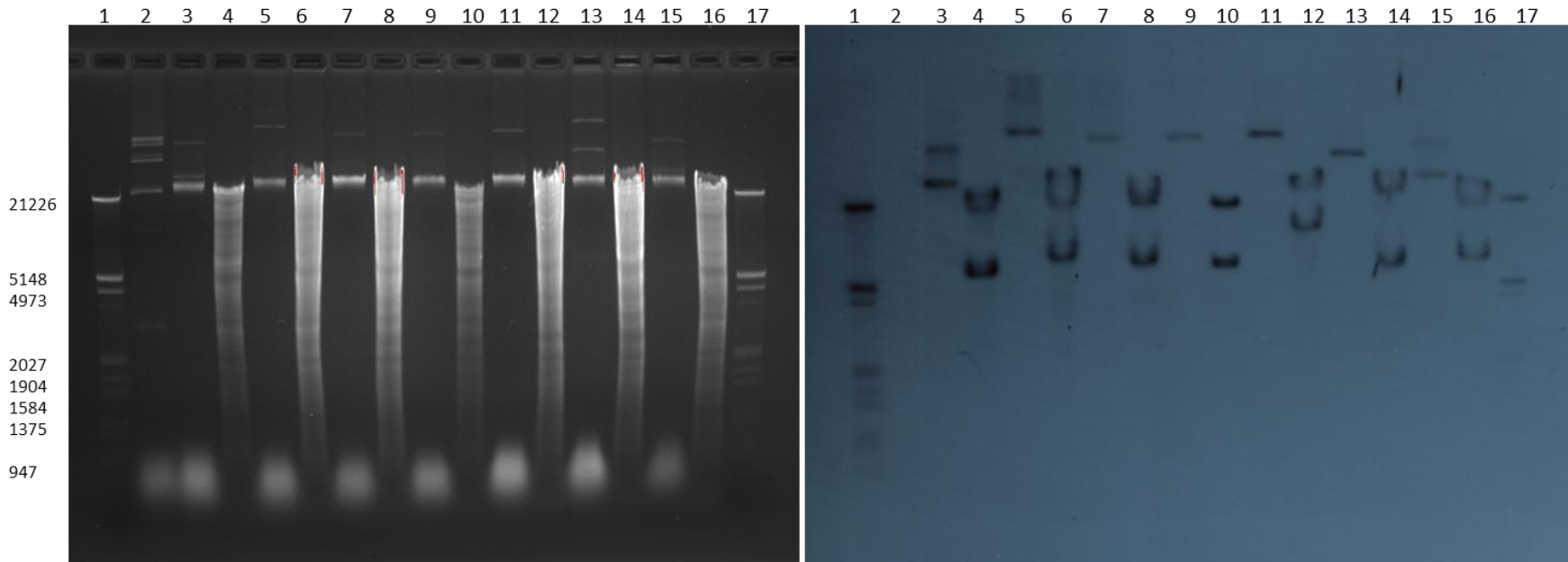


Figure 4-4. Total genomic and plasmid extractions of strains were subjected to electrophoresis (left) and probed with pthA probe (using primer pthAF/R DIG as the probe) by Southern hybridization (right). Lanes 1 and 17= DNA Molecular Weight Marker III DIG labeled; 2= *Erwinia stewartii* SW2; 3= Xc-A306 plasmid extraction (pXc-A306); 4=Xc-A306 genomic DNA restricted with *EcoRI* (Xc-A306 *EcoRI*); 5= pXc-A44; 6=Xc-A44 *EcoRI*; 7= pXc-A2090; 8= Xc-A2090 *EcoRI*; 9= pXc-A1660; 10= Xc-A2090 *EcoRI*; 11= pXc-AEtrog; 12= Xc-AEtrog *EcoRI*; 13=pXc-A100-Japan; 14= Xc-A100 Japan *EcoRI*; 15= pXc-A109 India; 16= Xc-A109 India *EcoRI*. Left panel= Ethidium bromide stained gel (agarose 0.7%). Right panel= Southern blot of gel in left. Number in left indicates size in Kbp of DIG labeled marker only.



Figure 4-5. Two functional copies of the gene, *pthA4* were identified in cosmid library clones 'NLS8' and '5-4-2'. GF leaves were infiltrated with 5×10^8 CFU/ml suspensions of strains: *Xc-A306* Δ *pthA4* (left leaf, left side of midrib); *Xp 91-118:5-4-2*' (left leaf, right side of midrib; *Xc-A306* Δ *pthA4*: 'NLS8' (right leaf, left side of midrib); *Xc-A306* Δ *pthA4*: '5-4-2' (right leaf, right side of midrib).

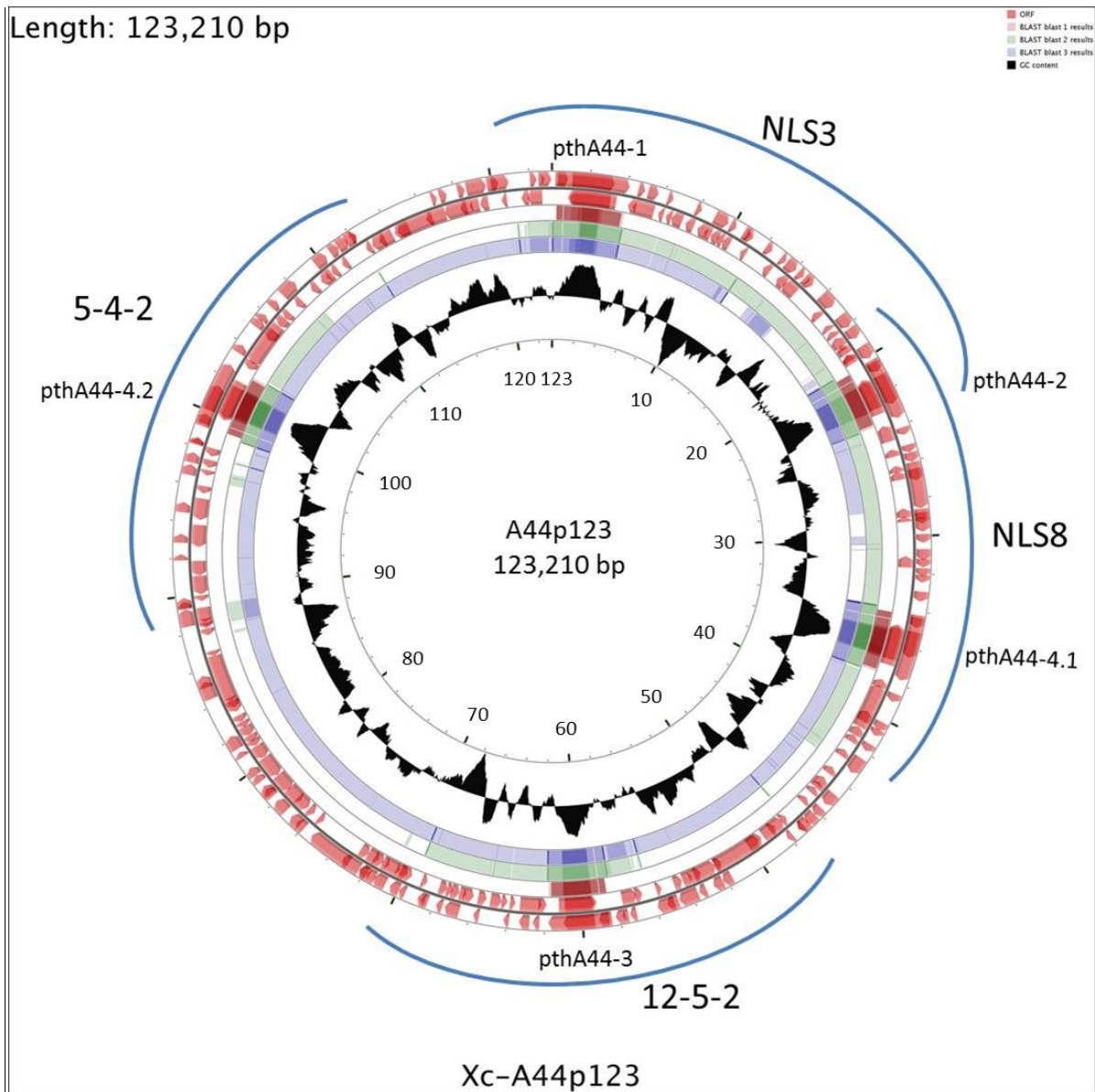


Figure 4-6. Circular representation of Xc-A44p123 using CGView server (Stothard Research Group) based on sequences obtained from Xc-A44 high-throughput sequencing contigs and library clones. Circles from outside to inside: first, scale bar in Kbp; second, G+C content showing % of GC bases out of the four nucleotides; third, BLASTn alignment using pXAC64 as a subject sequence; fourth, BLASTn alignment using pXAC33 as a subject sequence; fifth, BLASTn alignment using as a subject sequences Xc-A44 *pthA* genes (*pthA-1*, *-2*, *-3*, *-4.1*, *-4.2*). Blue Arcs represent the sequences of the Xc-A44 library cosmid clones 'NLS3', 'NLS8', '12-5-2', and '5-4-2'.

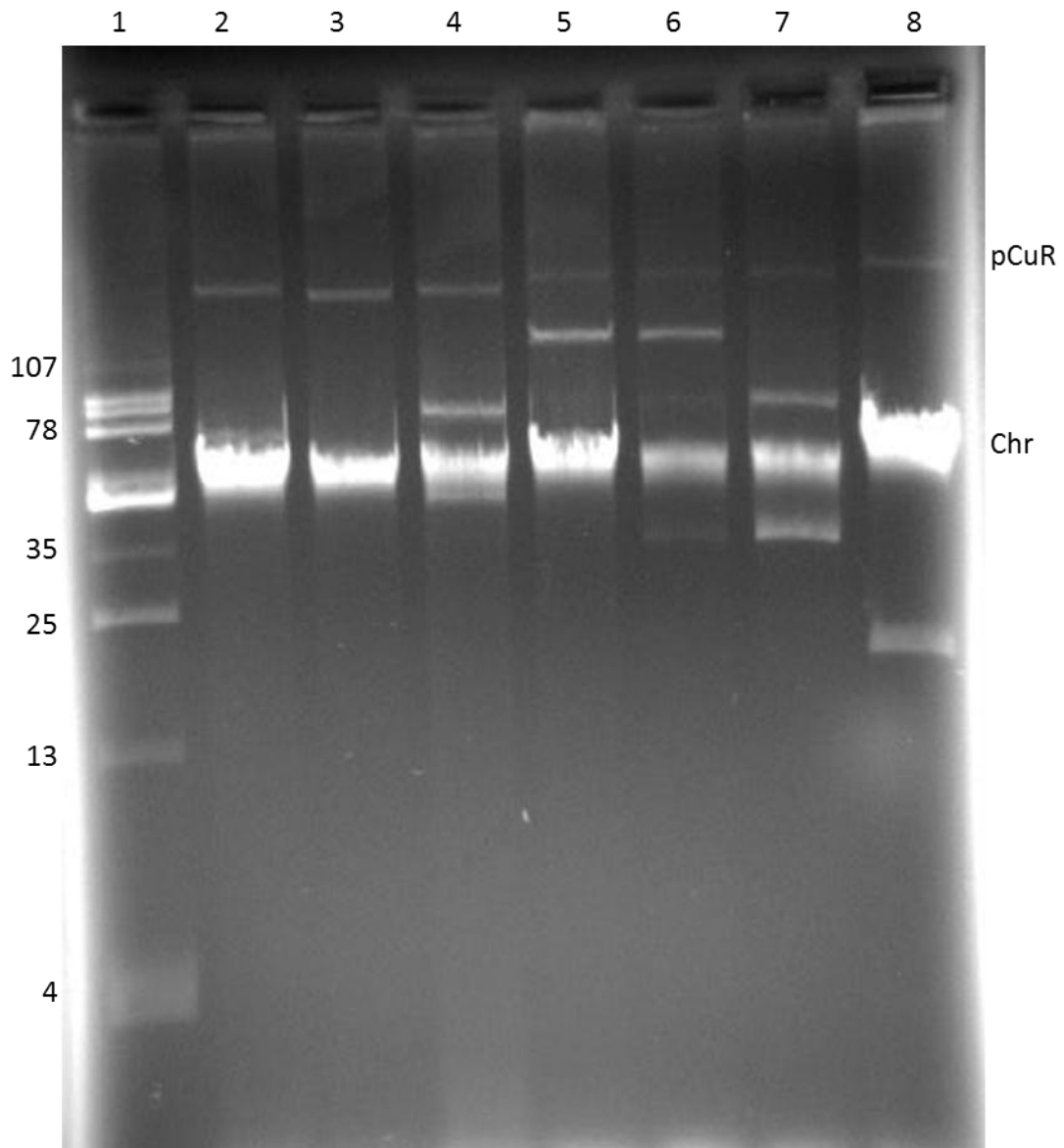
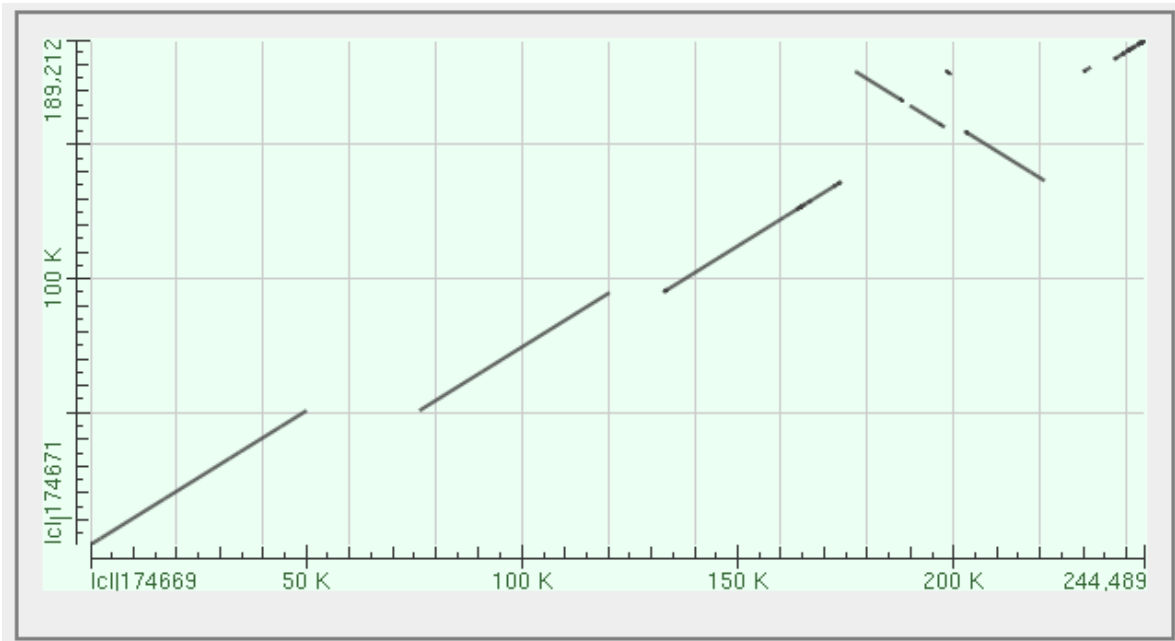


Figure 4-7. Plasmid profiles of *Xanthomonas* CuR strains following agarose gel electrophoresis. Number in the left indicates size in kbp. pCuR indicates CuR plasmids position. Chr indicates position of chromosomal DNA. Lanes 1 to 8 are: *Erwinia stewartii* SW2; *Xanthomonas perforans* (Xp1-7); *X. vesicatoria* (Xv1111); *X. vesicatoria* (BV5-4a); *X. citri* (Xc-A44); *X. citri* (Xc-A86); *X. citri* (Xc-A104); *X. citri* (Xc-A79).

A



B

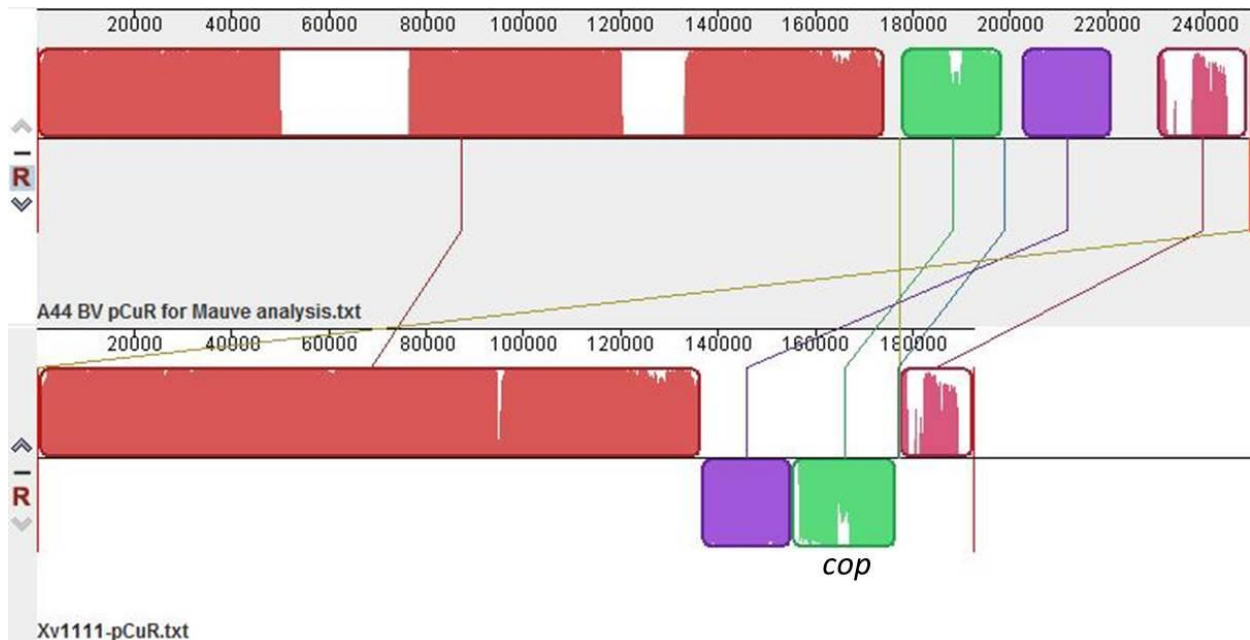


Figure 4-8. A. BLAST Dot Matrix representation for the alignment obtained for sequence comparison between Xv1111 pCuR (Y axis) and Xc-A44 pCuR (X axis). B. Plasmid rearrangement representation for the sequences of Xc-A44pCuR (above) and Xv1111 (below) using MAUVE. Conserved and highly related regions are colored and low identity unique regions are in white. The colored lines indicate translocations of the genome sections. Same colored blocks on opposite sides of the line indicate inversions. The *cop* green blocks represent the location of the *cop* operon.

Table 4-2. General features of Xc-A44 and Xv1111 CuR plasmids analyzed using Gene Calling method in IMG/ER

	A44	Xv1111
DNA, total number of bases	249703	192587
DNA G+C number of bases	58.81%	59.13%
Genes	269	200
Protein coding genes	267 (99.26%)	199 (99.5%)
RNA coding genes	2 (0.74%)	1 (0.5%)
Protein coding genes with predicted function	118 (43.87%)	89 (44.5%)
Without predicted function	149 (55.39%)	110 (55 %)

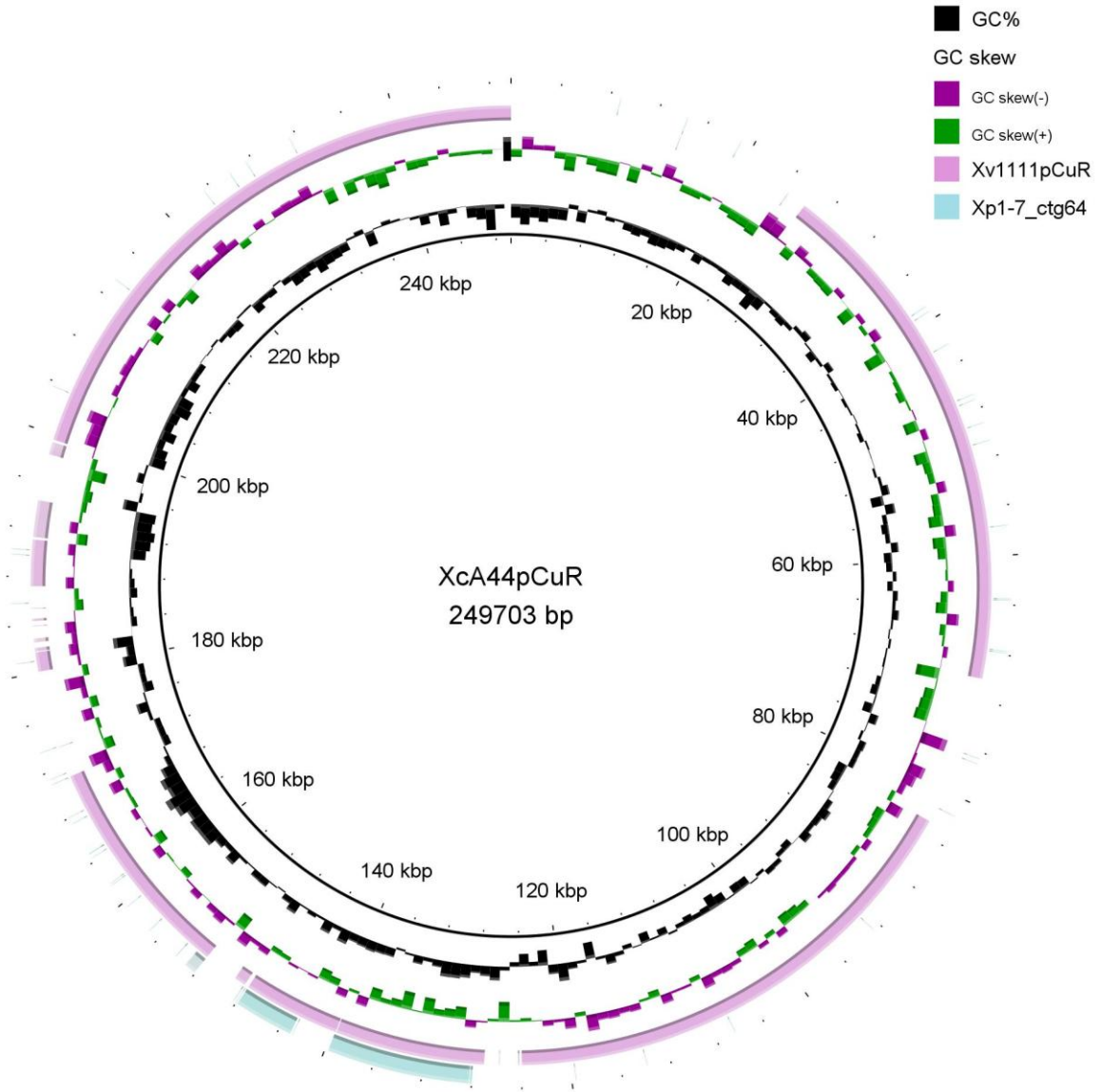


Figure 4-9. Circular representation of Xc-A44pCuR using BRIG. Circles from outside to inside: first, scale bar in Kbp; second and third: G+C content showing % of GC bases out of the four nucleotides, and G+C skew showing excess of C over G (purple), or G over C (green); fourth, BLASTn alignment using Xv1111pCuR as a subject sequence; fifth, BLASTn alignment using Xp1-7 Contig_64 (41783 bp) as a subject sequence.

Table 4-3. Gene summary of Xc-A44pCuR region '00056' (26132bp), obtained using IMG/ER Gene calling method, and Xc-A306 region '4624091; 4651419' (27328 bp) from GenBank. The genes identified as 'hypothetical protein' were not included in the list

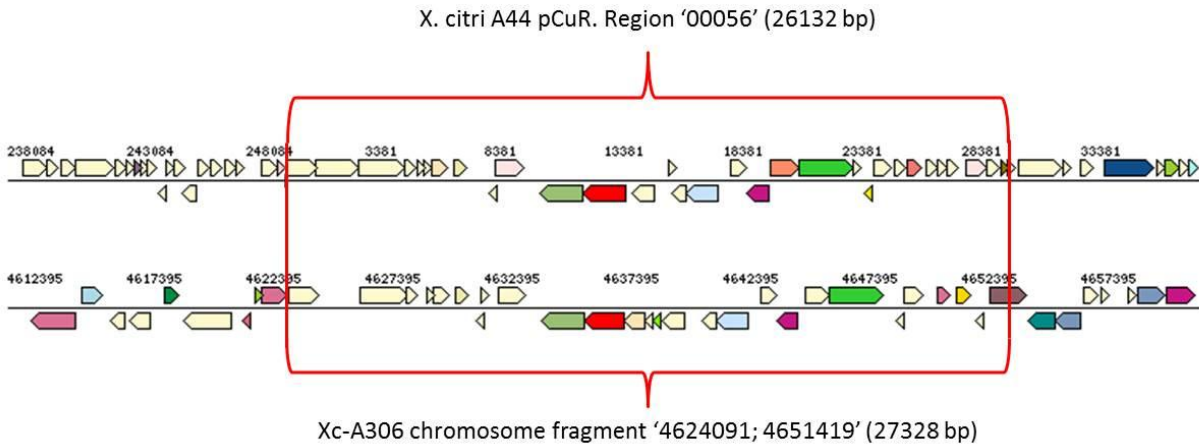
Designation	Gene ID	Locus Tag	Gene Product Name
Xc-A44pCuR region '00056' (position '1...26132')	2520013283	XcA44BVpCuR_00001	Phage integrase family
	2520013289	XcA44BVpCuR_00007	Transposase and inactivated derivatives.
	2520013290	XcA44BVpCuR_00008	PemK-like protein.
	2520013292	XcA44BVpCuR_00010	Restriction endonuclease.
	2520013293	XcA44BVpCuR_00011	Superfamily I DNA and RNA helicases.
	2520013294	XcA44BVpCuR_00012	Predicted ATP-dependent endonuclease of the OLD family.
	2520013295	XcA44BVpCuR_00013	Endodeoxyribonuclease RusA.
	2520013297	XcA44BVpCuR_00015	HNH endonuclease.
	2520013298	XcA44BVpCuR_00016	AAA domain.
	2520013300	XcA44BVpCuR_00018	Predicted transcriptional regulator.
	2520013302	XcA44BVpCuR_00020	Enzymes involved in molybdopterin and thiamine biosynthesis.
	2520013304	XcA44BVpCuR_00022	Helix-turn-helix.
	2520013307	XcA44BVpCuR_00025	PAPS reductase/FAD synthetase and related enzymes.
	2520013313	XcA44BVpCuR_00031	Nucleotidyltransferases.
	Xc-A306 chromosome (AE008923.1), fragment (position '4624091; 4651419')	21110336	AAM38769.1
21110340		AAM38772.1	<i>IS1389</i> transposase.
21110341		AAM38773.1	<i>IS1389</i> transposase.
21110343		AAM38775.1	<i>ISxac3</i> transposase.
21110344		AAM38776.1	<i>ISxac2</i> transposase.
21110346		AAM38778.1	DNA helicase.
21110348		AAM38780.1	<i>ISxac2</i> transposase*
21110349		AAM38781.1	<i>ISxac2</i> transposase*
21110350		AAM38782.1	recombination related protein
21110362		AAM38792.1	competence related protein

(*) Gene not present in Xc-A44 pCuR '00056' region.

Table 4-4. Gene summary of Xc-A44pCuR region '00052', obtained using IMG/ER Gene calling method, and Xc-A306 region '3399205; 3411434' from GenBank. (12230 bp; 100% identity). The genes identified as 'hypotetical protein' were not included in the list.

Designation	Gene ID	Locus Tag	Gene Product Name
Xc-A44pCuR region '00052' (position '69875... 82468')	2520013359	XcA44BVpCuR_00077	Site-specific recombinase XerD.
	2520013360	XcA44BVpCuR_00078	Phage integrase family Type I restriction-modification system methyltransferase subunit (EC:2.1.1.72).
	2520013364	XcA44BVpCuR_00082	
	2520013365	XcA44BVpCuR_00083	Type I site-specific deoxyribonuclease (EC:3.1.21.3).
	2520013366	XcA44BVpCuR_00084	Type I site-specific restriction-modification system, R (restriction) subunit and related helicases (EC:3.1.21.3).
	2520013372	XcA44BVpCuR_00090	ATP-dependent DNA helicase RecG (EC 3.6.1.).
	2520013373	XcA44BVpCuR_00091	Tetratricopeptide repeat/Sel1 repeat.
	2520013374	XcA44BVpCuR_00092	Putative helicase. Conjugative coupling factor TraD, SXT/TOL subfamily.
	2520013375	XcA44BVpCuR_00093	
	2520013376	XcA44BVpCuR_00094	Domain of unknown function (DUF4400). Putative conjugative transfer and/or transposition protein.
Xc-A306 chromosome, region '3399205; 3411434'	21109200	AAM37743.1	Type I restriction-modification system endonuclease.
	21109201	AAM37744.1	Type I restriction-modification system specificity determinant.
	21109202	AAM37745.1	Type I restriction-modification system DNA methylase.
	21109206	AAM37749.1	Integrase/recombinase.

A



B

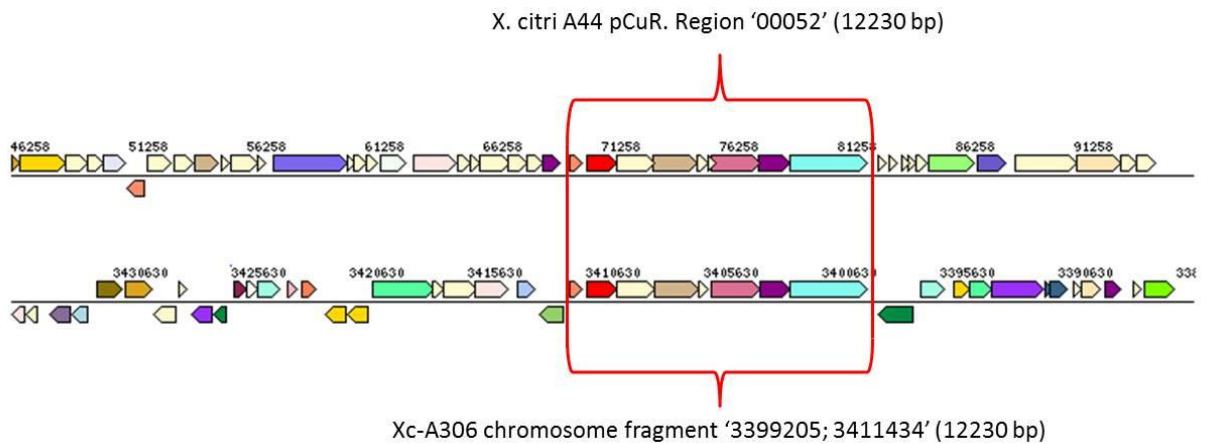


Figure 4-10. Gene Orthologous Neighborhoods comparison among (A) Xc-A44pCuR region designated '00056' ('1... 26132'), and Xc-A306 chromosome (AE008923.1) region '4624091; 4651419' (27328 bp); (B) Xc-A44pCuR region '00052' ('69875... 82468'), and Xc-A306 chromosome (AE008923.1) region '3399205; 3411434' (12230 bp). The area compared is delimited in red. The conserved neighborhood for the predicted genes in each Xc-A44 region was compared using IMG/ER database via top COG hit homolog.

CHAPTER 5

SUMMARY AND DISCUSSION

Citrus canker is a bacterial disease incited by *Xanthomonas citri* type A (Xc-A) and *X. fuscans* pv. *aurantifolii* (Xfa) species. The major objectives of this dissertation were 1) to identify and characterize the gene from Xfa type C that elicits a hypersensitivity response (HR) in certain *Citrus* species and 2) to characterize chromosomal and plasmid structural arrangements in copper resistant (CuR) strain, Xc-A44. The gene responsible for the Xfa type C strain eliciting an HR in all citrus species except Key lime (*C. aurantifolia*) was identified and designated *avrGf2*. A non-functional copy of this effector is present in Xfa-B strains, which suggests that Xfa-C is the progenitor strain. The gene *avrGf2* was not found in strains Xfa-#93 (an Xfa-C variant that does not produce HR in *Citrus*) and Xc-A* 290 (Xc-A* 1974), which induces a slow type of necrosis in grapefruit (GF) leaves after infiltration. For strain Xc-A*290, the visual comparison of the HR induced in GF leaves and the bacterial growth curves in GF leaves were different compared to the results in Xc-A306 strain carrying *avrGf1* and *avrGf2* genes. Compared with the previously characterized, *avrGf1* gene, *avrGf2* elicited a faster type of HR in citrus. The two avirulence genes, *avrGf1* and *avrGf2*, both members of the XopAG family, share low sequence identity at the nucleotide level, but 45% identity at the amino acid level and both contain chloroplast localization signals. Based on amino acid sequence comparisons, two C-terminal motifs were identified in AvrGf1 and AvrGf2 effectors and also in several XopAG related members described for *Xanthomonas* spp., *Pseudomonas* spp., *Acidovorax citrulli*, and *Ralstonia solanacearum*. Given that only the C terminal parts of *avrGf1* and *avrGf2* effectors have a high degree of similarity, the C terminal part of the *avrGf1* effector was swapped in the

corresponding terminal part of *avrGf2* to create the hybrid protein N-AvrGf2:C-AvrGf1. No difference was observed between the strain (Xc-A306) that carried the construct N-AvrGf2:C-AvrGf1, and the wild-type strain carrying empty vector (Xc-A306:pLAFR3), indicating a possible non-functionality of the hybrid protein due to incorrect folding of the effector. A putative C-terminal domain shows a conserved site, CLNAXYD was determined to be essential for HR elicitation based on characterization of mutants at this site. A cyclophilin (Cyp) binding site (GPXL) also conserved in all the XopAG class effector family members was determined to be essential for HR elicitation, although slight modification delayed the HR. The interaction between both avirulence proteins and the plant cyclophilin protein was confirmed using yeast two-hybrid experiments between GF-Cyp, and T3E *avrGf1* or *avrGf2*. A transient approach with *Agrobacterium* was used to down-regulate gene GF-Cyp in Duncan GF leaves. A delay in the HR elicitation for *avrGf2* in leaves with reduced GF-Cyp expression was quantified by changes in electrolyte leakage over time.

After completing genome sequencing of CuR strain Xc-A44, the strain was determined to have a similar T3E profile as well as high sequence identity with the chromosome of the reference strain Xc-A306; however, there were considerable differences in the plasmid profiles. Comparison of plasmid profiles in several copper resistant strains revealed differences in size for the pathogenicity and CuR plasmids. All the Xc-A strains isolated in Bella Vista region showed relatively similar pCuR sizes, which were larger than the pCuRs in strains Xp1-7, Xv1111, and Xv BV5-4a (isolated also in Bella Vista region). The Xc-A44 pathogenicity plasmid, which has an approx. size of 123 kbp (plasmid Xc-A44p123) has differences in the sequence and number of

its TALEs. The nucleotide sequences in Xc-A44 p123 indicate a recombination has occurred between plasmids pXAC33 and pXAC64 that were identified in strain Xc-A306. The identification of two copies of the TALE *pthA4* in two dissimilar clones in the Xc-A44 library suggests the presence of two homologs of *pthA4* in strain Xc-A44. Both *pthA4* homologs, *pthA44-4.1* and *pthA44-4.2*, confer pustule formation, and indicate that five copies of TALEs are present in plasmid Xc-A44p123. Based on the analysis of several cosmid clones from an Xc-A44 library and contigs that show homology with the sequences obtained from individual characterization of clones, a draft model and possible structure for Xc-A44 p123 was generated in order to explain how the TALEs are ordered in the plasmid. To confirm the sequence of the proposed Xc-A44 p123 molecule, it will be necessary to screen more clones from the Xc-A44 library, and the sequences obtained will need to be corroborated using a combination of the 454 and Illumina contig databases, as well as alternative techniques such as single molecule real time (SMRT). The second plasmid rearrangement was observed in the 250 kbp pCuR which mediated copper resistance. Plasmid Xc-A44pCuR has two insertion sequences with chromosome homology in Xc-A44 and Xc-A306. The percent identity between Xc-A44 pCuR and Xv1111 pCuR is high (>94.9% identity), but does not contain the transposon insertion present in Xc-A44pCuR. It is plausible that the insertion event could have occurred after the acquisition of the plasmid by Xc-A strains. The insertions found in Xc-A44 pCuR have sequence identities with bacterial endonucleases, recombinases, integrases, and transposases. Some of the transposases present in Xc-A44pCuR, such as *IS1389* and *ISxac*, were previously described in *Xanthomonas*, and represent families of transposons disseminated in

several *Xanthomonas* genomes, but were never described in plasmids that mediate resistance to copper.

LIST OF REFERENCES

- Ah-You N, Gagnevin L, Grimont Pa, *et al.*, 2009. Polyphasic characterization of xanthomonads pathogenic to members of the Anacardiaceae and their relatedness to species of *Xanthomonas*. *Int J Syst Evol Microbiol* **59**, 306-18.
- Alizadeh A, Rahimian H, 1990. Citrus canker in Kerman Province. *Iranian Journal of Plant Pathology* **26**, 118.
- Altschul Sf, Madden TI, Schäffer Aa, *et al.*, 1997. Gapped BLAST and PSI-BLAST: a new generation of protein database search programs. *Nucleic acids research* **25**, 3389-402.
- Amuthan G, Mahadevan A, 1994. Replicon typing of plasmids of phytopathogenic xanthomonads. *Plasmid* **32**, 328-32.
- Arlat M, Gough C, Barber Ce, Boucher C, Daniels Mj, 1991. *Xanthomonas campestris* contains a cluster of hrp genes related to the larger hrp cluster of *Pseudomonas solanacearum*. *Mol. Plant-Microbe Interact* **4**, 593-601.
- Aumüller T, Jahreis Gn, Fischer G, Schiene-Fischer C, 2010. Role of prolyl cis/trans isomers in cyclophilin-assisted *Pseudomonas syringae* AvrRpt2 protease activation. *Biochemistry* **49**, 1042-52.
- Bailey TI, Williams N, Mischel C, Li Ww, 2006. MEME: discovering and analyzing DNA and protein sequence motifs. *Nucleic acids research* **34**, W369-W73.
- Barash I, Manulis-Sasson S, 2009. Recent evolution of bacterial pathogens: the gall-forming *Pantoea agglomerans* case. *Annual review of phytopathology* **47**, 133-52.
- Basim H, Stall Re, Minsavage Gv, Jones Jb, 1999. Chromosomal gene transfer by conjugation in the plant pathogen *Xanthomonas axonopodis* pv. *vesicatoria*. *Phytopathology* **89**, 1044-9.
- Behlau F, Belasque J, Graham J, Leite R, 2010. Effect of frequency of copper applications on control of citrus canker and the yield of young bearing sweet orange trees. *Crop Protection* **29**, 300-5.
- Behlau F, Canteros Bi, Minsavage Gv, Jones Jb, Graham Jh, 2011. Molecular characterization of copper resistance genes from *Xanthomonas citri* subsp. *citri* and *Xanthomonas alfalfae* subsp. *citrumelonis*. *Appl Environ Microbiol* **77**, 4089-96.

- Bender Cl, Cooksey Da, 1986. Indigenous plasmids in *Pseudomonas syringae* pv. tomato: conjugative transfer and role in copper resistance. *Journal of bacteriology* **165**, 534-41.
- Berger E, 1914. Citrus canker in the Gulf Coast country, with notes on the extent of citrus culture in the localities visited. *Florida State Hort. Soc. Proc* **15**.
- Block A, Alfano Jr, 2011. Plant targets for *Pseudomonas syringae* type III effectors: virulence targets or guarded decoys? *Current opinion in microbiology* **14**, 39-46.
- Block A, Guo M, Li G, Elowsky C, Clemente Te, Alfano Jr, 2010. The *Pseudomonas syringae* type III effector HopG1 targets mitochondria, alters plant development and suppresses plant innate immunity. *Cellular microbiology* **12**, 318-30.
- Bogdanove Aj, Schornack S, Lahaye T, 2010. TAL effectors: finding plant genes for disease and defense. *Current opinion in plant biology* **13**, 394-401.
- Bonas U, Schulte R, Fenselau S, Minsavage G, Staskawicz B, Stall R, 1991. Isolation of a gene cluster from *Xanthomonas campestris* pv. vesicatoria that determines pathogenicity and hypersensitive response on pepper and tomato. *Mol Plant Microbe Interact* **4**, 81 - 8.
- Brunings A, Gabriel D, 2003. *Xanthomonas citri*: breaking the surface. *Molecular Plant Pathology* **4**, 141 - 57.
- Brunings Amey, B. Yuan, Q. Shanker, S. Gabriel, D. W. A self-transmissible plasmid carries at least two non-hrp genes required to cause citrus canker disease. In: Microbiology Asf, ed. *Proceedings of the General Meeting Of The American Society For Microbiology, 2001*. Orlando, Florida, 96.
- Bui Tn, Verniere C, Jarne P, *et al.*, 2009. From local surveys to global surveillance: three high-throughput genotyping methods for epidemiological monitoring of *Xanthomonas citri* pv. *citri* pathotypes. *Appl Environ Microbiol* **75**, 1173-84.
- Bull C, De Boer S, Denny T, *et al.*, 2010. Comprehensive list of names of plant pathogenic bacteria, 1980-2007. *Journal of Plant Pathology* **92**, 551-92.
- Bull C, De Boer S, Denny T, *et al.*, 2012. List of New Names of Plant Pathogenic Bacteria (2008-2010). *Journal of Plant Pathology* **94**, 21-7.
- Campos Bm, Sforça MI, Ambrosio AI, *et al.*, 2013. A Redox 2-Cys Mechanism Regulates the Catalytic Activity of Divergent Cyclophilins. *Plant physiology*.
- Canteros Bi, 1984. Disminuye la infección de cancrisis en los montes cítricos. In. *Sintesis Tecnologica*. Bella Vista, Corrientes: INTA, 2.

- Canteros Bi, 1990. *Diversity of Plasmids and Plasmid-encoded Phenotypic Traits in Xanthomonas Campestris Pv. Vesicatoria*. University of Florida.
- Canteros Bi. Copper resistance in *Xanthomonas campestris* pv. citri. In: A. M, ed. *Proceedings of the International Conference on Plant pathogenic Bacteria*. 26-29 August, 1996. Madras, Chennai, India, 455-9.
- Canteros Bi, 2005. Ecología de la cancrrosis de los citrus en Argentina. In: Aaf, ed. *XIII Congreso Latinoamericano de Fitopatología y III Taller de la Asociación Argentina de Fitopatólogos*. Villa Carlos Paz, Cordoba, Argentina: AAF, 57-60.
- Canteros Bi, Gochez Am, Hermosis F, Soliz J, Benitez R, 2013. Estado actual de la resistencia al cobre en la bacteria causal de la cancrrosis de los citrus en argentina. In: Inta, ed. *VII Congreso Argentino de Citricultura*. Puerto Iguazu, Misiones, 1.
- Canteros Bi, Hermosís F, Solíz Ja, Benítez R, Gochez Am. Bacteriocinas producidas por cepas grupo A contra cepas grupo B de *Xanthomonas axonopodis* pv. citri causantes de cancrrosis de los citrus. *Proceedings of the Congreso Argentino de Fitopatología*. 2. 2011 06 01-03, 1, 2 y 3 de Junio de 2011. Mar del Plata, Buenos Aires. AR., 2011.
- Canteros Bi, Rybak M, Naranjo M, et al., 2004. Caracterización molecular de la resistencia al cobre en *Xanthomonas axonopodis* pv. citri. In. Resúmenes de los trabajos presentados. XVº Reunión de Comunicaciones Científicas y Técnicas: UNNE.
- Canteros De Echenique B, Zagory D, Stall Re, 1985. A medium for cultivation of the B-strain of *Xanthomonas campestris* pv. citri, cause of cancrrosis B in Argentina and Uruguay. *Plant disease* **69**.
- Carvalho Fmds, Caramori Lpc, Leite Júnior Rp, 2005. Genetic diversity of *Xanthomonas axonopodis* pv. citri based on plasmid profile and pulsed field gel electrophoresis. *Genetics and Molecular Biology* **28**, 446-51.
- Cervantes C, Gutierrez-Corona F, 1994. Copper resistance mechanisms in bacteria and fungi. *FEMS microbiology reviews* **14**, 121-37.
- Cha J-S, Cooksey Da, 1993. Copper hypersensitivity and uptake in *Pseudomonas syringae* containing cloned components of the copper resistance operon. *Applied and environmental microbiology* **59**, 1671-4.
- Chandrika R, Gabriel D, 2003. Towards genetically engineered citrus plants with canker resistance. In: Aps, ed. *2003 APS Annual Meeting*. Charlotte, NC: Phytopathology, S15. (93.)

- Chiesa Ma, Siciliano Mf, Ornella L, *et al.*, 2013. Characterization of a Variant of *Xanthomonas citri* subsp. *citri* that Triggers a Host-Specific Defense Response. *Phytopathology* **103**, 555-64.
- Civerolo E, 1984. Bacterial canker disease of citrus. *Journal of the Rio Grande Valley Horticultural Society* **37**, 127 - 45.
- Civerolo E, Fan F, 1982. ***Xanthomonas campestris* pv. *citri* Detection and Identification by Enzyme-Linked Immunosorbent Assay.** . In. Plant Disease: APS, 231-6. (66.)
- Coaker G, Falick A, Staskawicz B, 2005. Activation of a phytopathogenic bacterial effector protein by a eukaryotic cyclophilin. *Science* **308**, 548-50.
- Coaker G, Zhu G, Ding Z, Van Doren Sr, Staskawicz B, 2006. Eukaryotic cyclophilin as a molecular switch for effector activation. *Molecular microbiology* **61**, 1485-96.
- Collmer A, Badel JI, Charkowski Ao, *et al.*, 2000. Pseudomonas syringae Hrp type III secretion system and effector proteins. *Proceedings of the National Academy of Sciences* **97**, 8770-7.
- Conover Ra, Gerhold Nr. Mixtures of copper and maneb or mancozeb for control of bacterial spot of tomato and their compatibility for control of fungus diseases [Phytophthora infestans, Stemphylium solani, Xanthomonas campestris pv. vesicatoria, Florida]. *Proceedings of the Proceedings of the... annual meeting of the Florida State Horticultural Society, 1981.*
- Cook A, Stall R, 1968. Effect of Xanthomonas vesicatoria on loss of electrolytes from leaves of Capsicum annuum. *Phytopathology* **58**, 617-9.
- Cooksey Da, 1990a. Genetics of bactericide resistance in plant pathogenic bacteria. *Annual review of phytopathology* **28**, 201-19.
- Cooksey Da, 1990b. Plasmid-determined copper resistance in Pseudomonas syringae fromimpatiens. *Applied and environmental microbiology* **56**, 13-6.
- Cooksey Da, Azad Hr, Cha J-S, Lim C-K, 1990. Copper resistance gene homologs in pathogenic and saprophytic bacterial species from tomato. *Applied and environmental microbiology* **56**, 431-5.
- Coplin D, Rowan R, Chisholm D, Whitmoyer R, 1981. Characterization of plasmids in Erwinia stewartii. *Applied and environmental microbiology* **42**, 599-604.
- Cornelis G, Biot T, Rouvroit Cl, *et al.*, 1989. The Yersinia yop regulon. *Molecular microbiology* **3**, 1455-9.

- Cubero J, Graham J, 2002. Genetic relationship among worldwide strains of *Xanthomonas* causing canker in citrus species and design of new primers for their identification by PCR. *Appl Environ Microbiol* **68**, 1257 - 64.
- Da Silva Ac, Ferro Ja, Reinach Fc, *et al.*, 2002. Comparison of the genomes of two *Xanthomonas* pathogens with differing host specificities. *Nature* **417**, 459-63.
- Daniels Mj, Barber Ce, Turner Pc, Cleary Wg, Sawczyk Mk, 1984. Isolation of mutants of *Xanthomonas campestris* pv. *campestris* showing altered pathogenicity. *Journal of general microbiology* **130**, 2447-55.
- Das A, Rangaraj N, Sonti R, 2009. Multiple adhesin-like functions of *Xanthomonas oryzae* pv. *oryzae* are involved in promoting leaf attachment, entry, and virulence on rice. *Mol Plant Microbe Interact* **22**, 73 - 85.
- Davis J, Wang J, Tropea Je, *et al.*, 2008. Novel fold of VirA, a type III secretion system effector protein from *Shigella flexneri*. *Protein Science* **17**, 2167-73.
- Defeyter R, Kado Ci, Gabriel Dw, 1990. Small, stable shuttle vectors for use in *Xanthomonas*. *Gene* **88**, 65-72.
- Deng Xx, Grosser Jw, Gmitter Jr Fg, 1992. Intergeneric somatic hybrid plants from protoplast fusion of *Fortunella crassifolia* cultivar 'Meiwa' with *Citrus sinensis* cultivar 'Valencia'. *Scientia horticulturae* **49**, 55-62.
- Derso E, Vernière C, Pruvost O, 2009. First report of *Xanthomonas citri* pv. *citri*-A* causing citrus canker on lime in Ethiopia. *Plant Disease* **93**, 203-.
- Ditta G, Stanfield S, Corbin D, Helinski Dr, 1980. Broad host range DNA cloning system for gram-negative bacteria: construction of a gene bank of *Rhizobium meliloti*. *Proceedings of the National Academy of Sciences* **77**, 7347-51.
- Domingues Mn, De Campos Bm, De Oliveira Mlp, De Mello Uq, Benedetti Ce, 2012. TAL Effectors Target the C-Terminal Domain of RNA Polymerase II (CTD) by Inhibiting the Prolyl-Isomerase Activity of a CTD-Associated Cyclophilin. *PLoS one* **7**, e41553.
- Dominguez-Solis Jr, He Z, Lima A, Ting J, Buchanan Bb, Luan S, 2008. A cyclophilin links redox and light signals to cysteine biosynthesis and stress responses in chloroplasts. *Proceedings of the National Academy of Sciences* **105**, 16386-91.
- Doyle Sm, Diamond M, McCabe Pf, 2010. Chloroplast and reactive oxygen species involvement in apoptotic-like programmed cell death in *Arabidopsis* suspension cultures. *Journal of experimental botany* **61**, 473-82.
- Dunger G, Pereda R, Farah C, Orellano E, Jorgelina O, 2008. Protein-protein interactions identified for effector proteins of the phytopathogen *Xanthomonas*

- axonopodis pv. citri [abstract]. *Proceedings of the V Congreso Argentino de Microbiologia General*.
- Dunger G, Relling Vm, Tondo MI, *et al.*, 2007. Xanthan is not essential for pathogenicity in citrus canker but contributes to Xanthomonas epiphytic survival. *Archives of microbiology* **188**, 127-35.
- El Yacoubi B, Brunings A, Yuan Q, Shankar S, Gabriel D, 2007. In planta horizontal transfer of a major pathogenicity effector gene. *Applied and Environmental Microbiology* **73**, 1612 - 21.
- El-Goorani Ma, 1989. The Occurrence of Citrus Canker Disease in United Arab Emirates (U.A.E.). *Journal of Phytopathology* **125**, 257-64.
- Erhardt M, Namba K, Hughes Kt, 2010. Bacterial nanomachines: the flagellum and type III injectisome. *Cold Spring Harbor perspectives in biology* **2**.
- Escalon A, Javegny S, Vernière C, *et al.*, 2013. Variations in type III effector repertoires, pathological phenotypes and host range of Xanthomonas citri pv. citri pathotypes. *Molecular plant pathology*.
- Fao, 2013. FAOSTAT. In. UN: FAO. (2014.)
- Fawcett Hs, Bitancourt Aa, 1937. Relatorio sobre as doenças dos Citrus nos Estados de Pernambuco, Bahia, São Paulo e Rio Grande do Sul *Rodriguesia* **3**, 23.
- Fee Ja, 1975. copper proteins systems containing the “Blue” copper center. In. *Biochemistry*. Springer, 1-60.
- Figueiredo Jf, Römer P, Lahaye T, Graham Jh, White Ff, Jones Jb, 2011. Agrobacterium-mediated transient expression in citrus leaves: a rapid tool for gene expression and functional gene assay. *Plant cell reports* **30**, 1339-45.
- Finn R, Tate J, Mistry J, *et al.*, 2008. The Pfam protein families database. *Nucleic Acids Research*, D281 - 8.
- Friedman Am, Long Sr, Brown Se, Buikema Wj, Ausubel Fm, 1982. Construction of a broad host range cosmid cloning vector and its use in the genetic analysis of *Rhizobium* mutants. *Gene* **18**, 289-96.
- Fu A, He Z, Cho Hs, Lima A, Buchanan Bb, Luan S, 2007. A chloroplast cyclophilin functions in the assembly and maintenance of photosystem II in Arabidopsis thaliana. *Proceedings of the National Academy of Sciences* **104**, 15947-52.
- Furutani A, Takaoka M, Sanada H, *et al.*, 2009. Identification of novel type III secretion effectors in Xanthomonas oryzae pv. oryzae. *Mol Plant Microbe Interact* **22**, 96 - 106.

- Gochez A, Minsavage G, Potnis N, Canteros B, Stall R, Jones J, 2012. Comparison between *avrGf1* and *avrGf2* which elicit hypersensitive reactions (HR) in grapefruit and sweet orange. *Phytopathology* **102**, S4.45.
- Gochez A, Rinsdahl-Canavosio M, Canteros B. Pathogenicity of strains of the C group and B group of *Xanthomonas axonopodis* in Duncan grapefruit (*Citrus paradisi*) and Key lime (*C. aurantifolia*). In: Deng X, ed. *Proceedings of the 11th International Citrus Congress, 2008*. Wuhan: International Society of Citriculture, 3.
- Gophna U, Ron Ez, Graur D, 2003. Bacterial type III secretion systems are ancient and evolved by multiple horizontal-transfer events. *Gene* **312**, 151-63.
- Goto M, 1972. Survival of *Xanthomonas citri* in the bark tissues of citrus trees. *Canadian Journal of Botany* **50**, 2629-35.
- Goto M, Takahashi T, Messina M, 1980. A comparative study of the strains of *Xanthomonas campestris* pv. *citri* isolated from citrus canker in Japan and cancrisis B in Argentina. *Annals of the Phytopathological Society of Japan* **46**, 329-38.
- Gottwald Tr, Graham Jh, 1992. A Device for Precise and Nondisruptive Stornata! Inoculation of Leaf Tissue with Bacterial Pathogens. *Phytopathology* **82**, 930-5.
- Graham Jh, Gottwald Tr, Cubero J, Achor Ds, 2004. *Xanthomonas axonopodis* pv. *citri*: factors affecting successful eradication of citrus canker. *Mol Plant Pathol* **5**, 1-15.
- Guidot A, Prior P, Schoenfeld J, Carrere S, Genin S, Boucher C, 2007. Genomic structure and phylogeny of the plant pathogen *Ralstonia solanacearum* inferred from gene distribution analysis. *Journal of Bacteriology* **189**, 377 - 87.
- Gullino MI, Tinivella F, Garibaldi A, Kemmitt Gm, Bacci L, Sheppard B, 2010. Mancozeb: past, present, and future. *Plant Disease* **94**, 1076-87.
- Gupta R, Mould Rm, He Z, Luan S, 2002. A chloroplast FKBP interacts with and affects the accumulation of Rieske subunit of cytochrome bf complex. *Proceedings of the National Academy of Sciences* **99**, 15806-11.
- Gurlebeck D, Thieme F, Bonas U, 2006. Type III effector proteins from the plant pathogen *Xanthomonas* and their role in the interaction with the host plant. *Journal of Plant Physiology* **163**, 233 - 55.
- Guttman Ds, Vinatzer Ba, Sarkar Sf, Ranall Mv, Kettler G, Greenberg Jt, 2002. A functional screen for the type III (Hrp) secretome of the plant pathogen *Pseudomonas syringae*. *Science* **295**, 1722-6.
- Gómez P, Ribas-Aparicio Rm, Peléez A, Rodicio Mr, 1999. Characterization of IS1389, a new member of the IS3 family of insertion sequences isolated from

- Xanthomonas campestris pv. amaranthicola. *Archives of microbiology* **172**, 15-21.
- Göthel S, Marahiel M, 1999. Peptidyl-prolyl cis-trans isomerases, a superfamily of ubiquitous folding catalysts. *Cellular and Molecular Life Sciences CMLS* **55**, 423-36.
- Hajri A, Brin C, Hunault G, *et al.*, 2009. A «repertoire for repertoire» hypothesis: Repertoires of type three effectors are candidate determinants of host specificity in Xanthomonas. *PLoS One* **4**, e6632.
- Hasse Ch, 1915. Pseudomonas citri, the cause of citrus canker. <A preliminary report>. *Journal of agricultural research*. **IV**, 97-100.
- He Z, Li L, Luan S, 2004. Immunophilins and parvulins. Superfamily of peptidyl prolyl isomerases in Arabidopsis. *Plant physiology* **134**, 1248-67.
- Heitman J, Movva N, Hall M, 1992. Proline isomerases at the crossroads of protein folding, signal transduction, and immunosuppression. *The New biologist* **4**, 448-60.
- Hibberd A, Bassett M, Stall R, 1987a. Allelism tests of three dominant genes for hypersensitive resistance to bacterial spot of pepper. *Phytopathology* **77**, 1304-7.
- Hibberd A, Stall R, Bassett M, 1987b. Different phenotypes associated with incompatible races and resistance genes in bacterial spot disease of pepper. *Plant disease* **71**.
- Horvath Dm, Stall Re, Jones Jb, *et al.*, 2012. Transgenic resistance confers effective field level control of bacterial spot disease in tomato. *PLoS One* **7**, e42036.
- Hu Y, Zhang J, Jia H, *et al.* Diverse TAL effectors converge on a single host susceptibility gene in citrus canker. *Proceedings of the PHYTOPATHOLOGY, 2013: AMER PHYTOPATHOLOGICAL SOC 3340 PILOT KNOB ROAD, ST PAUL, MN 55121 USA*, 62-.
- Huguet E, Hahn K, Wengelnik K, Bonas U, 1998. hpaA mutants of Xanthomonas campestris pv. vesicatoria are affected in pathogenicity but retain the ability to induce host-specific hypersensitive reaction. *Mol Microbiol* **29**, 1379-90.
- Ibrahim G, Bayaa B, 1989. Fungal, bacterial and nematological problems of citrus, grape and stone fruits in Arab countries. *Arab Journal of Plant Protection* **7**, 190-7.
- Ishiga Y, Ishiga T, Wangdi T, Mysore Ks, Uppalapati Sr, 2012. NTRC and chloroplast-generated reactive oxygen species regulate Pseudomonas syringae pv. tomato disease development in tomato and Arabidopsis. *Molecular Plant-Microbe Interactions* **25**, 294-306.

- Jaciani F, Destefano S, Rodrigues Neto J, Belasque Jr J, 2009. Detection of a New Bacterium Related to *Xanthomonas fuscans* subsp. *aurantifolii* Infecting Swingle Citrumelo in Brazil. *Plant Disease* **93**, 1074.
- Jaciani F, Ferro J, Ferro M, Verniere C, Pruvost O, Belasque Jr J, 2012. Genetic Diversity of a Brazilian Strain Collection of *Xanthomonas citri* subsp. *citri* Based on the Type III Effector Protein Genes. *Plant Disease* **96**, 193-203.
- Jalan N, Deng X, Jones J, Wang N. Pan-genome analysis of *Xanthomonas citri* subsp. *citri* provides insights into bacterial evolution and pathogenicity. *Proceedings of the Phytopathology, 2013a*: Amer Phytopathological Soc 3340 PILOT KNOB ROAD, ST PAUL, MN 55121 USA, 67-.
- Jalan N, Kumar D, Andrade Mo, *et al.*, 2013b. Comparative genomic and transcriptome analyses of pathotypes of *Xanthomonas citri* subsp. *citri* provide insights into mechanisms of bacterial virulence and host range. *BMC genomics* **14**, 551.
- Jalan N, Kumar D, Wang N, 2012. Gene content or gene expression: Which determines the difference in the host specificity and virulence of strains of *Xanthomonas citri* subsp. *citri*? . In: Aps, ed. *2012 APS Meeting*. Providence, Rhode Island: Phytopathology, S58. (102.)
- Jamir Y, Guo M, Oh Hs, *et al.*, 2004. Identification of *Pseudomonas syringae* type III effectors that can suppress programmed cell death in plants and yeast. *The Plant Journal* **37**, 554-65.
- Jelenska J, Yao N, Vinatzer Ba, Wright Cm, Brodsky JI, Greenberg Jt, 2007. AJ Domain Virulence Effector of *Pseudomonas syringae* Remodels Host Chloroplasts and Suppresses Defenses. *Current Biology* **17**, 499-508.
- Jones J, Lacy G, Bouzar H, Stall R, Schaad N, 2004. Reclassification of the xanthomonads associated with bacterial spot disease of tomato and pepper. *Syst Appl Microbiol* **27**, 755 - 62.
- Jones J, Woltz S, Jones J, Portier K, 1991. Population dynamics of *Xanthomonas campestris* pv. *vesicatoria* on tomato leaflets treated with copper bactericides. *Phytopathology* **81**, 714-9.
- Jones J, Woltz S, Kelly R, Harris G. The role of ionic copper, total copper, and select bactericides on control of bacterial spot of tomato. *Proceedings of the Florida State Horticultural Society. Meeting, 1992*.
- Kado C, Amp, Liu S, 1981. Rapid procedure for detection and isolation of large and small plasmids. *Journal of bacteriology* **145**, 1365-73.
- Kearney B, Staskawicz B, 1990. Widespread distribution and fitness contribution of *Xanthomonas campestris* avirulence gene *avrBs2*. *Nature* **346**, 385 - 6.

- Kim J, Li X, Roden J, *et al.*, 2009. Xanthomonas T3S Effector XopN Suppresses PAMP-Triggered Immunity and Interacts with a Tomato Atypical Receptor-Like Kinase and TFT1. *Plant Cell* **21**, 1305 - 23.
- Kim J-G, Choi S, Oh J, Moon Js, Hwang I, 2006. Comparative analysis of three indigenous plasmids from *Xanthomonas axonopodis* pv. *glycines*. *Plasmid* **56**, 79-87.
- Kirchner J, Roy B, 2002. Evolutionary implications of host-pathogen specificity: fitness consequences of pathogen virulence traits. *Evolutionary ecology research* **4**, 27-48.
- Klement Z, Goodman R, 1967. The hypersensitive reaction to infection by bacterial plant pathogens. *Annual Review of Phytopathology* **5**, 17-44.
- Klement Z, Rudolph K, Sands D, 1990. *Methods in phytopathology*. Akademiai Kiado.
- Kuhara S, 1978. Present epidemic status and control of the citrus canker disease (*Xanthomonas citri* (Hasse) Dowson) in Japan. *Rev. Plant Prot. Res* **11**, 132-42.
- Lee H, 1921. The increase in resistance to citrus canker with the advance in maturity of citrus trees. *Phytopathology* **11**, 331-9.
- Leite Jr R. Surviving with citrus canker in Brazil. *Proceedings of the Proc. Int. Soc. Citriculture IX Congress, 2000*, 890-6.
- Lin H, Hsu S, Hwang A, Tzeng K, 2005. Phenotypic and genetic characterization of novel strains of *Xanthomonas axonopodis* pv. *citri* which induce atypical symptoms on citrus leaves in Taiwan. *Plant Pathology Bulletin* **14**, 227-38.
- Lin H-C, Chang Y-A, Chang H, 2013. A pthA homolog from a variant of *Xanthomonas axonopodis* pv. *citri* enhances virulence without inducing canker symptom. *European Journal of Plant Pathology* **137**, 677-88.
- Lin H-C, Chu M-K, Lin Y-C, *et al.*, 2011. A single amino acid substitution in PthA of *Xanthomonas axonopodis* pv. *citri* altering canker formation on grapefruit leaves. *European Journal of Plant Pathology* **130**, 143-54.
- Lindgren P, Panopoulos N, Staskawicz B, Dahlbeck D, 1988. Genes required for pathogenicity and hypersensitivity are conserved and interchangeable among pathovars of *Pseudomonas syringae*. *Molecular and General Genetics MGG* **211**, 499-506.
- Loucks Kw, 1934. Citrus Canker and its Eradication in Florida. . In. Unpublished manuscript archives of the Florida Department of Agriculture, Division of Plant Industry, Gainesville, FL., 110. (Florida Department of Agriculture, Division of Plant Industry; vol.)

- Madden Lv, Hughes G, Van Den Bosch F, 2007. *The study of plant disease epidemics*. American Phytopathological Society St Paul, MN.
- Marco G, Stall R, 1983. Control of bacterial spot of pepper initiated by strains of *Xanthomonas campestris* pv. *vesicatoria* that differ in sensitivity to copper. *Plant Disease* **67**, 779-81.
- Mark Osborn A, Böltner D, 2002. When phage, plasmids, and transposons collide: genomic islands, and conjugative-and mobilizable-transposons as a mosaic continuum. *Plasmid* **48**, 202-12.
- Marshall J, 1968. Methods of leaf area measurement of large and small leaf samples. *Photosynthetica* **2**, 41-7.
- Mclean Ft, Lee Ha, 1922. Pressures required to cause stomatal infections with the citrus canker organism. *Philipp. J. Sci* **20**, 309-20.
- Metz M, Dahlbeck D, Morales Cq, Al Sady B, Clark Et, Staskawicz Bj, 2005. The conserved *Xanthomonas campestris* pv. *vesicatoria* effector protein XopX is a virulence factor and suppresses host defense in *Nicotiana benthamiana*. *Plant J* **41**, 801-14.
- Mills S, Jasalavich C, Cooksey D, 1993. A two-component regulatory system required for copper-inducible expression of the copper resistance operon of *Pseudomonas syringae*. *Journal of bacteriology* **175**, 1656-64.
- Minsavage G, Canteros B, Stall R, 1990a. Plasmid-mediated resistance to streptomycin in *Xanthomonas campestris* pv. *vesicatoria*. *Phytopathology* **80**, 719-23.
- Minsavage G, Dahlbeck D, Whalen M, *et al.*, 1990b. Gene-for-gene relationships specifying disease resistance in *Xanthomonas campestris* pv. *vesicatoria*-pepper interactions. *Mol Plant Microbe Interact* **3**, 41 - 7.
- Mohammadi M, Mirzaee M, Rahimian H, 2001. Physiological and biochemical characteristics of iranian strains of *Xanthomonas axonopodis* pv. *citri*, the causal agent of citrus bacterial canker disease. *Journal of Phytopathology* **149**, 65-75.
- Moreira L, Almeida N, Potnis N, *et al.*, 2010a. Novel insights into the genomic basis of citrus canker based on the genome sequences of two strains of *Xanthomonas fuscans* subsp. *aurantifolii*. *BMC Genomics* **11**, 238.
- Moreira L, Almeida N, Potnis N, *et al.*, 2010b. Novel insights into the genomic basis of citrus canker based on the genome sequences of two strains of *Xanthomonas fuscans* subsp. *aurantifolii*. *BMC Genomics* **11**, 238.
- Moreira Lm, Almeida Nf, Potnis N, *et al.*, 2010c. Novel insights into the genomic basis of citrus canker based on the genome sequences of two strains of *Xanthomonas fuscans* subsp. *aurantifolii*. *BMC Genomics* **11**, 238.

- Muraro R, Roka F, Spreen T. An overview of Argentina's citrus canker control program with applicable costs for a similar program in Florida. *Proceedings of the Abstr.) In: Proceedings of the International Citrus Canker Research Workshop, Ft. Pierce FL, 2000.*
- Namekata T, Oliveira Ad. Comparative serological studies between *Xanthomonas citri* and a bacterium causing canker on Mexican lime. *Proceedings of the Proceeding of the Third Internacional Conference on Plant Pathogenic Bacteria (ed. HP Maas Geesteranus), Centre for Agricultural Publication and Documentation, Wageningen, The Netherlands, 1972, 151-2.*
- Narra Hp, Saripalli Cs, Gopalakrishnan J, 2013. Host induced changes in plasmid profile of *Xanthomonas axonopodis* pv. *malvacearum* races. *African Journal of Biotechnology* **10**, 2451-4.
- Neale Hc, Slater Rt, Mayne L-M, Manoharan B, Arnold DI, 2013. *In planta* induced changes in the native plasmid profile of *Pseudomonas syringae* pathovar *phaseolicola* strain 1302A. *Plasmid* **70**, 420-4.
- Ngoc L, Verniere C, Vital K, *et al.*, 2009. Development of 14 minisatellite markers for the citrus canker bacterium, *Xanthomonas citri* pv. *citri*. *Molecular Ecology Resources* **9**, 125-7.
- Ngoc Lbt, Vernière C, Jouen E, *et al.*, 2010. Amplified fragment length polymorphism and multilocus sequence analysis-based genotypic relatedness among pathogenic variants of *Xanthomonas citri* pv. *citri* and *Xanthomonas campestris* pv. *bilvae*. *International journal of systematic and evolutionary microbiology* **60**, 515-25.
- Nociti Las, Camargo M, Rodrigues Neto J, Francischini Fjb, Belasque Júnior J, 2006. Agressividade de linhagens de *Xanthomonas axonopodis* pv. *aurantifolii* Tipo C em lima ácida 'Galego'. *Fitopatologia Brasileira* **31**, 140-6.
- Noel L, Thieme F, Nennstiel D, Bonas U, 2002. Two novel type III-secreted proteins of *Xanthomonas campestris* pv. *vesicatoria* are encoded within the *hrp* pathogenicity island. *J Bacteriol* **184**, 1340 - 8.
- Occhialini A, Cunnac S, Reymond N, Genin S, Boucher C, 2005. Genome-wide analysis of gene expression in *Ralstonia solanacearum* reveals that the *hrpB* gene acts as a regulatory switch controlling multiple virulence pathways. *Molecular plant-microbe interactions* **18**, 938-49.
- Park D, Hyun J, Park Y, *et al.*, 2006. Sensitive and specific detection of *Xanthomonas axonopodis* pv. *citri* by PCR using pathovar specific primers based on *HrpW* gene sequences. *Microbiol Res* **161**, 145 - 9.

- Parsons Im, Edgington Lv, 1981. The possible role of fixed coppers in combination with ethylenbisdithiocarbamates for control of *Pseudomonas syringae* pv. tomato. In. *Phytopathology*: APS, 563. (71.)
- Patel M, Allayyanavaramath S, Kulkarni Y, 1953. Bacterial shot-hole and fruit canker of *Aegle marmelos* Correa. *Curr Sci* **22**, 216-7.
- Petnicki-Ocwieja T, Schneider Dj, Tam Vc, *et al.*, 2002. Genomewide identification of proteins secreted by the Hrp type III protein secretion system of *Pseudomonas syringae* pv. tomato DC3000. *Proceedings of the National Academy of Sciences* **99**, 7652-7.
- Phan J, Austin Bp, Waugh Ds, 2005. Crystal structure of the *Yersinia* type III secretion protein YscE. *Protein science* **14**, 2759-63.
- Pohronezny K, Stall Re, Canteros Bi, Kegley M, Datnoff Le, Subramanya R, 1992. Sudden shift in the prevalent race of *Xanthomonas campestris* pv. *vesicatoria* in pepper fields in southern Florida. *Plant disease* **76**, 118-20.
- Portnoy D, Moseley S, Falkow S, 1981. Characterization of plasmids and plasmid-associated determinants of *Yersinia enterocolitica* pathogenesis. *Infection and immunity* **31**, 775-82.
- Potnis N, Krasileva K, Chow V, *et al.*, 2011. Comparative genomics reveals diversity among xanthomonads infecting tomato and pepper. *BMC Genomics* **12**, 146.
- Potnis N, Minsavage G, Smith Jk, *et al.*, 2012. Avirulence Proteins AvrBs7 from *Xanthomonas gardneri* and AvrBs1. 1 from *Xanthomonas euvesicatoria* Contribute to a Novel Gene-for-Gene Interaction in Pepper. *Molecular Plant-Microbe Interactions* **25**, 307-20.
- Poueymiro M, Cunnac S, Barberis P, *et al.*, 2009. Two type III secretion system effectors from *Ralstonia solanacearum* GMI1000 determine host-range specificity on tobacco. *Molecular plant-microbe interactions* **22**, 538-50.
- Rademacher C, Masepohl B, 2012. Copper-responsive gene regulation in bacteria. *Microbiology* **158**, 2451-64.
- Rigano La, Siciliano F, Enrique R, *et al.*, 2007. Biofilm formation, epiphytic fitness, and canker development in *Xanthomonas axonopodis* pv. *citri*. *Molecular Plant-Microbe Interactions* **20**, 1222-30.
- Roden J, Belt B, Ross J, Tachibana T, Vargas J, Mudgett M, 2004. A genetic screen to isolate type III effectors translocated into pepper cells during *Xanthomonas* infection. *Proc Natl Acad Sci USA* **101**, 16624 - 9.
- Rodriguez Ds, 2012. *Origen y Desarrollo de los Citrus en Bella Vista, Corrientes*. Bella Vista, Corrientes: INTA.

- Rodríguez-Herva Jj, González-Melendi P, Cuartas-Lanza R, *et al.*, 2012. A bacterial cysteine protease effector protein interferes with photosynthesis to suppress plant innate immune responses. *Cellular microbiology* **14**, 669-81.
- Rohmer L, Guttman D, Dangl J, 2004. Diverse evolutionary mechanisms shape the type III effector virulence factor repertoire in the plant pathogen *Pseudomonas syringae*. *Genetics* **167**, 1341 - 60.
- Romano Pg, Horton P, Gray Je, 2004. The Arabidopsis cyclophilin gene family. *Plant Physiology* **134**, 1268-82.
- Rosetti V, 1977. Citrus canker in Latin America: a review. In. *Proceedings 2th International Citrus Congress* Orlando, Florida, 918-24. (3.)
- Ryan Rp, Ryan Dj, Sun Yc, Li Fm, Wang Y, Dowling Dn, 2007. An acquired efflux system is responsible for copper resistance in *Xanthomonas* strain IG-8 isolated from China. *FEMS microbiology letters* **268**, 40-6.
- Ryan Rp, Vorhölter F-J, Potnis N, *et al.*, 2011. Pathogenomics of *Xanthomonas*: understanding bacterium–plant interactions. *Nature Reviews Microbiology* **9**, 344-55.
- Rybak M, 2005. *Genetic determinants of host range specificity of the Wellington strain of Xanthomonas axonopodis pv. citri*. 1453 Fifield Hall: University of Florida, Philosophical Doctor.
- Rybak M, Minsavage G, Stall R, Jones J, 2009. Identification of *Xanthomonas citri* ssp *citri* host specificity genes in a heterologous expression host. *Molecular Plant Pathology* **10**, 249 - 62.
- Sambrook J, Fritsch Ef, Maniatis T, 1989. *Molecular cloning*. Cold spring harbor laboratory press New York.
- Sambrook Jj, Russell Ddw, 2001. *Molecular cloning: a laboratory manual*. Vol. 2. Cold Spring Harbor Laboratory Press.
- Santo Ce, Lam Ew, Elowsky Cg, *et al.*, 2011. Bacterial killing by dry metallic copper surfaces. *Applied and environmental microbiology* **77**, 794-802.
- Saunt J, 2000. *Citrus Varieties of the World: An illustrated Guide*. Sinclair International Business Resources.
- Schaad N, Postnikova E, Lacy G, *et al.*, 2005. Reclassification of *Xanthomonas campestris* pv. *citri* (ex Hasse 1915) Dye 1978 forms A, B/C/D, and E as *X. smithii* subsp. *citri* (ex Hasse) sp. nov. nom. rev. comb. nov., *X. fuscans* subsp. *aurantifolii* (ex Gabriel 1989) sp. nov. nom. rev. comb. nov., and *X. alfalfae* subsp. *citrumelo* (ex Riker and Jones) Gabriel *et al.*, 1989 sp. nov. nom. rev. comb. nov.; *X. campestris* pv *malvacearum* (ex smith 1901) Dye 1978 as *X.*

- smithii subsp. smithii nov. comb. nov. nom. nov.; X. campestris pv. alfalfae (ex Riker and Jones, 1935) dye 1978 as X. alfalfae subsp. alfalfae (ex Riker et al., 1935) sp. nov. nom. rev.; and "var. fuscans" of X. campestris pv. phaseoli (ex Smith, 1987) Dye 1978 as X. fuscans subsp. fuscans sp. nov. *Syst Appl Microbiol* **28**, 494 - 518.
- Schaad Nw, Postnikova E, Lacy G, *et al.*, 2006. Emended classification of xanthomonad pathogens on citrus. *Systematic and Applied Microbiology* **29**, 690-5.
- Schein Ai, Kissinger Jc, Ungar Lh, 2001. Chloroplast transit peptide prediction: a peek inside the black box. *Nucleic Acids Res* **29**, E82.
- Schmid Fx, 1995. Protein folding: Prolyl isomerases join the fold. *Current Biology* **5**, 993-4.
- Schubert Ts, Rizvi Sa, Sun X, Gottwald Tr, Graham Jh, Dixon Wn, 2001. Meeting the challenge of eradicating citrus canker in Florida-Again. *Plant Disease* **85**, 340-56.
- Serizawa S, Inoue K, 1975. Studies on citrus canker. III. The influence of wind on infection. *Bull. Shizuoka Citrus Exp. Stn* **11**, 54-67.
- Shantharaj D, Minsavage J, Stall R, *et al.*, 2013. Deciphering specificities of TAL effectors in *Xanthomonas citri* and prospects in citrus. *Phytopathology* **103**, S2.
- Soprano As, Abe Vy, Smetana Jh, Benedetti Ce, 2013. Citrus MAF1, a repressor of RNA Pol III, binds the *Xanthomonas citri* canker elicitor PthA4 and suppresses citrus canker development. *Plant physiology*.
- Stall R, Cook A, 1966. Multiplication of *Xanthomonas vesicatoria* and lesion development in resistant and susceptible pepper. *Phytopathology* **56**, 1152-4.
- Stall R, Marco G, Canteros B, 1981. Pathogenicity of three strains of the citrus canker organism on grapefruit In. *Proceedings 5th International Conference Plant Pathogenic Bacteria Cali, Colombia*, 334-40.
- Stall Re, 1964. Bacterial spot of tomato. Fungicide-Nematocide Tests. *Amer. Phytopathol. Soc.* **20**, 2.
- Stall Re, Loschke Dc, Jones Jb, 1986. Linkage of copper resistance and avirulence loci on a self-transmissible plasmid in *Xanthomonas campestris* pv. *vesicatoria*. *Phytopathology* **76**, 240-3.
- Stall Re, Marco G, Canteros Bi, 1979. *Cancrosis de los citrus. Informe Investig. Proyecto Cooperat. INTA-IFAS durante 1978-79. Informe Tecnico N°1*
- Stall Re, Marco Gm, Canteros De Echenique B, 1982. Importance of mesophyll in mature-leaf resistance to cancrrosis of citrus [caused by *Xanthomonas campestris citri*, *Citrus paradisi*, *Citrus sinensis*, *Citrus limonia*, cultivars]. *Phytopathology* **72**.

- Stall Re, Seymour Cp, 1983. Canker, a threat to citrus in the Gulf-Coast states. *Plant Disease* **67**, 581-5.
- Stamnes Ma, Rutherford Sl, Zuker Cs, 1992. Cyclophilins: a new family of proteins involved in intracellular folding. *Trends in cell biology* **2**, 272-6.
- Staskawicz B, Dahlbeck D, Keen N, Napoli C, 1987. Molecular characterization of cloned avirulence genes from race 0 and race 1 of *Pseudomonas syringae* pv. *glycinea*. *Journal of Bacteriology* **169**, 5789-94.
- Staskawicz Bj, Dahlbeck D, Keen Nt, 1984. Cloned avirulence gene of *Pseudomonas syringae* pv. *glycinea* determines race-specific incompatibility on *Glycine max* (L.) Merr. *Proc Natl Acad Sci U S A* **81**, 6024-8.
- Sun X, Stall R, Jones J, *et al.*, 2004. Detection and characterization of a new strain of citrus canker bacteria from key Mexican lime and Alemow in South Florida. *Plant Disease* **88**, 1179 - 88.
- Sundin G, Jones A, Fulbright D, 1989. Copper resistance in *Pseudomonas syringae* pv. *syringae* from cherry orchards and its associated transfer in vitro and in planta with a plasmid. *Phytopathology* **79**, 861-5.
- Swarup S, Yang Y, Kingsley M, Gabriel D, 1992. A *Xanthomonas citri* pathogenicity gene, *pthA*, pleiotropically encodes gratuitous avirulence on nonhosts. *Mol Plant Microbe Interact* **5**, 204 - 13.
- Tampakaki Ap, Skandalis N, Gazi Ad, *et al.*, 2010. Playing the “Harp”: Evolution of Our Understanding of *hrp/hrc* Genes 1. *Annual review of phytopathology* **48**, 347-70.
- Thieme F, Szczesny R, Urban A, Kirchner O, Hause G, Bonas U, 2007. New type III effectors from *Xanthomonas campestris* pv. *vesicatoria* trigger plant reactions dependent on a conserved N-myristoylation motif. *Mol Plant Microbe Interact* **20**, 1250 - 61.
- Timmer L, Gottwald T, Zitko S, 1991. Bacterial exudation from lesions of Asiatic citrus canker and citrus bacterial spot. *Plant disease* **75**, 192-5.
- Timmer Lw, Garnsey Sm, Graham Jh, Society Ap, 2000. *Compendium of citrus diseases*. APS Press.
- Uden Pc, Bigley Ie, 1977. High-pressure liquid chromatography of metal diethyl-dithiocarbamates with uv and dc argon-plasma emission spectroscopic detection. *Analytica Chimica Acta* **94**, 29-34.
- Vauterin L, Hoste B, Kersters K, Swings J, 1995. Reclassification of *xanthomonas*. *International Journal of Systematic Bacteriology* **45**, 472-89.

- Vauterin L, Swings J, 1997. Are classification and phytopathological diversity compatible in *Xanthomonas*? *Journal of Industrial Microbiology and Biotechnology* **19**, 77-82.
- Vellosillo T, Vicente J, Kulasekaran S, Hamberg M, Castresana C, 2010. Emerging complexity in reactive oxygen species production and signaling during the response of plants to pathogens. *Plant physiology* **154**, 444-8.
- Verniere C, Hartung J, Pruvost O, *et al.*, 1998. Characterization of phenotypically distinct strains of *Xanthomonas axonopodis* pv. *citri* from Southwest Asia. *European Journal of Plant Pathology* **104**, 477-87.
- Voloudakis Ae, Bender Cl, Cooksey Da, 1993. Similarity between copper resistance genes from *Xanthomonas campestris* and *Pseudomonas syringae*. *Applied and environmental microbiology* **59**, 1627-34.
- Wang P, Heitman J, 2005. The cyclophilins. *Genome biology* **6**, 226.
- Wei Z-M, Laby Rj, Zumoff Ch, *et al.*, 1992. Harpin, elicitor of the hypersensitive response produced by the plant pathogen *Erwinia amylovora*. *Science* **257**, 85-8.
- White F, Potnis N, Jones J, Koebnik R, 2009. The Type III effectors of *Xanthomonas*. *Mol Plant Pathol* **10**, 749 - 66.
- Willis Dk, Rich Jj, Hrabak Em, 1991. hrp Genes of phytopathogenic bacteria. *Mol. Plant-Microbe Interact* **4**, 132-8.
- Ye G, Hong N, Zou L-F, *et al.*, 2013. tale-Based Genetic Diversity of Chinese Isolates of the Citrus Canker Pathogen *Xanthomonas citri* subsp. *citri*. *Plant Disease* **97**, 1187-94.
- Young J, Park D, Shearman H, Fargier E, 2008. A multilocus sequence analysis of the genus *Xanthomonas*. *Syst Appl Microbiol* **31**, 366 - 77.
- Zhu W, Magbanua Mm, White Ff, 2000. Identification of Two Novelhrp-Associated Genes in the hrp Gene Cluster of *Xanthomonas oryzae* pv. *oryzae*. *Journal of bacteriology* **182**, 1844-53.

BIOGRAPHICAL SKETCH

Alberto Martin Gochez was born in Buenos Aires, Argentina, in 1978. From 1997 to 2002 he attended the National University of Misiones (Posadas, province of Misiones, Argentina), where he obtained a B.S. in Genetics. In 2003, he started to work in the National Institute of Agricultural Technology (INTA) in Bella Vista city (Corrientes, Argentina). In 2005, he was admitted for the Master of Science program in Plant Pathology at National University of Mar del Plata (Balcarce city, Buenos Aires, Argentina), under the supervision of Dr. Blanca I. Canteros. His master's research was focused on "Differential interaction among strains of *Xanthomonas* and diverse Rutaceae", upon graduation in 2007 he continued at INTA as a Research Plant Pathologist and in 2009 was awarded with a fellowship from INTA to pursue graduate studies. Alberto entered the University of Florida, Gainesville, FL, in the fall semester 2010, where he conducted research on "Host pathogen interaction and copper resistance in *Xanthomonads* associated with citrus canker" under the supervision of Dr. Jeffrey B. Jones. At the end of his studies he resumes his position in Argentina.